

# How unstable was the environment during the Penultimate Glacial in the South-Western Mediterranean? Vegetation, climate and human dynamics during MIS 6.

**Charton Liz<sup>1,2</sup>, Combourieu-Nebout Nathalie<sup>1</sup>, Bertini Adele<sup>2</sup>, Peyron Odile<sup>3</sup>, Robles Mary<sup>3</sup>, Lebreton Vincent<sup>1</sup>, Moncel, Marie-Hélène<sup>1</sup>.**

1 : UMR 7194 HNHP- « Histoire Naturelle des Humanités Préhistoriques », MNHN / CNRS / UPVD, Paris, France. [liz.charton@mnhn.fr](mailto:liz.charton@mnhn.fr)

2 : Dipartimento di Scienze della Terra, Università degli Studi di Firenze, Florence, Italy.

3: UMR 5554, ISEM-Institut des Sciences de l'Evolution de Montpellier, CNRS, Université de Montpellier, Montpellier, France.

## Abstract

The impact of rapid climate variability on Neanderthal population in Europe during the Last Glacial (Marine Isotope Stages 4-2), including Dansgaard-Oeschger cycles and Heinrich events, has been the subject of a long-standing debate. However, few studies have focused on the nature and impact of such rapid variations on human population during earlier periods. A growing number of high-resolution paleoclimatic archives supports the persistence of rapid oscillations during the penultimate glaciation (MIS 6), and the close response of Mediterranean ecosystems to these. Still, few palynological sequences in the Mediterranean region offer sufficient resolution to document vegetation dynamics during this time. Pollen records are especially lacking in the western Mediterranean, a key region to understand the connection between North Atlantic and Mediterranean climatic influences. This region is also traditionally considered a climatic refugium for human population during unfavourable periods. We provide new palynological data covering MIS 6 from the long and continuous marine record of ODP 976 in the Alboran Sea. A total of 200 samples, spanning the interval from 196 to 127 ka Before Present (BP), reveal both long-term trends and rapid fluctuations in regional vegetation composition. A multi-method approach, including modern analogues, regression, and machine learning approaches, was applied to ODP 976 pollen assemblages to reconstruct the annual/seasonal temperatures and precipitation. Results show that three phases can be identified. The first phase (187-166 ka BP) is characterized by significant oscillations of temperate trees and rather cool and humid conditions during early MIS 6, coincident with a sapropel layer deposition in both the western and eastern Mediterranean. In the second phase (165-144 ka BP), arid herbaceous vegetation is dominant, marking the main imprint of glacial maxima conditions and reduced climate variability. The third phase (144-129 ka BP) is marked by the development of Ericaceae and increased annual precipitations. At the end of MIS 6 glaciation, an [episode of](#) strong cooling and

a mis en forme : Anglais (Royaume-Uni)

a mis en forme : Anglais (Royaume-Uni)

35 ~~intense episode of~~ steppe and semi-desert expansion is identified as Heinrich Stadial 11 (135-129 ka  
36 BP), marking a distinct pattern for Termination II in the Western Mediterranean. Rapid oscillations  
37 appear like a pervasive feature of the Penultimate glacial in the SW Mediterranean, though they  
38 present reduced amplitude and frequency compared to the Last Glacial. A synthesis of human  
39 occupation during MIS 6 shows that a mosaic of traditional (Mode 2) and innovative (Mode 3) lithic  
40 technological features is observed in the archaeological record. Although the data are scarce,  
41 Neanderthals seems to have continuously inhabited Western Mediterranean regions across the  
42 penultimate glacial. The severe climate conditions during Heinrich Stadial 11 (~133-129 ka BP) might  
43 have played a role in the apparent population contraction at the end of MIS 6, and perhaps also in the  
44 definitive abandonment of Lower Palaeolithic industries.

## 45 1. Introduction

46 Rapid climate oscillations occurred during the last Glacial period (MIS 4-2). Dansgaard-  
47 Oeschger (DO) cycles have been well identified in ice-core records (Bond et al., 1999; Dansgaard et al.,  
48 1993; Johnsen et al., 1992; Rasmussen et al., 2014) and recognized in Atlantic sedimentary cores (e.g.  
49 Bond et al., 1993, 1997; Roucoux et al., 2005; Sánchez Goñi et al., 2002; Shackleton et al., 2000,  
50 Zumaque et al., 2025). Short periods of intense cold named Heinrich Stadials (HS) and linked with  
51 intense iceberg discharges were also evidenced in Atlantic sediments (Bond et al., 1992; Heinrich,  
52 1988; Hemming, 2004; Rasmussen et al., 2003; Ruddiman, 1977; Shackleton et al., 2004). Major cooling  
53 events also occurred during MIS 5 and the penultimate deglaciation (e.g. Chapman & Shackleton, 1999;  
54 Oppo et al., 2001). These high-frequency oscillations reflect major changes at global scale in the  
55 oceanic circulation and the Atlantic Meridional Overturning Circulation (AMOC), that are important  
56 features particularly during glacial terminations (Barker and Knorr, 2021). The Mediterranean region  
57 has been very sensitive to the rapid climate oscillations of MIS 5 to MIS 1, with changes recorded in  
58 both marine and continental environments (Cacho et al., 1999, 2006; Combourieu-Nebout et al., 2002,  
59 2009; Fletcher et al., 2010; Martrat et al., 2007; Penaud et al., 2016; Sánchez Goñi et al., 2002, 2022).

60 The penultimate glacial (MIS 6), took place between ~185 and 130 ka BP and presented a  
61 different ice-sheet and global climate configuration compared to the last glacial (MIS 4-2). It is  
62 considered among the coldest glacial periods of the past 800 ka BP (Masson-Delmotte et al., 2010),  
63 characterized by larger European Ice-Sheet and smaller Laurentide ice-sheet extension (Colleoni et  
64 al., 2016; Ehlers et al., 2018; Ehlers & Gibbard, 2007; Rohling et al., 2017). In Europe, it corresponds to  
65 the Riss glaciation in the Alpine area, and to the late Saalian glaciation complex in northern and central  
66 Europe, with two major ice-sheet advances identified in Germany: the Drenthe advance (~170-155 ka  
67 BP) characterized by the maximum ice extent in Europe, and the less extensive Warthe advance during

a mis en forme : Anglais (Royaume-Uni)

68 the younger stage of MIS 6 (Ehlers et al., 2011). The exact chronology of the Penultimate Glacial  
69 Maximum (i.e. the maximum extension of the northern hemisphere ice-sheet) is still not well  
70 constrained (Svendsen et al., 2004), but is usually considered around 140 ka BP (Colleoni et al., 2016).  
71 Five marine isotopic substages were identified from MIS 6e to 6a, reflecting variations of global sea  
72 temperatures : three cold substages (6e : ~180 ka BP, 6c : ~160 ka BP, 6a : ~136 ka BP) with increasing  
73 cold intensity, and two warm substages (6d : ~170 ka BP and 6b : ~149 ka BP) (Railsback et al., 2015).  
74 Different speleothem records revealed that MIS 6 glaciation in Europe, including the Mediterranean  
75 region, was characterized by wetter conditions in comparison with the last glacial (Ayalon et al., 2002;  
76 Koltai et al., 2017; Nehme et al., 2018; Regattieri et al., 2014). Furthermore, various studies highlighted  
77 the apparent higher stability of the Laurentide ice-sheets during the penultimate glacial, leading to the  
78 absence of typical “Heinrich layers” in the North Atlantic sediments, with the exception of the large  
79 event recorded at the MIS 6 to MIS 5 transition, HS11 (~135-129 ka BP) (de Abreu et al., 2003;  
80 McCarron et al., 2021; McManus et al., 1999; Obrochta et al., 2014; Ovsepyan and Murdmaa, 2017;  
81 Shackleton et al., 2003).

82 Human Palaeolithic groups in Europe were likely affected by rapid climate changes  
83 (Bradt Möller et al., 2012; Dennell et al., 2011; Raia et al., 2020; Willis et al., 2004). The South-Western  
84 Mediterranean probably played a major role as one of the climate refugia areas around the  
85 Mediterranean Basin during the most unfavourable climatic periods, permitting the persistence of  
86 “source” population able to recolonize the northernmost areas during more favourable periods (Bailey  
87 et al., 2008; Bicho & Carvalho, 2022). Neanderthal presence in very distinct ecotones in Eurasia proves  
88 it could adapt to a very wide range of environments. However, recent niche modelling approaches  
89 together with palaeoecological data from archaeological sites strengthened the view that warm  
90 forested landscapes like the MIS 5e environments represented the most suitable habitats for  
91 Neanderthals, where they could persist during colder periods (Carrión et al., 2026; Ochando et al.,  
92 2019; Stewart et al., 2019; Trájer, 2023). This conception leads to the overlap of the notions of  
93 refugium for vegetation and human populations, despite the greatest adaptability and niche extension  
94 of humans.” Many studies focused on the potential impact of abrupt environmental changes on  
95 Neanderthal populations, especially those associated with Heinrich Stadials during MIS 3 (e.g. Charton  
96 et al., 2025; D’Errico & Sánchez Goñi, 2003; Finlayson & Carrión, 2007; Melchionna et al., 2018). During  
97 the previous climatic cycles of the Middle Pleistocene, when Early to Middle Palaeolithic cultures  
98 developed, repeated climate instability has been brought forward as an explanation for the large  
99 variability in the lithic production (Dennell et al., 2011; Foerster et al., 2022; Sánchez-Yustos and Díez-  
100 Martín, 2015), and the non-linearity of ~~the biological processes linked with~~ Neanderthal biological  
101 evolution (Bermúdez de Castro & Martín-Torres, 2013; Hublin, 2009). Still, the short and long-term

Code de champ modifié

102 resilience of human populations in a globally unstable environment is poorly understood, and partially  
103 hindered by our limited knowledge of fast millennial-scale climate oscillations in older glaciations prior  
104 to MIS 4-2.

105 While the Greenland ice does not provide an adequate record for periods older than 123 ka BP  
106 (Chappellaz et al., 1997), the description of a precise stratigraphy of climate events at sub millennial  
107 scale for the previous glacial/interglacial cycles remains complex, and relies on the Antarctic isotope  
108 record (Bazin et al., 2013; Jouzel et al., 2007), the study of marine sediments (de Abreu et al., 2003;  
109 Lisiecki & Raymo, 2005; Margari et al., 2010, 2014; McManus et al., 1999; Obrochta et al., 2014) and  
110 high-resolution continental archives such as speleothems (Burns et al., 2019; Held et al., 2024; Hodge  
111 et al., 2008; Wainer et al., 2013; Wang et al., 2018; Wang et al., 2001). Benthic and planktonic isotopic  
112 ratios together with Sea Surface Temperatures (SSTs) reconstructions in the North Atlantic and the  
113 Western Mediterranean showcased the persistence of D-O-like events and interhemispheric bipolar  
114 see-saw heat transport during MIS 6, in addition to important reorganization of the water circulation  
115 during sapropel S6 deposition ~175 ka BP (Margari et al., 2010, 2014; Martrat et al., 2004, 2007, 2014;  
116 Rousseau et al., 2020; Sierro & Andersen, 2022). Nevertheless, MIS 6 is much less well documented  
117 than the last glacial in Mediterranean Europe. Few palynological sequences are available to document  
118 the vegetation changes across this interval (Camuera et al., 2019, 2022; Follieri et al., 1988; Margari et  
119 al., 2010; Okuda et al., 2001; Roucoux et al., 2011; Sadori et al., 2016; Sinopoli et al., 2019; Tzedakis et  
120 al., 2006; Wilson et al., 2021). Among them, only one in SW Europe provides sufficient resolution to  
121 document high-frequency changes: ~~the deep-sea core MD01-2444~~ (Margari et al., 2010, 2014). This  
122 record from the deep-sea core MD01-2444 showed that several While D-O-like events impacting  
123 impacted the vegetation the vegetation have been identified in this record especially during the lower  
124 part of MIS 6 (Margari et al., 2010). ~~†~~ The core is located out of the Mediterranean Sea, along the  
125 Portuguese margin in the Atlantic Ocean. Therefore, questions remain open concerning the impact of  
126 such rapid events on the Western Mediterranean region, considered a Pleistocene refugium for human  
127 populations.

128 To fill this gap, our study provides high-resolution pollen data and quantitative climate  
129 reconstructions from ODP site 976 in south-western Mediterranean focusing on MIS 6. We aim to (i)  
130 reconstruct the vegetation and climate changes in the SW Mediterranean during the penultimate  
131 glacial, (ii) identify abrupt climatic changes including potential Heinrich-like and D-O like events and  
132 connect-correlate them with other Atlantic and Mediterranean paleoenvironmental records, (iii)  
133 compare the nature of millennial-scale climate and vegetation dynamics during the last glacial period  
134 and the penultimate glacial using a single, continuous pollen record and (iv) explore the potential

135 impact of these climatic changes for Early Middle Palaeolithic human groups, with particular attention  
136 to the presence of climate refugia during the most extreme glacial phases.

## 137 2. Study site

138 Ocean Drilling Program (ODP) Site 976 (36°12 N, 4°18W, 1108 m depth) core was retrieved in  
139 1995 in the Alboran Sea (Zahn et al., 1999). The site is located about 110 km east of the Gibraltar Strait,  
140 70 km south of the Spanish coast, and 100 km north of Morocco (Fig. 1).

141 The Alboran Sea is the westernmost extensional basin of the Mediterranean Sea, bordered to  
142 the north by the Betic Cordillera and to the south by the Moroccan Rif mountains. Oceanic currents  
143 result from the water masses exchanges between the Atlantic Ocean and the Mediterranean Sea  
144 through the Gibraltar Strait. The surface currents are governed by the inflow of low-salinity Atlantic  
145 waters (Atlantic Jet) forming two anticyclonic gyres named Western and Eastern Alboran Gyres (WAG  
146 and EAG) (Renault et al., 2012) (Fig. 1). The Mediterranean high-salinity water masses flow out in the  
147 Atlantic basin through the intermediate depth currents.

148 The modern climate in the Alboran Sea region is typically Mediterranean, defined by long, hot,  
149 dry summers and mild and cool winters (Lionello et al., 2006; Sánchez-Laulhé et al., 2021). Atlantic  
150 westerlies dominate during winter, while subtropical high pressure masses generate intense drought  
151 during summer (Sumner et al., 2001). The current vegetation distribution on the Alboran borderlands  
152 follows a strong altitudinal climatic gradient : dry steppe elements such as *Artemisia* and *Lygeum* grow  
153 in the most arid lowlands along the coast, sclerophyllous evergreen taxa, including *Quercus ilex*, *Olea*  
154 and *Pistacia* are the main representatives of the thermo-to meso-Mediterranean belts, while  
155 temperate vegetation with deciduous trees constitutes the overlying supra-Mediterranean belt  
156 (Quézel, 2000). Finally, coniferous forests of *Abies* and *Pinus* and *Picea* grow in the oro-Mediterranean  
157 belt (above approximately 1200 m), with the presence of *Cedrus* in altitudinal vegetation of the  
158 Moroccan Rif mountains.

159 The main sedimentation processes in the area originate from the strong erosion in the Betic  
160 Cordillera (Alonso et al., 1999; Liqueste et al., 2005; Lobo et al., 2006) and the material transported by  
161 the surface Atlantic waters (Auffret et al., 1974), although a significant but unknown proportion of  
162 particles including pollen was transported by African winds as evidenced by the presence of Saharan  
163 clay particles and *Cedrus* pollen across the Pleistocene (Bout-Roumazeilles et al., 2007; Jiménez-  
164 Moreno et al., 2020; Magri & Parra, 2002). Therefore, the pollen assemblage is interpreted as reflecting  
165 the regional vegetation of the southern Iberian Peninsula, with smaller but variable contribution from  
166 Northern Africa. Previous studies have shown that the Alboran Sea palynological record displays close  
167 similarities with the Padul record in SE Spain (Camuera et al., 2019), indicating that ODP 976 is a valid

a mis en forme : Anglais (Royaume-Uni)

Code de champ modifié

168 archive to reconstruct the southern Iberian Peninsula vegetation changes (Fletcher & Sánchez Goñi,  
169 2008; Charton et al., 2025).

170 Two Organic-Rich Layers (ORLs) were identified in ODP 976 core during the MIS 6 interval, bed  
171 607 (50.43-49.93 m), and bed 606 (41.6-40.4 m) (Murat, 1999). The ages were recalculated based on  
172 the updated age model for MIS 6 presented here, giving 178.07-174.53 ka BP for bed 607, and 132.64-  
173 129.16 ka BP for bed 606. With a Total Organic Carbon (TOC) of 1.18% and 1.85% respectively, these  
174 layers have been described as “ghost sapropels”, as they present a lower organic matter content than  
175 the Eastern Mediterranean sapropels (Rogerson et al., 2008). Their relevance for hydrological and  
176 climatic inferences in the Alboran Sea will be discussed in the light of the vegetation dynamics.

a mis en forme : Anglais (États-Unis)

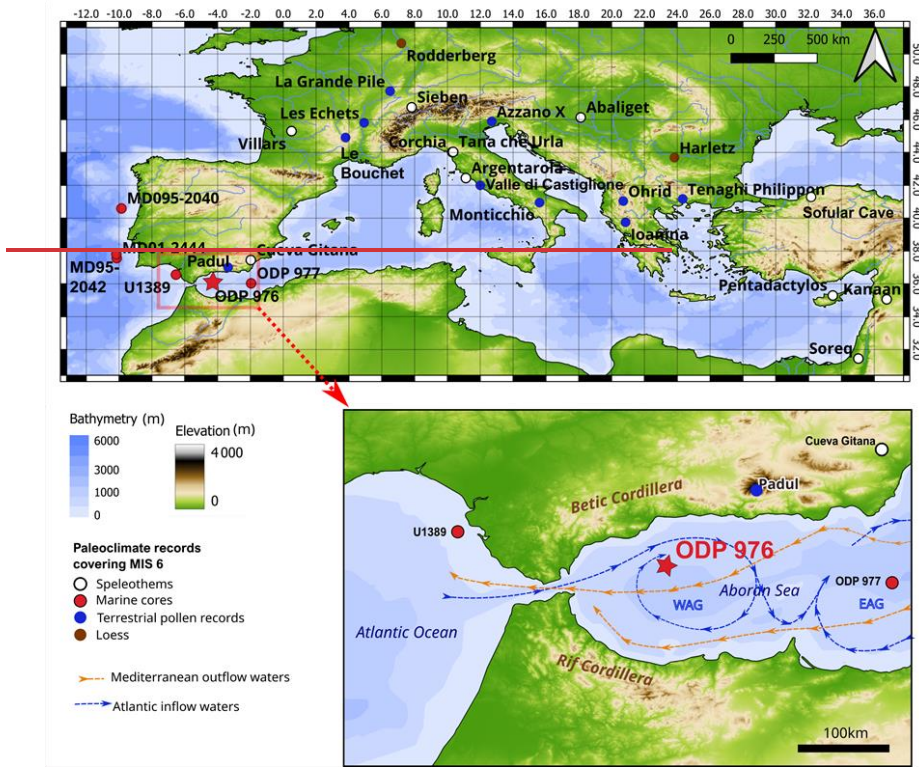




Fig. 1. Map showing the location of ODP 976 core together with other paleoenvironmental and paleoclimate records covering part or all of MIS 6, as discussed in the text.

177

### 3. Methods

178

#### 3.1. Age Model

179

180

The age model for the study interval uses three previously published tie-points between ODP 976 Mg/Ca-derived SST (Jiménez-Amat and Zahn, 2015) and the speleothem temperature records from Dongge cave in China (Kelly et al., 2006, [see Supplement Fig. S1](#)). [Several other marine records covering MIS 6 in the region are chronologically tuned to speleothems \(e.g. Sierra & Anderson, 2022; Tzedakis et al., 2018\).](#) -For the lower interval, the low resolution of planktonic isotopic data available for ODP 976 did not allow direct [correlation to global temperature stacks or orbital configuration](#) ~~orbital or~~ [temperature calibration](#) (von Grafenstein et al., 1999). Instead, we chose to align the higher-resolution pollen record produced in this study with the one from MD01-2444 core on the Portuguese margin (Margari et al., 2010, 2014; Tzedakis et al., 2018). Previous studies highlighted the strong similarities between pollen records on the Atlantic margin and the Alboran Sea during the last glacial period

189

a mis en forme : Anglais (Royaume-Uni)

190 (Fletcher et al., 2010a; Fletcher & Sánchez Goñi, 2008; Sánchez Goñi et al., 2002), supporting this  
 191 approach. MD01-2444 chronology is based on the alignment of benthic isotopic events with the  
 192 Antarctic temperature record, on AICC2012 timescale (Jouzel et al., 2007; Margari et al., 2010; Shin et  
 193 al., 2020). The eleven tie-points between MD01-2444 core and Epica Dome C can be found in  
 194 Supplement (Table S1). Five peaks of temperate forest in MD01-2444 were used as control-points for  
 195 ODP 976 (Table 1). The main assumptions of these tuning approaches with Dongge cave speleothem  
 196 and the Antarctic record are discussed in detail in Jiménez-Amat and Zahn (2015) and Margari et al.  
 197 (2010) respectively. The obtained chronology for ODP 976 core for MIS 6 prevents any assessment of  
 198 the southwestern Mediterranean vegetation response to global climatic events.

a mis en forme : Anglais (États-Unis)

a mis en forme : Anglais (États-Unis)

a mis en forme : Anglais (États-Unis)

Event type	ODP 976 meters composite Depth (mcd)	Age (ka BP)	References
Dongge cave speleothem D3	40.25	128.73	Jiménez-Amat and Zahn, 2015; Kelly et al., 2006
Dongge cave speleothem D2	42.61	135.57	Jiménez-Amat and Zahn, 2015; Kelly et al., 2006
Dongge cave speleothem D1	44.14	142.09	Jiménez-Amat and Zahn, 2015; Kelly et al., 2006
Temperate pollen peak in MD01-2444	46.4	149.43	(Margari et al., 2010; Shin et al., 2020)
Temperate pollen peak in MD01-2444	48.5	160.00	(Margari et al., 2010; Shin et al., 2020)
Temperate pollen peak in MD01-2444	49.3	170.07	(Margari et al., 2010; Shin et al., 2020)
Temperate pollen peak in MD01-2444	50.48	178.42	(Margari et al., 2010; Shin et al., 2020)
Temperate pollen peak in MD01-2444	53.2	193.758	(Margari et al., 2010; Shin et al., 2020)

a mis en forme le tableau

a mis en forme : Anglais (Royaume-Uni)

199 **Table 1. List of control points used to calibrate the ODP 976 record for the MIS 6 interval.** The tie-  
 200 points on MD01-2444 temperate pollen curve are on AICC2012 timescale.

201 A linear regression was applied to obtain a continuous age for the study interval, spanning from  
 202 126.4 to 196.6 ka BP, with a mean resolution of about 350 years for the record (Fig. 2).

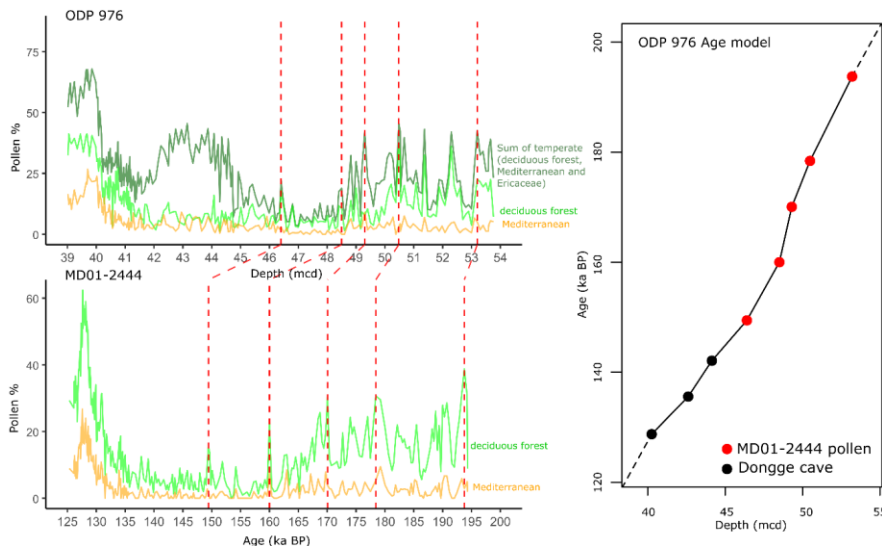


**Fig. 2.** Age versus depth model for the MIS 6 part of ODP 976 record, based on correlation between the Mg/Ca-based SST curve (Jiménez-Amat and Zahn, 2015) and the Dongge cave speleothem temperature record (Kelly et al., 2006) (black dots), and graphical correlation of the temperate pollen curve with the MD01-2444 palynological record (red dots and dotted lines) on AICC2012 timescale (Margari et al., 2010; Shin et al., 2020).

203

### 204 3.2. Pollen analyses

205 Two hundred samples have been analysed [herein this study](#), between 40 and 54 m (mcd)  
 206 depth. The sample processing followed the traditional steps used for pollen extraction (Faegri and  
 207 Iversen, 1964) and previously applied to the ODP 976 core (Combourieu-Nebout et al., 2002; 2009;  
 208 Sassoon et al., 2023, Charton et al., 2025). It included sample weighing between 5 and 10 g of  
 209 sediments, a 150  $\mu\text{m}$  sieving for ~~the~~ retrieving of macrofossils and macroparticles, followed by 10%  
 210 HCl, 40% HF, 20% HCl and a final 10  $\mu\text{m}$  sieving.

211 A minimum of 150 pollen grains were counted for each sample, excluding *Pinus* as it is usually  
 212 overrepresented in marine sequences (e.g. Combourieu-Nebout et al., 2002; Fletcher et al., 2010b;  
 213 Mudie, 2011 and references therein), and represents often more than 50% of the total pollen sum  
 214 [along in](#) the study interval (see Fig. 3).

215 Ecological groups of pollen taxa were defined following previous studies of the ODP 976 record  
 216 (Charton et al., 2025; Combourieu-Nebout et al., 2009; Sassoon et al., 2023). The percentage pollen  
 217 diagram was constructed using the *rioja* R package (Juggins, 2023). Constrained Incremental Sum-of-

218 Squares (CONISS) cluster analysis was applied for pollen zonation, using the *vegan* package on R  
219 (Oksanen et al., 2024).

### 220 3.3. Pollen-inferred climate reconstructions: a multi-method approach

221 Four methods were applied to the ODP 976 record to reconstruct past climate changes during  
222 MIS 6. This is the first time this approach is used for the entire MIS 6 interval (Sinopoli et al., 2019). ~~As~~  
223 ~~already pointed out, t~~ The multi-method approach allows for a more accurate climate reconstruction  
224 (trends and rapid events) compared to the traditional single-method approach (Chevalier et al., 2020;  
225 Peyron et al., 2011, 2013; Salonen et al., 2019; Sassoon et al., 2025). It also allows us to compare the  
226 reliability and biases of the different methods, which are based on different ecological principles and  
227 mathematical algorithms. Four methods were used in this study.

228 The Modern Analogue Technique (MAT) is the first “assemblage” method ever developed to  
229 estimate climate parameters based on pollen assemblages, and is still the most widely used (Guiot,  
230 1990). It is based on the calculation of a dissimilarity index between the fossil samples and samples  
231 from a modern pollen dataset. The values of the closest modern analogues selected (here, 4) are  
232 averaged to reconstruct the climate parameters for each fossil sample. Weighted-Averaging Partial  
233 Least Squares (WA-PLS) (ter Braak and Juggins, 1993) is the second most widely used method, and is  
234 based on a different mathematical approach using non-linear regression. Assuming that taxa are most  
235 abundant where they find their optimum climatic conditions, WA-PLS models the plant/climate  
236 relationships from the modern calibration dataset, weighing the climatic values based on the pollen  
237 taxa percentage. These plant pollen abundance / climate transfer functions are then used to calculate  
238 the climate parameters of the fossil samples. The last two methods, Random Forest (RF) and Boosted  
239 Regression Trees (BRT), rely on a completely different approach using machine learning: they generate  
240 a large set of regression trees based on a randomised pollen dataset by bootstrapping (with pollen  
241 taxa selected randomly). Contrary to RF (Prasad et al., 2006), BRT (Salonen et al., 2012) assigns a higher  
242 probability to select samples that have not been selected before (boosting), increasing the  
243 performance of the model for elements that are less well predicted (Chevalier et al., 2020). The  
244 application of these machine learning methodologies in paleoclimatology is very promising, especially  
245 for BRT, and they have already been validated through different European and Mediterranean pollen  
246 records, for different time periods (Charton et al, 2025; D’Oliveira et al., 2023; Robles et al., 2022,  
247 2023; Salonen et al., 2019; Sassoon et al., 2025).

248 The four methods were run on R using the *Rioja* packages *Rioja* for MAT and WA-PLS (Juggins,  
249 2024), *dismo* for BRT (Hijmans et al., 2023) and *randomForest* for RF (Liaw and Wiener, 2022).

250 We used the modern pollen dataset compiled by Peyron et al. (2013, 2017) and updated by  
251 Dugerdil et al. (2021a) and Robles et al. (2023). Samples belonging to non-relevant biomes for this  
252 study were excluded (Taiga, Tundra, Pioneer Forest, warm steppe and hot desert), resulting in 2373  
253 samples for calibration dataset spanning ~~across~~ Eurasia and NW Africa (see Supplement, Fig. S2). A  
254 total of 103 harmonized pollen taxa are included in the dataset, excluding *Pinus* and aquatic taxa.

a mis en forme : Police :Italique

255 Six climate variables were reconstructed: PANN (annual ~~precipitations~~precipitation), MAAT  
256 (annual temperatures), SUMMERPR (summer ~~precipitations~~precipitation), WINTERPR (winter  
257 ~~precipitations~~precipitation), MTWA (mean temperature of the warmest month) and MTCO (mean  
258 temperature of the coldest month). The climatic tolerance spectra of the ten most abundant pollen  
259 taxa in the ODP 976 record have been reconstructed based on the modern dataset (Supplement, Fig.  
260 S3). They show that steppe and semi-desert taxa display the highest tolerance to low winter  
261 temperature and precipitation, while Mediterranean taxa (*Olea* and *Quercus ilex*-type) are the most  
262 tolerant taxa to high annual and summer temperature, and *Cedrus* and *Ericaceae* to higher annual and  
263 seasonal precipitation. SUMMERPR and MTWA values were poorly reconstructed according to the  
264 accuracy indicators (Table 2). This is in agreement with previous studies showing the poor reliability of  
265 summer parameters (e.g. Camuera et al., 2022). Therefore, we chose to represent seasonal  
266 parameters as contrast values for a better visualization: TCON (temperature contrast) = MTCO -  
267 MTWA, and PCON (precipitation contrast) = WINTERPR - SUMMERPR. The MTWA and SUMMERPR  
268 results can be found in Supplementary Supplement (Fig. S4).

a mis en forme : Police :Italique

a mis en forme : Police :Italique

a mis en forme : Police :Italique

a mis en forme : Police :Italique

269 For comparison with the present-day climate, and the calculation of anomalies, the modern  
270 values were extracted from ERA 5 reanalysis of the ECMWF (European Centre for Medium-Range  
271 Weather Forecasts), based on data assimilation into meteorological modelling from 1960 to 2022  
272 (Hersbach et al., 2020). Pollen dispersal is reduced beyond a radius of 175 km (Rojo et al., 2016).  
273 However, other studies suggest that pollen can be transported up to distances of 200-300 km  
274 (Fernández-Rodríguez et al., 2014) and even over distances greater than 500 km (Bayr et al., 2023;  
275 Damialis et al., 2017). Sediments from marine cores such as ODP 976 can therefore include close and  
276 long-distance pollen. To account for these observations, An averaged value of the climate parameters  
277 on a 400 km radius around the ODP 976 site was extracted (Supplement, Fig. S5), giving MAP = 478  
278 mm, MAAT = 16.78°C, MTCO = 13.78 °C, WINTERPR = 172 mm, TCON = -9.59, PCON = 141.5 mm. These  
279 values for modern climate, averaged temporally and spatially, provide a better basis for understanding  
280 the nature of the climate signal extracted from a marine palynological sequence at a regional pluri-  
281 annual scale.

a mis en forme : Anglais (Royaume-Uni)

a mis en forme : Anglais (Royaume-Uni)

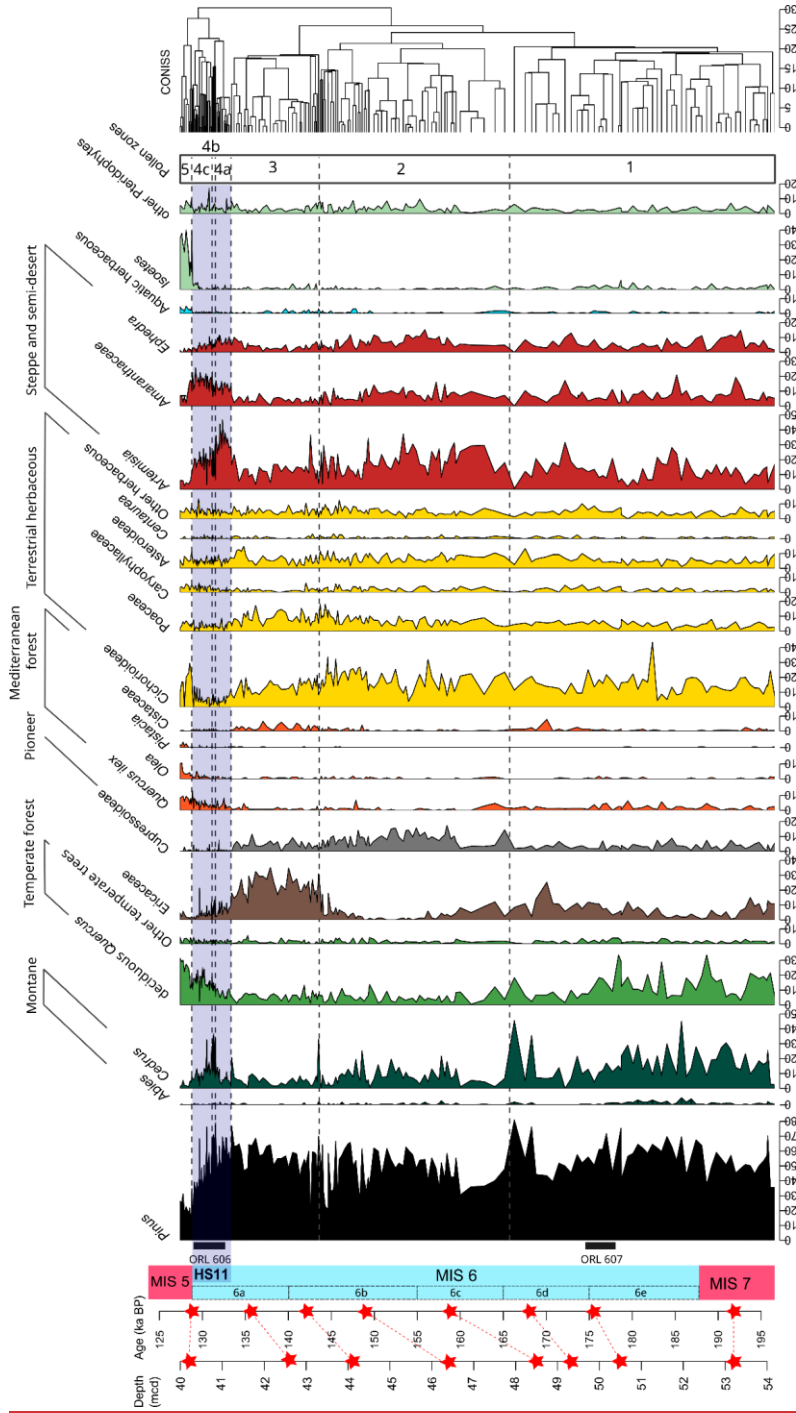
a mis en forme : Anglais (Royaume-Uni)

282           The reliability of the different methods and climate parameters reconstructed is evaluated with  
283 bootstrapping cross-validation through two indicators: the correlation coefficient between the  
284 variables ( $R^2$ ) and the root mean square error (RMSE).

## 285 4. Results

### 286 4.1. Pollen record

287           The pollen diagram shows the vegetation dynamics between 196.6 and 127.5 ka BP, spanning  
288 late MIS 7 to early MIS 5 (Fig. 3). Five pollen zones were separated by CONISS cluster analysis, with  
289 zone 4 being divided in three subzones (Table 2).



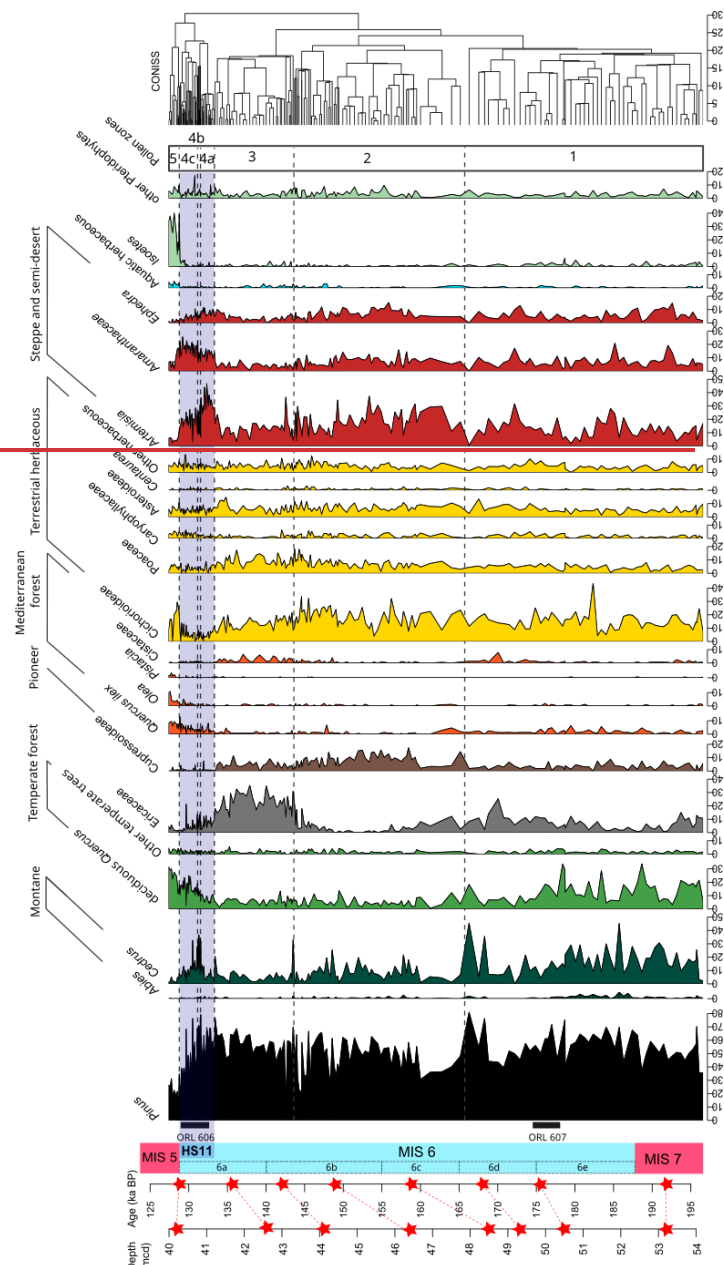


**Fig. 3.** Pollen diagram of selected taxa for MIS 6 interval in the ODP 976 record, plotted against age. Taxa are grouped by ecological groups (see Table 2). Red stars indicate control points used for the age calibration, and their correspondence with mcd (meters composite depth) (see Table 1). The blue bar indicates Heinrich Stadial 11. ORL : Organic Rich Layers from ODP 976 (Murat, 1999).

291 Zone 1 most represented taxa are deciduous *Quercus* and *Cedrus*, with important abundance  
292 variability showing an unstable ~~and rather cool and humid~~ phase at the transition from MIS 7 to MIS  
293 6e and 6d. Zone 2 displays the maximum expansion of steppe and semi-desert vegetation together  
294 with other open vegetation taxa and Cupressoideae, ~~characteristic of the vegetation maximum glacial~~  
295 ~~stage~~ during the MIS 6b and 6c. An additional noteworthy observation within this interval is the  
296 presence of gastropod shells identified as *Limacina retroversa* (Jeanne Rampal, personal  
297 communication, [2023](#)), recovered during sieving of a sample at 46.4 m, corresponding to around  
298 155.5 ka BP (Fig. 4). This species is usually most abundant in temperate to subpolar waters in the  
299 North-Atlantic (Thabet et al., 2015). Zone 3 is mainly characterized by the abundance of Ericaceae ~~and~~  
300 ~~indicates cold and humid conditions~~ at the final stage of MIS 6 (6b and 6a). Zone 4, at the end of MIS  
301 6a, is divided into 3 subzones which display fast vegetation changes during the transition from MIS 6  
302 to MIS 5 (Termination II), and Heinrich Stadial 11. The fast expansion of steppe and semi-desert taxa  
303 (*Artemisia*, *Amaranthaceae*, *Ephedra*) occurs simultaneously with the first increase of deciduous  
304 temperate and Mediterranean forest indicative of the initialization of interglacial conditions (zone 4a).  
305 This episode of arid vegetation dominance is interrupted in zone 4b by the fast expansion of montane  
306 vegetation mainly represented by *Cedrus*. A new steppe and semi-desert vegetation increase is  
307 observed in zone 4c, while the deciduous temperate forest and the Mediterranean vegetation  
308 continue to expand. Finally, zone 5 is characterized by the maximum abundance of mesophilous and  
309 thermophilous elements, mainly represented by deciduous *Quercus* and *Quercus ilex*, typical of the  
310 MIS 5 interglacial ~~optimum~~.

311

312

313

314

315

316

317

318

319

320

321

322

323

324

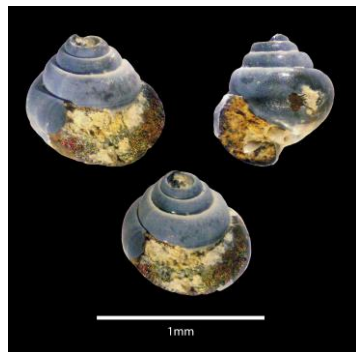
Pollen zone	Depth (mcd) and Age (ka BP)	Description of the pollen assemblage (Fig. 3)	Climate reconstructions (Fig. 5)
5	40.25-39.98 m 128.73-127.47 ka BP	Peak abundance of deciduous <i>Quercus</i> (up to 32%), <i>Quercus ilex</i> (4-10%), <i>Olea</i> (2-11%), <i>Pistacia</i> (up to 4%), aquatic herbaceous (up to 5%) and <i>Isoetes</i> (up to 38%). High values of Cichorioideae (up to 30%). Low percentages of <i>Pinus</i> (<35%), <i>Artemisia</i> (<11%), Amaranthaceae (<18%) and <i>Ephedra</i> (<3%).	Rapid increase of temperature, precipitation and seasonal contrast close to the modern value
4c	41.08-40.28 m 131.13-128.81 ka BP	New increase of <i>Artemisia</i> (up to 29%) and Amaranthaceae (up to 26%). High values of <i>Cedrus</i> (5-28%), and increasing percentages of deciduous <i>Quercus</i> (10-23%), Cichorioideae (0-14%) and <i>Quercus ilex</i> (1-13%). Decrease of Ericaceae (13-0%). Increasing percentages of <i>Isoetes</i> (0-5%) and Pteridophytes spores (0-17%).	First decrease, and then increase in temperatures and <del>precipitations</del> precipitation, with low PCON.
4b	41.21-41.09 m 131.51-131.16 ka BP	Peak abundance of <i>Cedrus</i> (up to 37%). Decrease of <i>Artemisia</i> (30-7%), Amaranthaceae (6-13%) and <i>Ephedra</i> (6-4%). Notable abundance of deciduous <i>Quercus</i> (6-15%) and <i>Quercus ilex</i> (1-3%).	Abrupt rise in precipitation contrast, but still cold conditions.
4a	41.82-41.22 m 133.28-131.54 ka BP	Peak abundance of <i>Artemisia</i> , (24-47%), Amaranthaceae (14-6%) and <i>Ephedra</i> (5-11%). Decreasing trend of Ericaceae percentages (12-2%), and progressive increasing of deciduous <i>Quercus</i> (4-11%) and <i>Quercus ilex</i> (1-8%). Decrease of Cichorioideae (<11%) and Cupressoideae (<8%).	Rapid decrease in temperature, precipitation and seasonal contrast.
3	44.57-41.85 m 143.49-133.37 ka BP	Peak abundance of Ericaceae (12-35 %), and high values of Cichorioideae (8-22%). Notable presence of Cupressoideae (2-11%). Peak abundance of <i>Artemisia</i> (37%) at 44.28 m / 142.54 ka BP and <i>Cedrus</i> (33%) at 44.57 m/143.49 ka BP.	Increase of temperatures (but still lower than present), and important <del>precipitations</del> precipitation rise until values higher-than-present. Seasonal contrast close to present-day.
2	48.91-44.63 m 165.16-143.68 ka BP	High percentages of Cichorioideae (11-34 %), Poaceae (4-18%), <i>Artemisia</i> (4-	Decline of temperatures and <del>precipitations</del> precipitation, both lower than the modern

		37%), Amaranthaceae (3-16%) and <i>Ephedra</i> (3-12%). Cupressoideae maximum between 150-160 ka BP (up to 17%), and abundant <i>Cedrus</i> (up to 25%). Very low values of deciduous <i>Quercus</i> (<10%), Mediterranean taxa (<4%) and Ericaceae (<12%), with minimum values between 150 and 158 ka BP.	values, reaching a minimum between ~164-155 ka BP. Afterwards, progressive rise in temperature, precipitation and seasonal contrast.
1	53.76-49 m 196.15-166.29 ka BP	High percentages of <i>Cedrus</i> (8 to 45%) and deciduous <i>Quercus</i> (4 to 34%), with important variations. Abundant Cichorioideae (up to 43%) and Ericaceae (up to 25%), with notable presence of <i>Abies</i> (up to 5%), <i>Quercus ilex</i> (up to 6%) and <i>Isoetes</i> (up to 6%). Relatively low values of semi-desert elements ( <i>Artemisia</i> , Amaranthaceae, <i>Ephedra</i> ) but with two increases at 49.6 m /172 ka BP and at 51.6 m / 185 ka BP.	Rather stable conditions expressed by the smoothed lines, but important and numerous rapid oscillations. In general, values of precipitation and seasonal contrast are close or higher than the modern value, while temperature is cooler than present.

325

326 **Table 2. Description of the pollen zones identified through CONISS cluster analysis, including the**  
 327 **main characteristics of their pollen assemblage and associated climate reconstructions.**

328



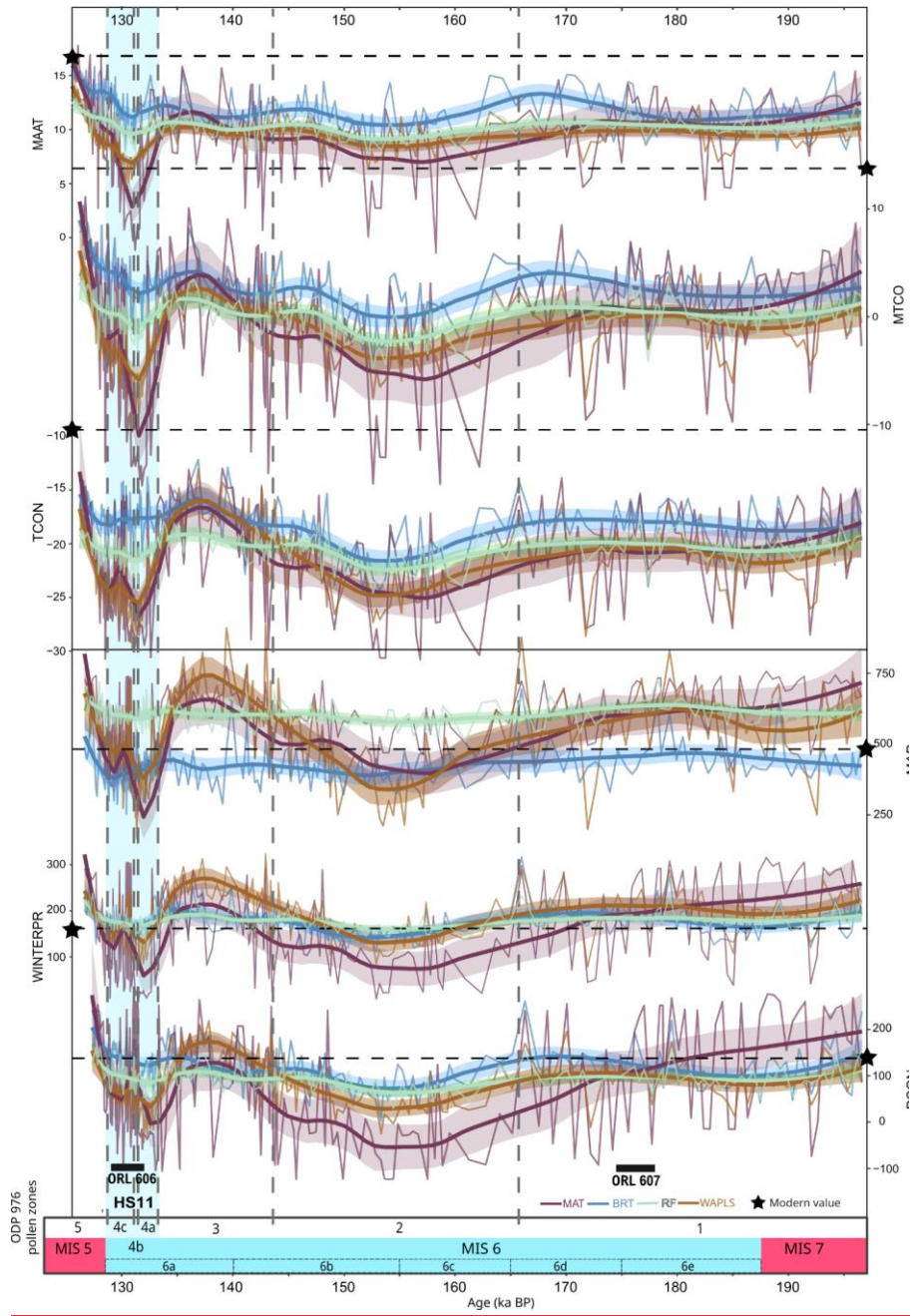
329 **Fig. 4. *Limacina retroversa* specimen found in sample B6H4 130-132** (identification: Jeanne Rampal personal communication, 2023). Photo: Dael Sassoon.

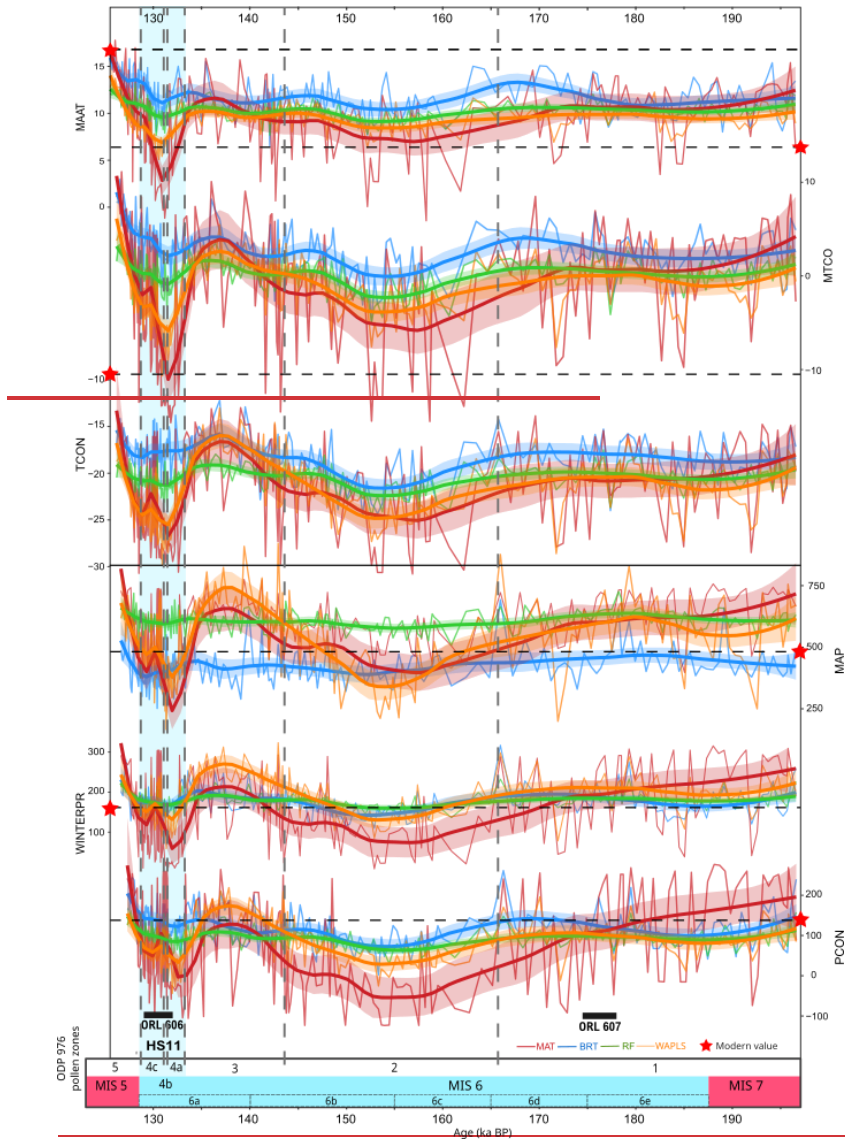
330 4.2. Pollen-inferred climate reconstructions

331 Results show significant temperatures and precipitation variations in connection with the  
332 glacial / interglacial cyclicality and shorter-term variability (Fig. 5, Table 2). The most reliable methods  
333 according to the two  $R^2$  and RMSE indicators are MAT and BRT, and the most accurately reconstructed  
334 parameters are MAAT and MTCO (Table 3). The four methods are in agreement for the general trends,  
335 although MAT shows the widest amplitude of variations, and RF has the smoothest curve.

336 Temperatures are lower than the present ~~all along during the complete~~ MIS 6 interval, except  
337 at the onset of MIS 5. A cooling trend is reconstructed during the final stage of MIS 7 (pollen zone 1,  
338 MIS 6e and 6d), while MTCO and the seasonal temperature contrast (TCO) are stable. The methods  
339 do not agree on the precipitation patterns during this phase, with MAT showing a trend toward aridity,  
340 decreasing WINTERPR and seasonal precipitation contrast (PCON), while the three other methods  
341 display a slight precipitation increase and stable PCON. From 166 ka BP onward (pollen zone 2, MIS 6c  
342 and 6b), both temperatures and precipitation decrease, and the seasonal contrast between winter and  
343 summer climate conditions reduced progressively. The MIS 6 minimum temperatures and precipitation  
344 are reconstructed in pollen zone 2 between around 150 and 160 ka BP, corresponding to the transition  
345 between MIS 6c and 6b. Subsequently, both temperatures and precipitation increase progressively in  
346 the late pollen zone 2 and early pollen zone 3 (MIS 6b to 6a). Between 140-135 ka BP (early MIS 6a),  
347 the four methods reconstruct temperatures similar to late MIS 7, a seasonal contrast close to the  
348 present, and precipitation higher than the present (except for BRT). This climate optimum is abruptly  
349 interrupted by the HS11 extreme arid event between ~134 and ~129 ka BP (pollen zone 4, late MIS 6a),  
350 during which temperatures, precipitation and seasonal contrasts are significantly reduced, reaching  
351 climate conditions similar to the MIS 6 glacial maxima ~155 ka BP. A short climate amelioration is  
352 evidenced at ~132 ka BP (pollen zone 4b), where precipitation and seasonal contrasts increase  
353 abruptly. Finally, after 130 ka BP the climate amelioration toward the MIS 5 interglacial conditions  
354 happens very fast (pollen zone 5).

355





356 **Fig. 5. Pollen-based climate reconstructions for MIS 6 interval from the ODP 976 record.** MAAT (Mean  
 357 Annual Temperature), MTCO (Mean Temperature of the Coldest Month), TCON (Temperature  
 358 Contrast, see methods), MAP (Mean Annual ~~Precipitations~~Precipitation), WINTERPR (Winter  
 359 ~~Precipitations~~Precipitation) and PCON (Precipitation contrast, see methods) for the four different  
 360 methods applied: MAT (Modern Analogue Technique), WA-PLS (Weighted Averaging Partial Least  
 361 Square), BRT (Boosted Regression Trees) and RF (Random Forest). The light-coloured interval  
 362 represents the 95% confidence window, and the bold curves the loess smoothed values (alpha = 0.25).  
 363 Modern values (see methods)- are indicated by the horizontal dashed line and the ~~red-black~~ star. Grey  
 364 vertical dashed lines separate the pollen zones defined by CONISS cluster analysis.

365

	BRT		MAT		WA-PLS		RF	
	R <sup>2</sup>	RMSE	R <sup>2</sup>	RMSE	R <sup>2</sup>	RMSE	R <sup>2</sup>	RMSE
MTCO	<b>0.87</b>	2.96	<b>0.88</b>	3.19	<b>0.71</b>	4.44	<b>0.77</b>	3.88
MAAT	0.83	2.31	0.83	2.48	0.66	3.22	0.69	3.00
SUMMERPR	0.77	44.86	0.82	46.61	0.52	66.87	0.65	56.48
MAP	0.77	148.52	0.79	163.70	0.50	225.68	0.66	182.32
MTWA	0.76	2.25	0.79	2.33	0.53	3.16	0.61	2.81
WINTERPR	0.69	60.69	0.72	65.81	0.43	82.58	0.59	69.34

a mis en forme : Police :Gras

a mis en forme : Police :Gras

a mis en forme : Police :Gras

a mis en forme : Police :Gras

366

367 **Table 3. R<sup>2</sup> (coefficient of determination) and RMSE (Root Mean Square Error) values for the different**  
 368 **climate parameters reconstructed with the four methods applied.** The lower the RMSE and the higher  
 369 the R<sup>2</sup> (in bold), the more reliable the reconstruction.

370

## 371 5. Discussion

### 372 5.1. Paleoenvironment of MIS 6 and Termination II in the western Mediterranean

373 Important changes are recorded during MIS 6, that are consistent with orbital-scale variability  
 374 during the different glacial substages ~~and with D-O like dynamics.~~

375 Three phases can be discerned. The early phase (pollen zone 1) spans late MIS 7, MIS 6e and  
 376 6d (~196-166 ka) and is characterized by high percentages of deciduous *Quercus*, *Cedrus* and  
 377 Cichorioideae, with marked variability and several abrupt semi-desert and steppe increases under cool  
 378 and humid climate conditions, with seasonal contrast similar to present-day. The middle phase (pollen  
 379 zone 2) extends from MIS 6c to late 6b (~165-143 ka), and displays the maximum expansion of steppe  
 380 and semi-desert taxa together with very low temperatures and precipitation between ~160 and ~150  
 381 ka BP, a chronology compatible with the maximum Drenthe ice advance (Ehlers et al., 2011). Finally,  
 382 the late phase (pollen zone 3), spanning late MIS 6b and 6a (~143-133 ka), is marked by a major  
 383 expansion of Ericaceae vegetation associated with higher reconstructed precipitation and winter  
 384 temperatures, as well as enhanced seasonal contrast during this phase.

385 Previous studies are consistent with a subdivision of MIS 6 is traditionally divided into three  
 386 phases characterized by different general trends and amplitude of millennial-scale oscillations  
 387 (Margari et al., 2014; Nehme et al., 2020). Margari et al. (2014) described an early phase between 185  
 388 and 160 ka BP, with warmer and wetter conditions and important rapid climate variability, a middle  
 389 transitional phase between 160 and 150 ka BP, and a late phase with stable glacial conditions between  
 390 150 and 135 ka BP. This three-phasing for MIS 6 glaciation matches our interpretation of ODP 976  
 391 pollen zones 1, 2 and 3.

392

393

394

395

396

397

398

399

400

401

402

403

404

405

406

407

408

409

410

411

412

413

414

415

416

417

418

419

420

421

422

423

424

The final phase of MIS 6 is characterized by important changes in vegetation and climate, indicating a rapid ~~reorganization~~modification of vegetation communities and atmospheric configuration at the transition between MIS 6 and MIS 5. Termination II (TII), defined as the period of fast reorganization of the climate system from full glacial (MIS 6) to full interglacial (MIS 5) conditions, is indeed characterized by extreme and fast internal dynamics including a major Heinrich Stadial, HS11 (Broecker & Henderson, 1998; Gouzy et al., 2004; Martrat et al., 2014; Moseley et al., 2015; Ovsepyan & Murdmaa, 2017). The ~~t~~Timing for TII has been estimated based on the initialisation and termination of Weak Asian Monsoon evidenced in the Dongge cave speleothems, lasting from ~136 to 129 ka BP (Bajo et al., 2020; Kelly et al., 2006; Menviel et al., 2019). These boundaries for TII give a total duration of about 7 ka. The timing of TII in the ODP 976 marine record is directly dependent on Dongge Cave chronology (see methods, section 3.1). Approximately the same duration is observed in the ~~Alboran~~ Sea-vegetation response to TII, but with ~1 ka delay; ~~the~~the imprint of HS11 on the vegetation in the Western Mediterranean region is indeed recorded here between 133.3 – 128.8 ka BP (pollen zone 4). This delay in marine and terrestrial proxies may reflect the vegetation response to the first cold pulse of HS11. ODP 976 provides for the first time a very detailed record of vegetation successions during this arid event (pollen zones 4a, 4b and 4c), in agreement with other SSTs and speleothem records that depict a three-phases or “~~double-UW~~” pattern for the event (see section ~~5.6~~.4). After the first rapid increase of steppe and semi-desert taxa (pollen zone 4a), the middle phase shows an abrupt decrease of steppe and semi-desert vegetation, and a fast increase of montane trees (mainly *Cedrus*) percentages (pollen zone 4b). Climate reconstructions reflect this event through a fast increase of both precipitation and temperatures. This pattern is fully compatible with the ODP 976 SSTs trend (Jiménez-Amat and Zahn, 2015; Martrat et al., 2014), although a delay of about 1 kyr is observed between the abrupt drop in alkenone-based SSTs at the onset of HS11 and the expansion of steppe and semi-desert vegetation. ~~In~~In the same way, the abrupt sea surface warming in the middle of HS11 (~133 ka BP) is shifted in the pollen record, to around 131.5 ka BP (pollen zone 4b).

## 5.2. ~~Atmospheric-Hydroclimate~~ connection with ORLs deposition during MIS 6

Pollen analyses help us to characterize the processes behind Organic Rich Layers (ORLs) deposition in this western Mediterranean region. Like sapropels, ~~they~~ORLs reveal important changes in the water stratification and circulation, with reduced bottom water ventilation and enhanced organic productivity in ~~straight~~direct connection with (i) increase in the freshwaters Atlantic inflow at times of deglaciation and (ii) enhanced rivers runoff regionally linked with increased precipitation (Murat, 1999; Pérez-Asensio et al., 2020; Rogerson et al., 2008). Although they are often considered as “ghost

a mis en forme : Espace Avant : 12 pt

a mis en forme : Non Surlignage

425 sapropels”, their timing and the mechanism behind them may differ from those of Eastern  
426 Mediterranean sapropels (Rogerson et al., 2008).

427 ORL bed 607 coincides with a period of enhanced precipitation around 176 ka reconstructed  
428 through our pollen-based approach (Fig. 7). Its basis appears almost synchronous with the onset of  
429 Sapropel S6 layer deposition in the Eastern Mediterranean (Emeis et al., 2003; Rohling et al., 2015;  
430 Savannah et al., 2024). Its duration also appears shorter than Sapropel S6, possibly indicating an  
431 interruption of favourable climate conditions in the Western Mediterranean region by a stadial event  
432 occurring around 172 ka BP and marked by an abrupt decrease in precipitation (Fig. 7).

433 ORL bed 606 was deposited during the second half of Termination II, at a time of deglaciation and  
434 directly following the first aridity pulse of HS11. Pollen-based reconstructions show enhanced  
435 precipitation and seasonal contrast during this time, suggesting intense precipitation together with  
436 deglacial freshwater input as combined causes for ORL deposition in the Western Mediterranean,  
437 which finds no counterpart in the Eastern Mediterranean. The implications of such organic layer  
438 deposition occurring at times of enhanced ~~precipitations~~precipitation or deglaciation will be further  
439 discussed in section 6.2.6.4.

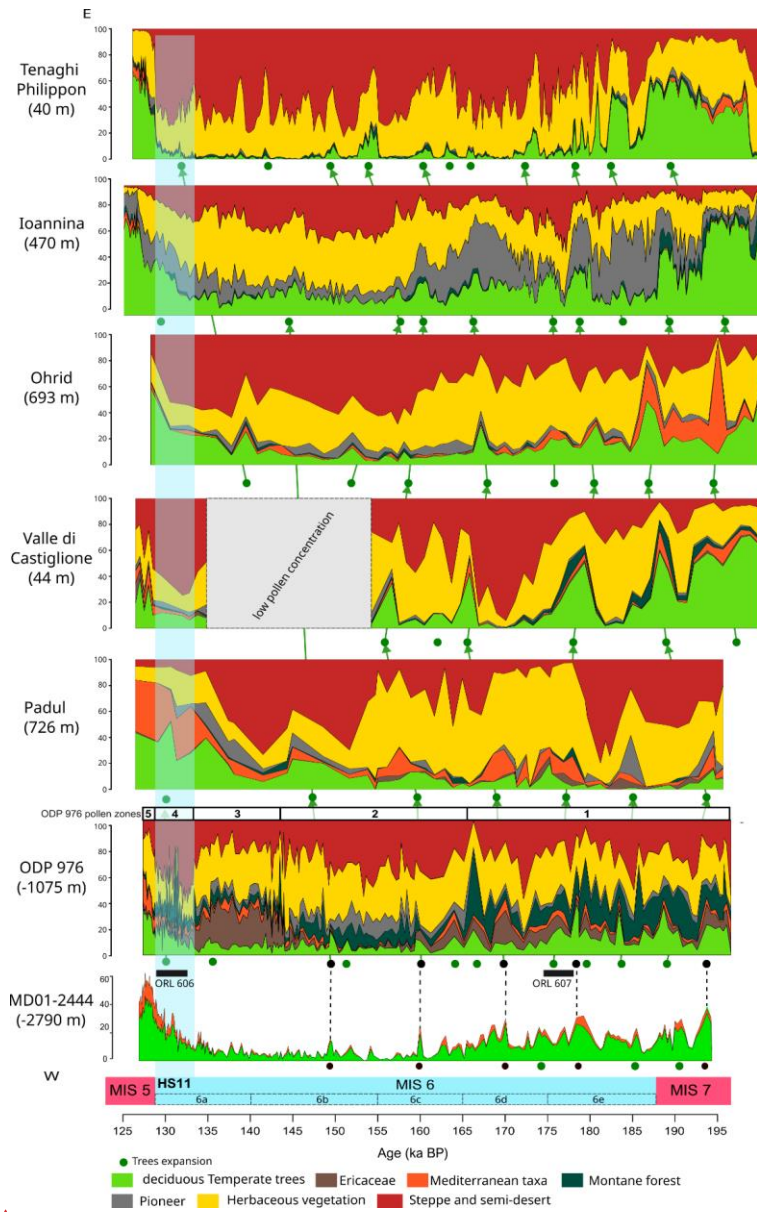
### 440 5.3. Mediterranean vegetation changes during the penultimate glaciation: a 441 synthesis

442 The ODP 976 pollen record documents MIS 6 vegetation changes in the Western  
443 Mediterranean with a temporal resolution comparable to the most detailed terrestrial palynological  
444 sequences from the Eastern Mediterranean (Tenaghi Philippon and Ioannina). ~~This~~A W-E transect of  
445 Mediterranean palynological records offers valuable insights on the spatial pattern of vegetation  
446 changes during the penultimate glaciation (Fig. 6).

447 At the MIS 7-6 transition, no abrupt decline of temperate forest is recorded in the ODP 976 and  
448 Padul records, in contrast with central and Eastern pollen records such as Tenaghi Philippon, Ioannina,  
449 Ohrid and Castiglione where the transition is very abrupt (Follieri et al., 1988; Koutsodendris et al.,  
450 2023; Roucoux et al., 2011; Sadori et al., 2016). ~~At these sites, a higher contrast has been described  
451 between interglacial periods with very high percentages of temperate deciduous forest taxa and glacial  
452 periods with very reduced tree cover (Tzedakis, 1993; Tzedakis et al., 2006). The western  
453 Mediterranean region, at the contrary, was generally characterized by a high proportion of herbaceous  
454 taxa, even during interglacial periods, attenuating the vegetation contrasts during transitions to glacial  
455 periods. This difference is probably linked with the lower percentages of deciduous forest in the  
456 Western Mediterranean region.~~

a mis en forme : Anglais (Royaume-Uni)

457           The first half of MIS 6 (~185-165 ka BP) is marked by relatively high percentages of arboreal  
458 pollen across all records, especially deciduous forest (Roucoux et al., 2011; Margari et al., 2010, 2014).  
459 The abundance of montane taxa (mainly *Cedrus*) is characteristic of ODP 976 record, and reflects the  
460 development of altitudinal trees on the Moroccan ~~Rif~~-mountains. Montane elements also increase  
461 during early MIS 6 at Valle di Castiglione, mainly represented by *Fagus* and *Abies* (Follieri et al., 1988),  
462 and at Ioannina, mainly represented by *Pinus* (Roucoux et al., 2011). No equivalent pattern is recorded  
463 in Padul where herbaceous vegetation is largely dominant. The scarcity of palynological data from the  
464 western Mediterranean, especially from North Africa, limits our understanding of the spatio-temporal  
465 significance of *Cedrus* expansions during MIS 6, and past glaciations in general.



a mis en forme : Anglais (Royaume-Uni)

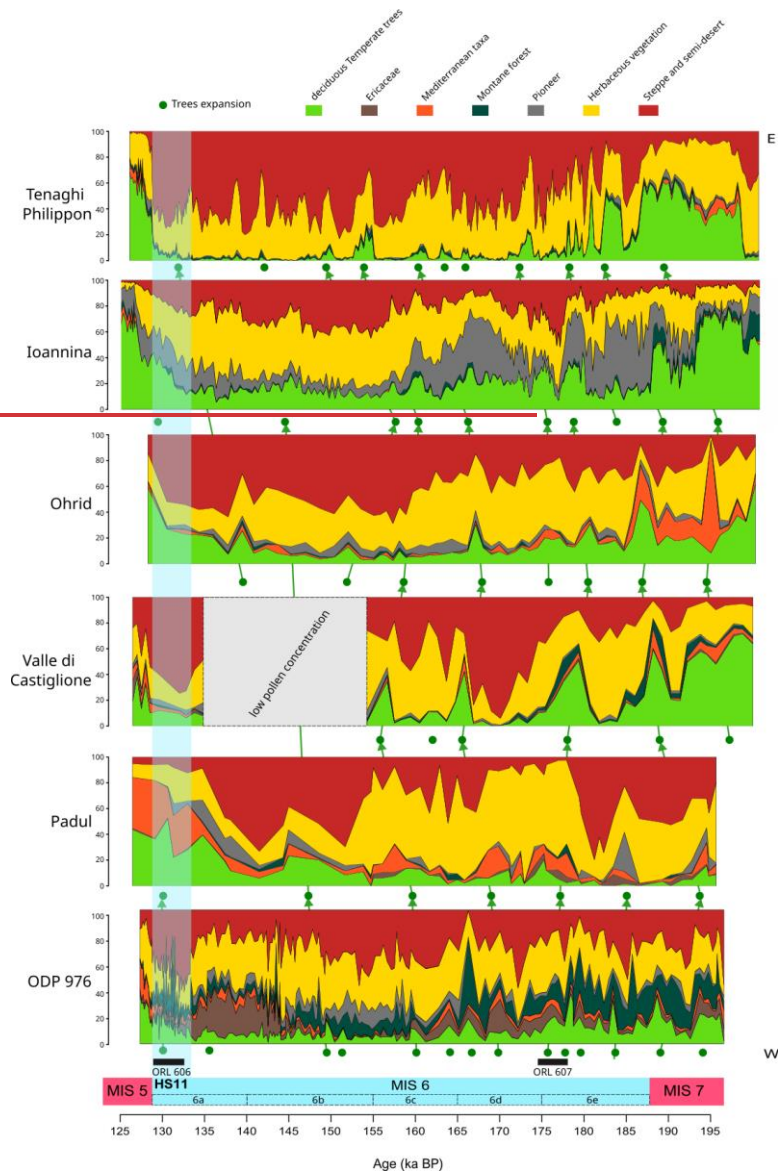


**Fig. 6. Synthesis of vegetation changes in the Mediterranean during MIS 6 based on available palynological sequences, from west (bottom) to east (top): MD01-2444 (Margari et al., 2010; Tzedakis et al., 2018), from east (top) to west (bottom): ODP 976 (this study), Padul (Camuera et al., 2019), Valle di Castiglione (Follieri et al., 1988), Ohrid (Sadori et al., 2016), Ioannina (Roucoux et al., 2011), Tenaghi Philippon (Koutsodendrīs et al., 2023).** Each synthetic pollen diagram is plotted according to its own age model. ODP 976 and Ioannina's chronologies are based on alignment with MD01-2444 temperate pollen curve on AICC2012 timescale. The ecological groups are the same as for ODP 976, except *Pinus* was included in pioneer vegetation at Ioannina, as it is the only record

Code de champ modifié

where *Pinus* is not over-represented. Green dots indicate temperate vegetation increases, with tentative correlations between records. The two Organic Rich Layers (ORLs) identified in the ODP 976 core (Murat, 1999), were placed at the bottom.

a mis en forme : Police :Italique

466 The main phase of steppe and semi-arid vegetation is recorded between ~165-145 ka BP in the  
467 Alboran Sea record, consistent with Ohrid and Ioannina pollen sequences (Fig. 6.6 Fig. 6). In Padul,  
468 however, the maximum expansion of steppe and semi-desert taxa occurs later, between ~155 and  
469 ~137 ka BP. This time window corresponds to the glacial maximum recorded at Azzano X (northern  
470 Italy) between 148 and 135 ka BP (Pini et al., 2009), and to a period of low pollen concentration at  
471 Valle di Castiglione, likely reflecting full glacial conditions. The ~10 ka lag in the vegetation glacial  
472 maxima between ODP 976 and Padul is probably the result of the low temporal resolution of the latter,  
473 in addition to differences in the age models used. However, the presence of pioneer vegetation and to  
474 a lesser extent of montane elements in Padul during the maximum glacial phase matches the ODP 976  
475 pattern in pollen zone 2, where Cupressoideae and *Cedrus* display high abundance.

476 A distinctive feature of the Western Mediterranean vegetation recorded during the final stage  
477 of MIS 6 (pollen zone 3) is the marked increase in Ericaceae observed in the ODP 976 record, and  
478 whereas Ericaceae are almost absent in the rest of the Mediterranean region. A similar expansion is  
479 observed in the Atlantic margin, where core MD01-2444 recorded patterns of Ericaceae expansion  
480 matching the three insolation minima during MIS 6 (Margari et al., 2014). Ericaceae development  
481 during minimal summer insolation is particularly favoured by reduced summer evaporation at times of  
482 low seasonal contrast in precipitation, as already noted in the Alboran Sea during the last glacial  
483 (Fletcher and Sánchez Goñi, 2008). Following the same interpretation, the expansion of heathland  
484 vegetation in the Iberian Peninsula as recorded in ODP 976 during the final stage of MIS 6 therefore  
485 marks may therefore mark the renewed influence of westerlies and Atlantic moisture preceding the  
486 onset of the transition to MIS 5 interglacial (Margari et al., 2014). Supporting this interpretation state,  
487 an increase in temperate deciduous forest at the end of MIS 6 is also seen in Padul, Ohrid and Ioannina  
488 records before the transition to MIS 5.

a mis en forme : Anglais (Royaume-Uni)

489 Despite some discrepancies due to the differences in age models and temporal resolutions, all  
490 records display comparable variations in temperate pollen percentages during the penultimate glacial.  
491 These variations support the persistent sensitivity of Mediterranean plant ecosystems to global-scale  
492 millennial climate variability during the penultimate glaciation, with modulation of the vegetation  
493 response depending on the local geography. Strong similarities can be observed between ODP 976 and  
494 Padul, despite the lower temporal resolution of Padul record. In both sequences, temperate pollen  
495 percentages reached ~25-30% of total pollen as a maximum during the rapid forest expansions events  
496 in the first half of MIS 6. This similarity supports the validity of the ODP 976 marine record to

497 reconstruct the SW Iberian Peninsula temperate forest history. However, ODP 976 sequence provides  
498 a more regional image of the vegetation, including higher percentages of Ericaceae pollen coming from  
499 the Atlantic coast, and *Cedrus* pollen from the Moroccan ~~Rif~~ mountains (Jiménez-Moreno et al., 2020),  
500 compared to Padul where percentages of Mediterranean taxa and hygrophyte herbaceous are higher  
501 due to the local nature of the signal (Camuera et al., 2019). Looking further east, Valle di Castiglione  
502 recorded various temperate trees expansions and contractions during the lower MIS 6, before the full  
503 glacial conditions. In the Italian Peninsula, various interstadials have also been identified further north  
504 at Azzano X (Pini et al., 2009). In the Balkans, Tenaghi Philippon shows the highest percentages of semi-  
505 desert and herbaceous vegetation ~~aeross-throughout~~ MIS 6, with more abrupt changes than all the  
506 other Mediterranean records, and more amplitude of the trees' contractions. This pattern was already  
507 described during the last climatic cycle and reflects the exacerbated vegetation dynamics locally, with  
508 episodes of rapid and enhanced colonization by tree vegetation ~~and probably linked with the lower~~  
509 ~~altitude of the site~~ (Koutsodendris et al., 2023; Tzedakis, 2005; Tzedakis et al., 2004). This has been  
510 mainly explained by the location of the site in a low altitudinal plain characterized by a more  
511 continental climate with lower winter precipitation: tree population at lower altitudinal location are  
512 closer to their ecological threshold in term of precipitation, and are likely to be very affected even by  
513 minimal changes in the amount of rainfall. On the contrary, the Ioannina record shows the highest  
514 deciduous forest percentages of all the records presented here, supporting its character as a local trees  
515 refugium (Roucoux et al., 2011).

a mis en forme : Anglais (Royaume-Uni)

516 Termination II displays a particular pattern in vegetation records from the Mediterranean  
517 region: while the expansion of trees and temperate vegetation is fast and continuous, HS11 represents  
518 at the same time a remarkable episode of abrupt steppe and semi-desert expansion. Although this  
519 event is visible in almost all the records, it is particularly prominent in ODP 976 record (pollen zone 4),  
520 and appears less pronounced in the eastern Mediterranean sequences. This observation is compatible  
521 with previous observations that Heinrich stadials during the last glacial had a minor impact on the  
522 eastern Mediterranean vegetation compared to the western Mediterranean, likely due to the already  
523 limited presence of tree vegetation in the eastern records during glacials (Tzedakis, 2005). A similar  
524 interpretation can be proposed for the differential response of eastern and western Mediterranean  
525 vegetation to HS11, supporting the major sensitivity of the southwestern Mediterranean vegetation  
526 to North Atlantic cold events. In Padul, no major expansion of xerophyte vegetation is detected, but a  
527 small decrease of temperate deciduous taxa was interpreted as the HS11 imprint (Camuera et al.,  
528 2019), and the signal might be hindered by the low resolution of the record. A pattern of fast arid  
529 vegetation increase contemporaneous to the temperate forest expansion is also found in central Italy

a mis en forme : Anglais (Royaume-Uni)

530 at Lago Grande di Monticchio, which was not presented in ~~Fig. 6-6~~Fig. 6 as its record does not extend  
531 beyond 132 ka BP (Allen and Huntley, 2009; Brauer et al., 2007).

532 ~~To sum up~~Finally, all palynological sequences reveal high-frequency oscillations of temperate  
533 and semi-desert pollen, compatible at first look with DO-like variability based on their duration and  
534 intensity with DO-like variability. They, and which are represent a particularly distinctive feature of the  
535 lower part of MIS 6.

#### 536 5.4. Rapid climate variability during MIS 6: a regional multiproxy comparison

537 In order to ~~disentangle-investigate~~ the character of rapid climate variability during MIS 6, a  
538 comparison with regional and global climatic archives is essential. The ~~events of increases in~~arboreal  
539 pollen ~~increase~~ observed in the ODP 976 record ~~are show percentages and timing consistent with~~  
540 comparable to those from the Portuguese margin core MD01-2444 (Margari et al., 2010, 2014;  
541 Tzedakis et al., 2018) (Fig. 7, m). However, the ODP 976 record generally presents lower ~~percentages~~  
542 values of temperate deciduous pollen percentages compared to the Atlantic record, due to its more  
543 ~~semiarid the~~Mediterranean influence as previously evidenced for the last glacial period (Charton et  
544 al., 2025; Fletcher et al., 2010b). To better capture temperate vegetation dynamics, we added  
545 Ericaceae, a clear marker of Atlantic influence in the ODP 976 record, to the deciduous temperate  
546 forest, to obtain a “total temperate pollen sum” which enhances the main warming peaks and  
547 strengthens the correlation between the two marine cores on both sides of Gibraltar Strait (Fig. 7, m  
548 and l). ~~Another striking correlation appears between the~~The ODP 976 pollen-inferred climate  
549 reconstructions ~~show generally consistent patterns with~~ the SSTs trends based on alkenones (Martrat  
550 et al., 2004, 2007), and the southern Iberian humidity recorded in the speleothem from data from  
551 Cueva Gitana (Hodge et al., 2008) (Fig. 7, e and g). The ODP 976 pollen and climate record therefore  
552 appears to reflect well regional variations in both temperature and humidity across MIS 6.

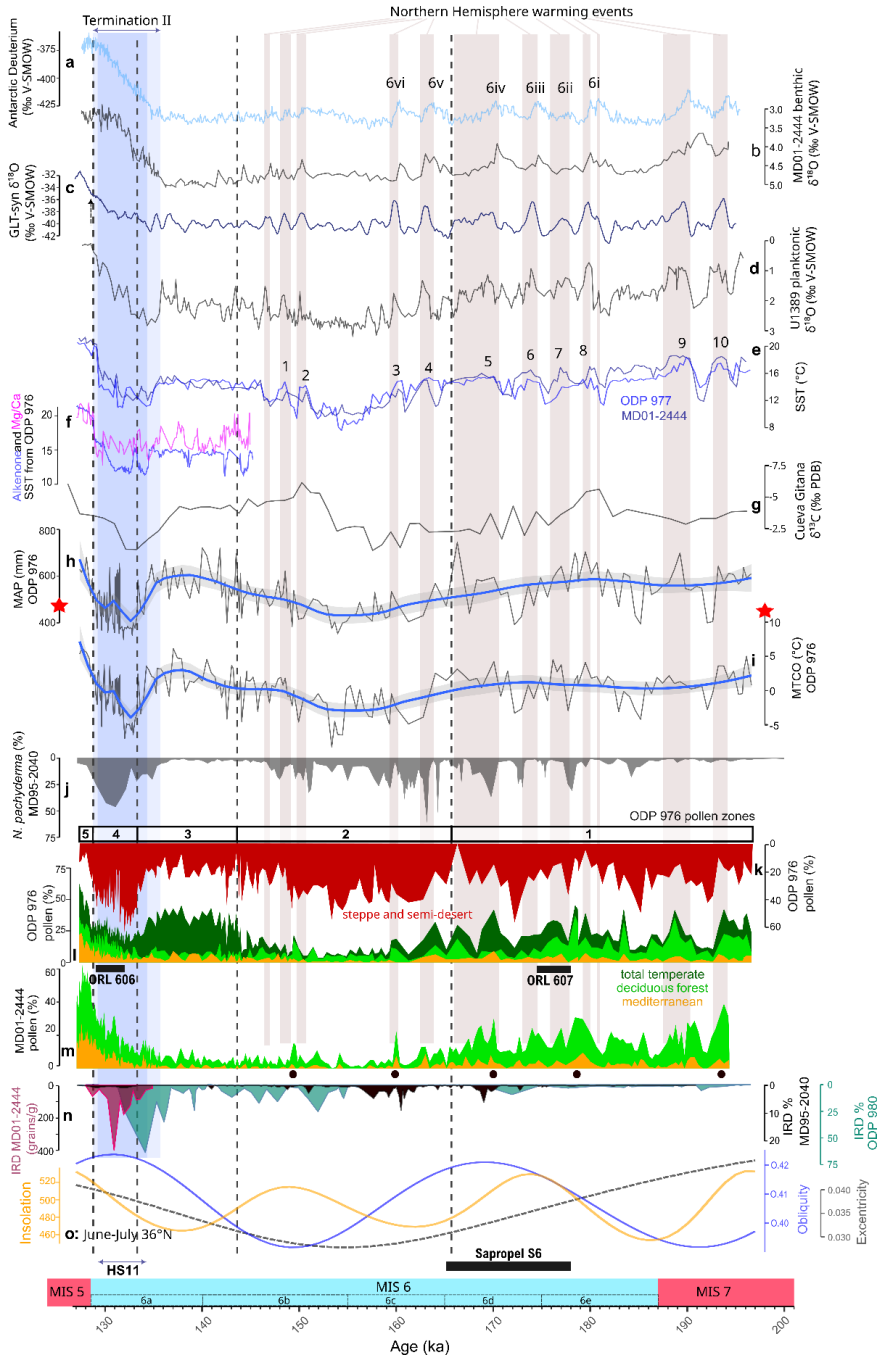
553 Warm events in the northern hemisphere are generally well-correlated to peaks in the ODP  
554 976 temperate pollen curve (Fig. 7, c and l). An active bipolar seesaw dynamics was described during  
555 the penultimate glacial Davtian & Bard, 2023; EPICA Community Members, 2006; Stocker, 1998), and  
556 the Antarctic record was used to elaborate the Greenland GL<sub>T</sub>-syn (Greenland temperature synthetic)  
557 curve showing predicted  $\delta^{18}\text{O}$  ~~D-O~~millennial-scale events for the past glacial eight climatic cycles,  
558 which are not directly recorded in Greenland ice (Barker et al., 2011; Bazin et al., 2013; Jouzel et al.,  
559 2007). Six Antarctic Isotopic maxima (AIM) events were recognized on the Deuterium curve during MIS  
560 6 (6i to 6vi), correlated with increases in CO<sub>2</sub> concentrations and benthic isotope minima in the North  
561 Atlantic (Barker et al., 2011; Hodell et al., 2023; Margari et al., 2010, 2014; Shin et al., 2020) (Fig. 7, a-  
562 c). These AIM and benthic minima in the Atlantic are not easily correlated with steppe expansions in

a mis en forme : Anglais (Royaume-Uni)

563 the ODP 976 record, indicating a limited response of vegetation in the Western Mediterranean to the  
564 Antarctic warm events.

565 Barker et al. (2011) predicted the occurrence of eleven ~~millennial-scale warming events~~  
566 ~~events~~ during MIS 6 (Fig. 7, c), while nine interstadials were recognized in the Alboran Sea from the  
567 alkenone record (Fig. 7, e), (Martrat et al., 2004, 2007). In the loess record of Harletz in central Europe,  
568 ten interstadials were described (Rousseau et al., 2020), strongly matching the Chinese speleothems  
569 records of stadial and interstadial events related to the Asian Monsoon dynamics (Cheng et al., 2006;  
570 Li et al., 2014; Wang et al., 2018; Wang et al., 2001; Xue et al., 2019). The global nature of fast climate  
571 oscillations in the northern hemisphere thus appears controlled by the coupled influence of Atlantic  
572 cold events, and tropical monsoon variations as evidenced by the eastern Mediterranean speleothems  
573 records from Sofular, Soreq and Kanaan caves (Ayalon et al., 2002; Held et al., 2024; Matthews et al.,  
574 2021; Nehme et al., 2018).

575



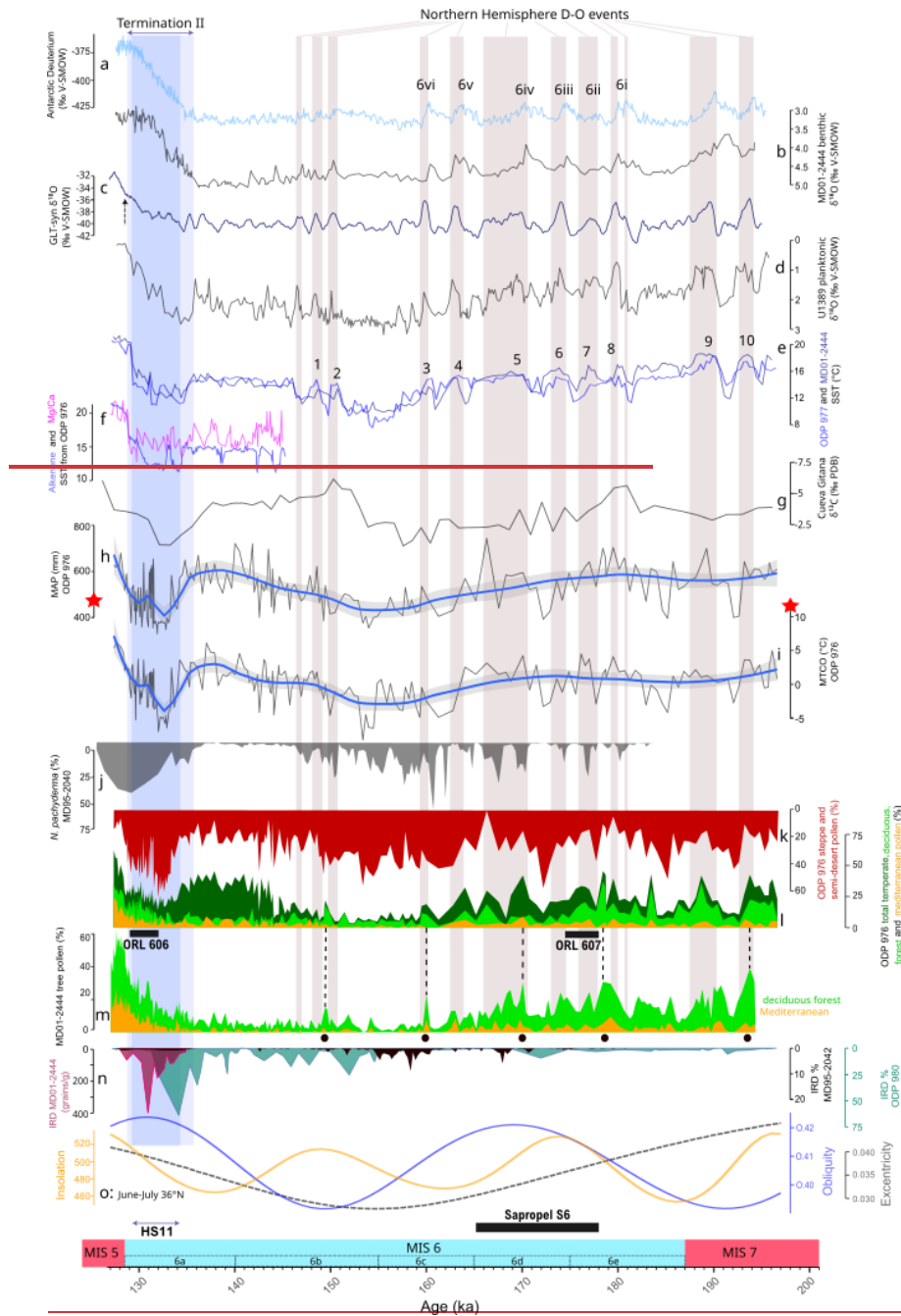


**Fig. 7. Millennial climate changes during MIS 6.** a) Antarctic Dome C  $\delta D$  (Bazin et al., 2013; Jouzel et al., 2007); b) Benthic  $\delta^{18}O$  from MD01-2444 (Margari et al., 2010); c) Greenland synthetic  $\delta^{18}O$

Code de champ modifié

(Barker et al., 2011); **d**) Planktonic  $\delta^{18}\text{O}$  from U1389 (Sierra & Andersen, 2022); **e**) alkenone-based SST from ODP 977 (darker blue) and MD01-2444 (lighter blue) (Martrat et al., 2004, 2007); **f**) Alkenone-based SST (Martrat et al., 2014) and Mg/Ca-based SST (Jiménez-Amat and Zahn, 2015) from ODP 976; **g**)  $\delta^{13}\text{C}$  from Cueva Gitana (Hodge et al., 2008); **h**) Mean Annual Precipitation (MAP) reconstructed from ODP 976 pollen assemblage, mean of the four methods used in this study (MAT, WA-PLS, RF, BRT), with the red star showing the modern value; **i**) Mean Temperature of the Coldest Month (MTCO) reconstructed from ODP 976 pollen assemblage, mean of the four methods used in this study (MAT, WA-PLS, RF, BRT), with the red star showing the modern value; **j**) *N. pachyderma* percentages from MD95-2040 (de Abreu et al., 2003; Voelker & de Abreu, 2011); **k**) ODP 976 pollen percentages of semi-desert and steppe taxa, with ODP 976 pollen zones (this study); **l**) ODP 976 pollen percentages of total temperate taxa including temperate deciduous forest + Ericaceae + Mediterranean (dark green), deciduous forest (light green), Mediterranean (orange) (this study); **m**) MD01-2444 pollen percentages of temperate tree (light green) and Mediterranean (orange) taxa (Margari et al., 2010; Tzedakis et al., 2018); **n**) Ice-Rafted Debris (IRD) percentages from MD01-2444, 37° N (pink) (Skinner & Shackleton, 2006) redrawn from Tzedakis et al. (2018), MD95-2040 (red/black), 40°N (de Abreu et al., 2003) and ODP 980 (blue), 55°N (McManus et al., 1999; Oppo et al., 2001, 2006); **o**) orbital parameters (Laskar et al., 2004) calculated for June-July at 36°N: Eccentricity (black), Obliquity (blue) and Insolation (yellow). The black rectangle indicates the interval of deposition of Sapropel layer S6 in the eastern Mediterranean (Ziegler et al., 2010). The marine substages MIS 6a-e follow (Railsback et al., 2015). All data are plotted on AICC2012 chronology (Bazin et al., 2013) following Sierra et al. (2020, 2022), except for the IRD records and Gitana Cave which is plotted on its own age model based on U-series absolute dating. The vertical grey bars indicate the Northern Atlantic interstadial events based on the planktonic isotope record and the predicted millennial-scale warming  $\delta^{18}\text{O}$ -events from Greenland synthetic record, with the numbers of the Alboran interstadials (AI-1 to AI-10) from Martrat et al. (2004, 2007). Numbers 6i-6vi correspond to the Antarctic Isotope Maxima (AIM) from Margari et al. (2010). The vertical blue bar represents Heinrich Stadial 11 (HS11). Black dots and dotted lines show the five temperate pollen peaks in MD01-2444 used as control points for ODP 976 chronology.

MIS 6 is traditionally divided into three phases characterized by different general trends and amplitude of millennial scale oscillations (Margari et al., 2014; Nehme et al., 2020). Margari et al. (2014) described an early phase between 185 and 160 ka BP, with warmer and wetter conditions and important rapid climate variability, a middle transitional phase between 160 and 150 ka BP, and a late phase with stable glacial conditions between 150 and 135 ka BP. This three phasing for MIS 6 glaciation matches our interpretation of ODP 976 pollen zones 1, 2 and 3.

The three phases identified during MIS 6 based on the ODP 976 vegetation and climate record can be compared with regional and global records to be interpreted in a broader context, based on general climatic trends and the expression of climatic instability;

Early MIS 6 (187-166 ka BP): warm/wet conditions and instability. The first phase encompasses the two substages MIS 6e and 6d, and is characterized by humid and rather warm climate conditions in the Mediterranean at the transition from MIS 7 to MIS 6. This phase aligns well with the deposition of ORL bed 607 in the Alboran Sea, and the sapropel layer S6 in the Eastern Mediterranean, associated with the maximum summer insolation and increased intensification of the summer monsoonal system

a mis en forme : Non souligné

a mis en forme : Non souligné

a mis en forme : Non souligné

591 in the eastern Mediterranean between 178.5 to 165.5 ka (Emeis et al., 2003; Rohling et al., 2015;  
592 Ziegler et al., 2010). At the same time of S6 deposition, Cheddadi and Rossignol-Strick (1995) described  
593 an increase in temperate pollen in the Nile region, and Soreq cave speleothem records climatic  
594 conditions typical of an interglacial (Ayalon et al., 2002). Sapropel depositions usually occur during  
595 interglacial periods as MIS 1 (Holocene), which makes sapropel S6 an exceptional feature of early MIS  
596 6. It reflects particularly warm and humid conditions, and intense freshwater input in the  
597 Mediterranean which can result from various sources, including increased rainfall and monsoon  
598 activity, Atlantic freshwater entrance, and enhanced river discharges (Sierra & Andersen, 2022). The  
599 long speleothem records in China report a period of northern shift of the Intertropical Convergence  
600 Zone associated with enhanced Asian Monsoon activity during this phase (Wang et al., 2018). Higher  
601 pluviometry is also supported by foraminifera isotopic and SSTs signal throughout the Mediterranean  
602 Sea, which were used to reconstruct past salinity and freshwater budget regionally (Kallel et al., 2000).  
603 Enhanced rainfall in the Balkans is evidenced by the Ioannina lake deepening (Wilson et al., 2021), and  
604 a more humid period is documented in speleothem records from Argentarola cave in Italy (Bard et al.,  
605 2002) and Gitana cave in southern Spain (Hodge et al., 2008) (Fig. 7, g). Therefore, humid conditions  
606 during this phase were not restricted to the eastern Mediterranean where the sapropel deposition  
607 occurred. ODP 976 organic layer 607 together with the pollen-based climate reconstructions support  
608 this view, with enhanced seasonal precipitation contrast during this interval driven by enhanced winter  
609 precipitationsprecipitation (Fig. 5). Comparison with Padul pollen-based hydroclimate reconstructions  
610 (Camuera et al., 2022) further strengthens this scenario: despite the chronological delay between the  
611 two sequences, this early MIS 6 humid phase and ORL deposition likely matches the Western  
612 Mediterranean Humid Period (WMHP 6) dated between 180-155 ka BP (Fig. 8). The same study made  
613 the case for a co-occurrence of humid periods in the Western Mediterranean and in West Africa  
614 (African Humid Periods) during periods of high precipitationsprecipitation seasonality and enhanced  
615 West African Monsoon. Pollen-inferred climate reconstructions from lake Ohrid have also shown the  
616 phase relationship between African Monsoons and periods of high winter precipitationsprecipitation  
617 in the Mediterranean region (Wagner et al., 2019; Sinopoli et al., 2019).

618 Another characteristic of this early MIS 6 phase is the strong variations in pollen and isotopic  
619 curves in the Atlantic and Western Mediterranean (Fig. 7, a-d and l-m). Variations in temperate  
620 deciduous and Ericaceae percentages are observed in the ODP 976 record, in close correspondence  
621 with the Atlantic record from MD01-2444. The largest interstadial peak in ODP 976 around 179 ka BP  
622 is also identified in all the different records and marked by warmer conditions in the sea, and more  
623 effective precipitationsprecipitation in SE Iberia (Hodge et al., 2008). It is well correlated with the  
624 stadial following Antarctic event 6i (Margari et al., 2010), the associated predicted millennial-scale

625 ~~warming D-O~~ event in Greenland synthetic curve, and the Alboran Sea SST interstadial event 8 (Martrat  
626 et al., 2004). In Padul record, the temperate deciduous, Mediterranean and *Abies* percentages increase  
627 correlates well with this event (Camuera et al., 2019). It could also match the WMHP 6.1 interstadial  
628 (Camuera et al., 2022) (Fig. 8). This large interstadial was suggested to be at the origin of the  
629 initialisation of the sapropel S6 deposition (Sierro & Andersen, 2022), and could also have participated  
630 in the initialization of ORL 607 deposition in the Alboran Sea (Murat, 1999). On the other hand, the  
631 most important tree population decline and semi-desert expansion in ODP 976 is recorded at ~172 ka  
632 BP, which could match Antarctic event 6iv, and is associated to a moderate increase of IRD deposition  
633 at the latitude of ODP 980 (Fig. 7, n). A similar stadial can be observed in the Ioannina and Tenaghi  
634 Philippon records with a close chronology (Roucoux et al., 2011) (Fig. 6). Dry conditions at this time are  
635 also recorded in the eastern Mediterranean as shown in the Pentadactylos and Soreq speleothems  
636 (Ayalon et al., 2002; Nehme et al., 2018).



**Fig. 8. Comparison between the precipitation pattern reconstructed from ODP 976 with our multi-method approach (mean) (this study) and from Padul with only the WA-PLS method (Camuera et al., 2022).** Mean Annual Precipitation (MAP) and Winter Precipitation (WINTERPR) are represented, together with the two Organic Rich Layers (ORLs) identified in ODP 976 (Murat, 1999) and the Western Mediterranean Humid Period (WMHP) 6 defined by Camuera et al. (2022). Red arrows indicate tentative correlation between the two phases of WMHP 6, and the precipitation reconstructions from ODP 976. Red stars and dashed lines indicate the modern climate value (see methods).

637 Middle MIS 6 (165-144 ka BP): maximum glacial conditions and stability. This phase is marked  
638 by the maximum expansion of semi-desert vegetation and the almost complete collapse of forest  
639 vegetation between ~163 and 150 ka BP, according to the ODP 976 pollen and MD01-2444 records,  
640 synchronous with the minimum in orbital eccentricity. This is in agreement with the lowest SSTs values  
641 reconstructed in the Alboran Sea from the alkenone record occurring around 155 ka BP, and low SSTs  
642 in the Gulf of Lions too (Cortina et al., 2015). At the same time, high percentages of the cold species *N.*  
643 *pachyderma*, together with important ice-detritus pulses, are recorded on the Portuguese margin (de  
644 Abreu et al., 2003; Voelker & de Abreu, 2011), (Fig. 7, j and n). The occurrence of the cold Atlantic  
645 species *Limacina retroversa* shells in the ODP 976 sediments at ~155 ka BP is consistent with the  
646 enhanced entrance of cold subpolar water masses in the Alboran sea at the time of full glacial  
647 conditions. In parallel, there is an intensification of "Fleuve Manche" paleo river discharges evidenced  
648 in various sedimentary cores from the Bay of Biscay (Boswell et al., 2019; Eynaud et al., 2007; Penaud  
649 et al., 2009, 2016; Toucanne et al., 2009), and a fluvial aggradation linked with reduced vegetation  
650 cover in Spanish river basins (Macklin et al., 2002). A long-term aridification is recorded in SE Spain in  
651 Gitana cave close to the ODP 976 location (Hodge et al., 2008). The glacial maximum in Soreq cave  
652 speleothem is also recorded around 154 ka BP (Bard et al., 2002), and might be responsible for the  
653 hiatus in the Pentadactylos speleothem in Cyprus (Nehme et al., 2020). In Italy, the Tana che Urla cave  
654 also recorded cooling and aridification between 159-132 ka BP, indicated by both the carbon and  
655 oxygen isotopic ratio (Regattieri et al., 2014). The coolest phase in Abaliget Cave speleothem in central  
656 Europe is also recorded at that time (Koltai et al., 2017). Climate conditions reconstructed at ODP 976  
657 site during this phase show the maximum aridity and cold temperatures, which are consistent and fall  
658 within the range of reconstructed temperatures and ~~precipitations~~precipitation at the same time at  
659 Ohrid (Sinopoli et al., 2019). This main phase of glaciation in Europe took place after 163 ka BP,  
660 corresponding to the Drenthe glacial advance (Ehlers et al., 2018; Margari et al., 2014). The maximum  
661 ice expansion probably led to the almost complete collapse of temperate vegetation across the  
662 Mediterranean region, except in specific climate refugia's like Ioannina or Padul (Fig. 6-6Fig. 6). The  
663 Mediterranean vegetation taxa were particularly affected and almost disappeared at this time in the  
664 ODP 976 record.

Code de champ modifié

a mis en forme : Français (France)

a mis en forme : Français (France)

665 Few interstadial events are observed during this cold and dry phase, probably due to the  
666 extended ice volume reaching a critical threshold (McManus et al., 1999) and leading to higher climate  
667 stability at time of glacial maximum expansion (Sierro and Andersen, 2022). One moderate interstadial  
668 event around 150 ka BP is expressed in the ODP 976 and MD01-2444 records through an increase in  
669 temperate deciduous tree taxa (Fig. 7, l and m). It may correspond to the interstadial recognized in  
670 Gitana Cave speleothem approximately at the same time, and is compatible with the Alboran  
671 Interstadial events 1 or 2 (Martrat et al., 2004), while a larger trees increase in Padul record is also  
672 observed (Camuera et al., 2019) (Fig. 6). It is also compatible with interstadials recognized in other  
673 speleothem records in eastern and central Mediterranean (Ayalon et al., 2002; Bard et al., 2002;  
674 Regattieri et al., 2014). Sierro et al. (2022) described a major event of low Mediterranean overturning  
675 and high freshwater entrance through the Gibraltar Strait at that time and contemporaneous to the  
676 insolation maximum (Fig. 7, o). This configuration was similar to the one contemporaneous to sapropel  
677 S6 and ORL 607 deposition during early MIS 6, but did not lead to any new sapropel deposition at 150  
678 ka BP, probably because the climate conditions were more favourable but not enough for a sapropel  
679 deposition.

680 Late MIS 6 (144-129 ka BP): increased precipitation during the last glacial, and arid conditions  
681 during Heinrich Stadial 1+HS11. Between 150 and 140 ka BP, warmer and wetter conditions are  
682 indicated by ODP 976 pollen percentages of Ericaceae (pollen zone 3). Ericaceae expansions in the  
683 Iberian margin sediments were found to be associated to insolation minima in core MD01-2444  
684 (Margari et al., 2014). This pattern is consistent with the ODP 976 Ericaceae curve (Fig. 6-7 Fig. 7, j). The  
685 climate reconstructions evidenced high ~~precipitations~~precipitation and especially high WINTERPR  
686 values. These higher humidity and temperature values are supported by the carbon isotope record  
687 from Gitana Cave (Hodge et al., 2008) and the Alboran Sea SSTs (Martrat et al., 2007) (Fig. 7, e-g). In  
688 central Europe, Abaliget Cave speleothem also shows more favourable climate conditions during this  
689 phase (Koltai et al., 2017). Climatic oscillations appear subdued in the Western Mediterranean pollen  
690 records during this last phase. The high resolution ODP 976 record shows some SST variations  
691 (Jiménez-Amat and Zahn, 2015; Martrat et al., 2014) : Ericaceae pollen contractions and semi-desert  
692 elements expansions could be correlated to three abrupt drops in alkenone-based SSTs at 144, 142,  
693 and 139 ka BP (Fig. 6-7 Fig. 7, f, k and l). Fifteen Chinese Interstadials (CIS) were identified at Hulu Cave  
694 during late MIS 6, linked with Asian Monsoon dynamics (Q-Wang et al., 2018), and the ultra-high-  
695 resolution record of planktonic isotope ratio at U1389 by Sierro and Andersen (2022) also expresses  
696 some variability. However, the vegetation response in the SW Mediterranean was apparently limited.

697 Following the Ericaceae expansion, the most prominent feature of the late MIS 6 phase is the  
698 large and fast expansion of steppe and semi-desert vegetation during HS11, between 133 and 129 ka

a mis en forme : Anglais (Royaume-Uni)

Code de champ modifié

699 BP (pollen zone 4). It is characterized by a first large IRD peak at high latitude (ODP 980) around 134 ka  
700 BP, and later at the MD01-2444 latitude, around 131 ka BP (Skinner & Shackleton, 2006; Tzedakis et  
701 al., 2018). This event also corresponds to an increase in the oxygen isotopic ratio at the Portuguese  
702 margin (especially planktonic, starting around 136 ka BP), also broadly synchronous to an important  
703 decrease in SSTs of the Atlantic and the Mediterranean Sea (Jiménez-Amat and Zahn, 2015; Martrat et  
704 al., 2004, 2007, 2014). A pronounced increase in *N. pachyderma* (sinistral) abundance is also recorded  
705 on the Portuguese margin (Voelker & de Abreu, 2011). Climate reconstructions show particularly harsh  
706 conditions in the Western Mediterranean region during this event, compatible with the  
707 reconstructions from Lake Ohrid (Sinopoli et al., 2019) and from three French sites (Les Echets, la  
708 Grande Pile and Le Bouchet) for the latest phase of MIS 6 (Guiot et al., 1989, 1993). An arid phase is  
709 also evidenced at Gitana Cave (Hodge et al., 2008), which closely matches the trend of the ODP 976  
710 precipitation curve (Fig. 8). Aridity is evidenced in other speleothem records in Europe like Villars  
711 (Wainer et al., 2011), Sieben in the Alps (Moseley et al., 2015), and Abaliget cave in central Europe  
712 (Koltai et al., 2017). Dryness over western Europe is also supported by an episode of intense loess  
713 deposition in Rodderberg crater in northern Germany between 136-129 ka BP (Zhang et al., 2024). If  
714 HS11 is also recorded in China speleothems (Wang et al., 2018), it appears subdued in the eastern  
715 palynological Mediterranean records (Fig. 6), indicating that the Western Mediterranean region was  
716 more severely impacted by the dry and cold pulse of HS11. The “double u” shape of HS11 described in  
717 section 5.1 for the ODP 976 record matches well the Hulu cave record, where the particular event in  
718 the middle of HS11 was linked with a strong Asian Monsoon episode that could represent an analogue  
719 to the Bølling-Allerød during Termination I (Wang et al., 2018). The fast and multiphase vegetation and  
720 climate dynamics evidenced in the ODP 976 record is in agreement with the description of a “HS11  
721 complex” with multiple phases (Tzedakis et al., 2018), and will require more focused attention in the  
722 future.

723 HS11 has been described as a “pause” in the glacial termination II (Gouzy et al., 2004; Hodge  
724 et al., 2008). However, in the ODP 976 and MD01-2444 records, temperate vegetation keeps increasing  
725 all along the event, despite the supposed cessation of the warming and moistening trend for almost  
726 2000 years. Therefore, the trend toward increased temperate vegetation during Termination II did not  
727 seem to be strongly affected by the abrupt arid event, following the continuous climate amelioration  
728 described in various speleothem records from Italy covering Termination II, at Corchia cave, Tana che  
729 Urla and Argentarola (Bard et al., 2002; Drysdale et al., 2005; Regattieri et al., 2014). On the contrary,  
730 the Gitana Cave speleothem records a strong moisture deficit (Fig. 7, g), supporting a stronger impact  
731 of HS11 in the SW Mediterranean compared to the Italian Peninsula.

a mis en forme : Anglais (Royaume-Uni)

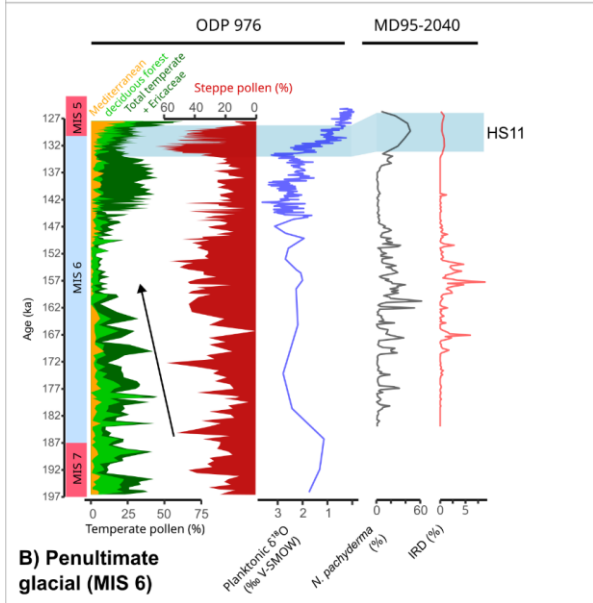
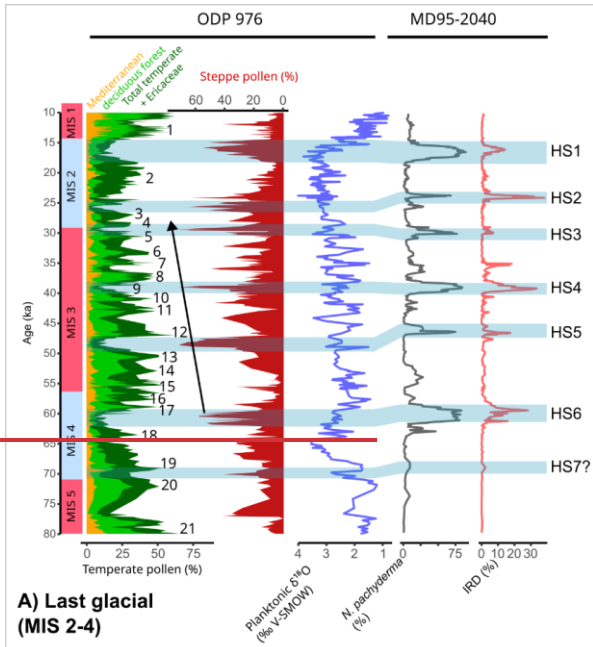
a mis en forme : Polonais

a mis en forme : Anglais (Royaume-Uni)

732 Finally, it is to be pointed out that HS12, occurring around 140 ka BP (Lisiecki & Stern, 2016),  
733 apparently did not have any imprint on the vegetation record of ODP 976, implying a subdued impact  
734 of this event on Mediterranean vegetation compared to HS11.

#### 735 5.5. Comparison of MIS 6 with the last glacial period (MIS 4-2)

736 Various studies have pointed out strong similarities between the millennial-scale oscillations  
737 of the last glacial period and the penultimate glacial period, with the division between MIS 3 and MIS  
738 2 being analogous to the early and mid-late phase of MIS 6 respectively (Held et al., 2024; Margari et  
739 al., 2010, 2014; Roucoux et al., 2011; Rousseau et al., 2020; Shin et al., 2020; Sierro et al., 2020). The  
740 same studies argued in favour of pervasive impact of stadial events on the continental climate and  
741 vegetation in the Mediterranean region, even in absence of typical Heinrich layers (Roucoux et al.,  
742 2011). The ODP 976 record shows a cooling and aridification trend during the first half of MIS 6 (Fig.  
743 9), with decreasing intensity of interstadials events, that recalls the pattern of MIS 3 D-O cycles (Bond  
744 et al., 1993).



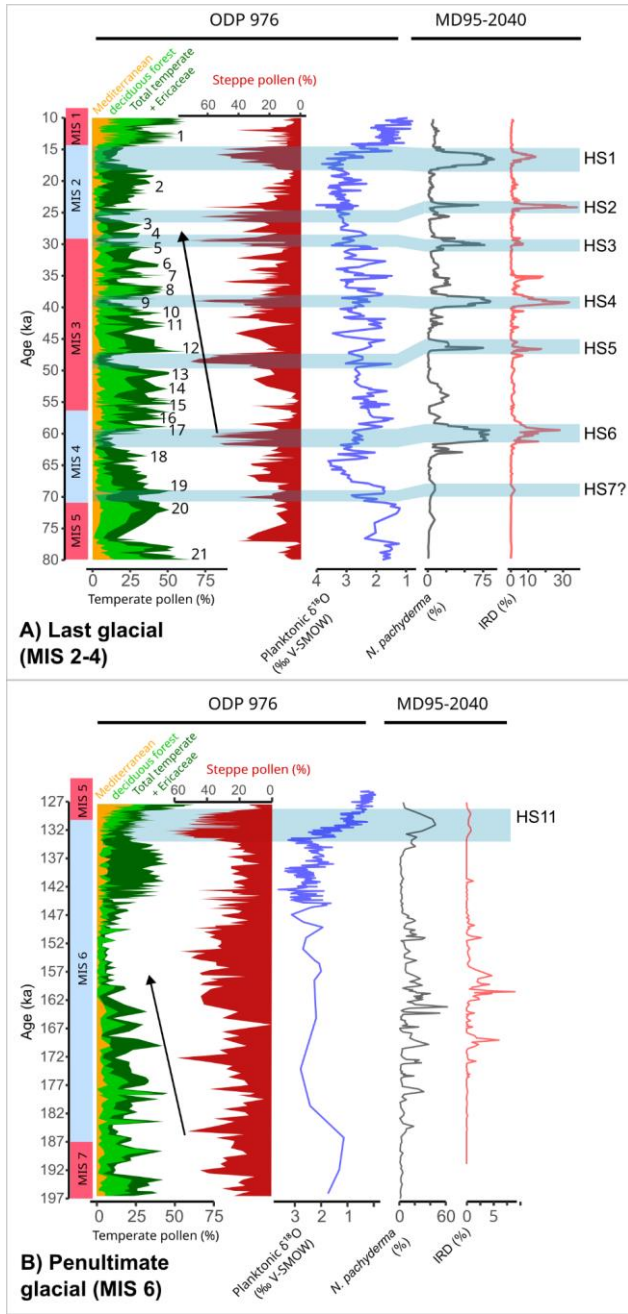


**Fig. 9.** Comparison of millennial changes during **A) the last glacial (MIS 2-4)** and **B) the penultimate glacial (MIS 6)**, including the main pollen data from ODP 976 (Charton et al., 2025; Combourieu-Nebout et al., 2002, 2009, and unpublished data for the last climatic cycle, and this study for MIS 6),

the ODP 976 planktonic isotopic ratio from *G. bulloides* (Combourieu-Nebout et al., 2002; Jiménez-Amat & Zahn, 2015; von Grafenstein et al., 1999, and unpublished data), and the *N. pachyderma* and IRD record from core MD95-2040 (de Abreu et al., 2003; Voelker and de Abreu, 2011). Marine Isotope Stages follow the boundaries from Lisiecki & Raymo (2005). Numbers on the Last Glacial correspond to the Greenland D-O events chronology (Fletcher et al., 2010a; Rasmussen et al., 2014). Black arrows mark the aridification trend and decreasing interstadials intensity during MIS 3 and early MIS 6.

a mis en forme : Anglais (Royaume-Uni)

745

746 However, the absence of clear successions of stadial events and especially Heinrich stadials,  
747 together with the more subdued expression of interstadials in the vegetation record, limits the  
748 resemblance between the two glacial periods. The pacing of interstadial peaks also seems to be  
749 reduced compared to the last glacial period high-frequency oscillations, as previously highlighted from  
750 the high-resolution speleothem record from Sofular cave in Turkey (Held et al., 2024).

751 A comparison of millennial-scale changes during the past two glacial periods based on the ODP  
752 976 and MD95-2040 records, on either side of the Gibraltar Strait, supports our view (Fig. 9). The last  
753 glacial period (encompassing MIS 4 to MIS 2) was characterized in the Alboran Sea by high-intensity  
754 oscillations in both temperate and semi-desert vegetation correlated with D-O cycles and intense ice-  
755 rafting events HE1 to HE7 in MD95-2040. During interstadial events, temperate and Mediterranean  
756 vegetation (deciduous forest + Mediterranean + Ericaceae) could reach values above 60 % of total  
757 pollen; during stadial events, the semi-desert pollen values reached values as high as 70% of total  
758 pollen (during HS3, HS4 and HS5). In comparison, the penultimate glacial (MIS 6) displays much lower  
759 intensity events, with interstadials characterized by 45% as a maximum value for temperate  
760 vegetation, and stadials with 65% for the steppe and semi-desert vegetation (during HS11). High-  
761 intensity cold episodes during MIS 6 are limited to the HS11, and the ~172 ka BP event. This is  
762 consistent with the multiproxy record of core MD95-2040 on the Portuguese margin, which evidenced  
763 reduced variability in the *N. pachyderma* abundance and IRD deposition during the penultimate glacial  
764 compared to the last glacial (de Abreu et al., 2003; Voelker & de Abreu, 2011). The ice rafting episodes  
765 appear to be of different nature during MIS 6 (Hodell et al., 2008; Liu et al., 2018; McCarron et al.,  
766 2021), with the main iceberg discharges originating from the European ice sheet, contrary to the typical  
767 Hudson Strait origin of the last glacial Heinrich events. SST reconstructions in the western  
768 Mediterranean also show less intense cooling during MIS 6 than during MIS 3 (Martrat et al., 2004,  
769 2007), supporting limited incursions of polar waters in the Mediterranean during MIS 6 compared to  
770 MIS 3 coldest stadials, and especially Heinrich stadials (Cacho et al., 1999).

771 Like ODP 976, Ioannina records lower intensity arboreal pollen oscillations during early MIS 6  
772 compared to the last glacial (Roucoux et al., 2011). In comparison, the Atlantic pollen record from  
773 MD01-2444 core displays similar amplitude of tree percentages during the last and the penultimate

774 glacial (Margari et al., 2010). This difference can be explained by the different climate conditions, and  
775 the higher sensitivity to cold and aridity of sclerophyllous and deciduous forest vegetation on the  
776 Mediterranean side, as recorded in the ODP 976 and Ioannina palynological sequence. It appears that  
777 temperate vegetation in SW Mediterranean responded to millennial climate oscillations with higher  
778 intensity during the last glacial compared to the penultimate, probably because the climate in Europe  
779 was colder during MIS 6 compared to MIS 2. This is supported by larger European ice-sheet extension  
780 during the penultimate glacial (Ehlers et al., 2011; Ehlers & Gibbard, 2007; Shackleton, 1987), favouring  
781 the long-term establishment of open landscapes mainly composed by steppe and semi-desert plants.  
782 The differences in humidity might not be as easily interpretable, with an early MIS 6 more humid, and  
783 a MIS 6 glacial maximum more arid, compared to MIS 3 and MIS 2 as also suggested by the Ioannina  
784 record (Roucoux et al., 2011). Future climate reconstructions applied to the complete last glacial cycle  
785 in ODP 976 and other Mediterranean long pollen sequences will help understanding the different  
786 climate configurations between the last two glacial periods.

#### 787 5.6. Human occupation during MIS 6 in SW Europe

788 Only a limited number of sites in South-Western Europe have yielded archaeological layers  
789 attributed to MIS 6, and even fewer of them have been radiometrically dated allowing for a robust  
790 comparison with the environmental changes during MIS 6 ([Fig. 10 and supplementary Supplements](#)  
791 [table S24](#)). The environmental proxies available in the archaeological layers (pollen, charcoal, macro  
792 and microfauna) can help the chronological attribution, but are often insufficient to establish a precise  
793 correlation with the high-resolution chrono-environmental framework of marine and glacial archives.  
794 Even when absolute dates are available, their large uncertainty range [and the poor resolution of the](#)  
795 [archaeological record represent a major limitation and makes](#) it difficult to correlate the human  
796 occupation phases with a specific substage of MIS 6.

797 It is generally accepted that the northern part of Europe was almost completely depopulated  
798 during MIS 6, with very few sites identified compared to the southern European fringes, indicating  
799 discontinuous occupation during more favourable climatic episodes (Hérisson et al., 2016) or total  
800 abandonment like in the British lands (Scott, 2011; Shaw et al., 2016; White and Pettitt, 2011).  
801 Southern France, Italy and the Iberian Peninsula could have represented climate refugia during the  
802 most extreme ice-cap advances (Bicho and Carvalho, 2022). Notably, Italy is particularly deprived of  
803 sites well-dated to MIS 6 including the isolated Neanderthal of Altamura, the short episode of elephant  
804 scavenging at Poggetti Vecchi, and the long sequence of San Bernardino cave which chronological  
805 range extends up to ~154 ka BP, a period marked by the most extensive glacial conditions of MIS 6.  
806 Some other few archaeological layers have been attributed to MIS 6, but they lack a robust

a mis en forme : Anglais (Royaume-Uni)

807 chronological attribution (Aureli & Ronchitelli, 2018; Fontana et al., 2010, Fig. 6.4 Fig. 10). One can  
 808 hypothesise that regional climate conditions in the peninsula were particularly harsh after 150 ka, and  
 809 that potential refugia sites remain to be identified in Italy. Palaeoecological reconstructions at the  
 810 Poggetti Vecchi site indicated cold and dry open environment (Aranguren et al., 2019; Benvenuti et al.,  
 811 2017). Interestingly, the chronological range for the site could coincide with a major stadial event at  
 812 171 ka BP identified in the ODP 976 core, and particularly well expressed in the Valle di Castiglione  
 813 record (Fig. 6).

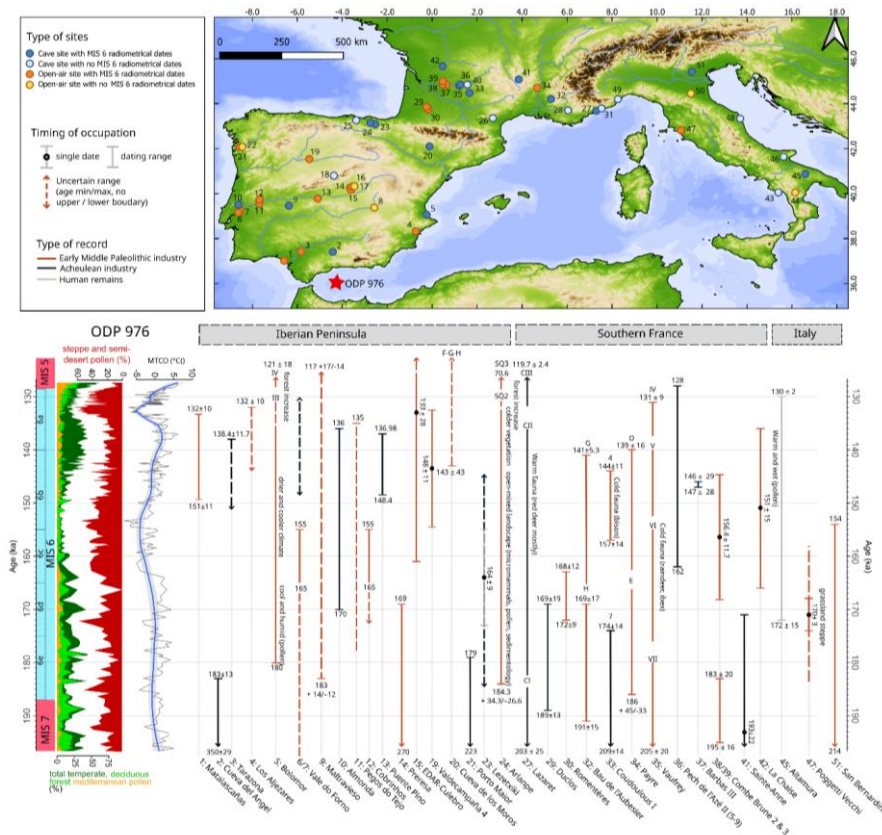


**Fig. 10.** Distribution of archaeological sites and radiometrically dated human occupation in western Mediterranean attributed to MIS 6, with some relevant palaeoecological information when available. The dates used and references can be found in Supplementary table S32. Sites on the map are numbered from south to north in each country: 1: Matalascañas ; 2: Cueva del Angel ; 3: Tarazona ; 4: Los Aljezares ; 5: Cueva del Bolomor ; 6: Vale do Forno ; 7: VF3 (Milharos) ; 8: El Provencio ; 9: Cueva de Maltravieso ; 10: Almonda ; 11: Pegos do Tejo ; 12: Cobrinhos ; 13: Puente Pino ; 14: Preresia ; 15: EDAR-Culebro 2 ; 16: Arriaga II/III ; 17: Arganda II (Valdocarros) ; 18: Villacastin ; 19: Valdecampana ; 20: Cueva de los Moros de Gabasa ; 21: Porto Maior ; 22 : Arbo ; 23 : Lezetxiki ; 24 : Arlanpe ; 25: Ventalaperra ; 26: Aldènes ; 27 : Grotte du Lazaret ; 28 : Baume Bonne ; 29 : Duclos

; **30**: Romenteres ; **31**: Grotte du Prince ; **32**: Bau de l'Aubesier; **33**: Coudoulous I ; **34**: Payre ; **35**: Grotte Vaufrey ; **36** : Pech de l'Aze II ; **37**: Barbas III ; **38**: Combe Brune 3 ; **39**: Combe Brune 2 ; **40**: Grotte Sirogne; **41**: Sainte -Anne ; **42**: La Chaise ; **43**: Riparo del Poggio; **44**: Rosaneto; **45**: Altamura; **46**: Riparo Paglicci; **47**: Poggetti Vecchi ; **48**: Monte Conero; **49**: Grotta del Colombo; **50**: Due Pozzi/Scornetta; **51**: Grotta di San Bernardino.

a mis en forme : Interligne : simple

814 In Southern France and the Iberian Peninsula, according to available radiometric dates, human  
815 occupation appears to have been continuous across MIS 6, even during the glacial maximum, with both  
816 cave and open-air sites. France provides a comparable number of cave and open-air sites mainly  
817 concentrated in the southwestern region. The Portuguese record is mainly constituted by open-air  
818 sites in fluvial terrace systems of the lower Tagus, offering important insights into short-term  
819 occupations during the full-glacial stage, but with complex chronological attribution (Cunha et al.,  
820 2012, 2017; Pereira et al., 2019). The Spanish record includes various open-air settlements in the upper  
821 Tagus valley (Panera et al., 2011, 2014; Yravedra et al., 2019), as well as the Duero (Diez-Martín, 2010)  
822 and the Guadalquivir (Caro Gómez et al., 2011) valleys. Cave sites are fewer and are mainly located  
823 closer to the coast (Cueva del Bolomor, Cueva del Angel, Lezetxiki, Arlanpe, Ventalaperra), with the  
824 two exceptions of Cueva de Maltravieso and Villacastín. Key sites like Lazaret ~~C~~eave (Late Acheulean,  
825 France) and Cueva del Bolomor (Middle Palaeolithic, Spain) evidence the persistence of human groups  
826 in possible climate refugia ~~where large game hunting of red deer was prevailed (Michel et al., 2013;~~  
827 ~~Valensi et al., 2013).~~ (Ochando et al., 2019; Valensi et al., 2005). ~~Cueva del Bolomor stands out in the~~  
828 ~~Iberian Peninsula record as it provides an exceptionally long and continuous record of human~~  
829 ~~presence, and the oldest evidence of fire use in Spain during the Middle Palaeolithic (Vidal-Matutano~~  
830 ~~et al., 2019). Climate changes during MIS 6 are documented in the cave's sediments through multiple~~  
831 ~~proxies, with a more humid and cool phase at the beginning, and the most arid phase taking place at~~  
832 ~~the middle of Phase III (layers X VIII) (Arsuaga et al., 2012; Fernández-Peris et al., 2008). The site is~~  
833 ~~described as a climate refugia where Mediterranean vegetation persisted during the colder phase of~~  
834 ~~MIS 6 thanks to the coastal reservoir character of the site (Ochando et al., 2019). ~~where large game~~~~  
835 ~~hunting of red deer was prevailed (Valensi et al., 2013).~~

a mis en forme : Français (France)

a mis en forme : Français (France)

Code de champ modifié

Code de champ modifié

Code de champ modifié

Code de champ modifié

Code de champ modifié

836 MIS 6 in Europe saw the final stage of the cultural transition from the Lower to the Middle  
837 Palaeolithic industries (MIS 8-5), mainly characterized by the emergence of more complex core  
838 technologies such as Levallois debitage and changes in subsistence strategies. No rupture is observed  
839 between the technocomplexes, as cultural diversity and the permanence of Acheulean bifacial tools  
840 associated to technological innovation mark these Early Middle Palaeolithic industries in Southern  
841 Europe (Santonja et al., 2016; Terradillos-Bernal et al., 2023). The distribution of archaeological sites  
842 and timing of human occupation in South-Western Mediterranean at that time reflects this pattern. A  
843 mosaic of traditional and innovative behavioural traits can be observed, with late Acheulean and Early

844 Middle Palaeolithic coexisting continuously (Cueto et al., 2016; de Lumley, 2018; Mathias et al., 2020;  
845 Moncel et al., 2025; Santonja et al., 2022; Torres et al., 2024; Valensi et al., 2013). Acheulean  
846 technocomplexes are progressively abandoned ~~aeross-during~~ MIS 6 in Europe (Álvarez-Alonso, 2014;  
847 Key et al., 2021), with the latest chronologies found possibly in the Manzanares basin in central Iberia  
848 at Arriaga sites (Panera et al., 2014; Rubio-Jara et al., 2016; Rubio-Jara and Panera, 2019; Silva et al.,  
849 2013), or at Lazaret cave (Michel et al., 2022), and dated to the beginning of MIS 5. No clear explanation  
850 is accepted for the emergence and generalization of the Levallois debitage, and while cognition might  
851 not be the only factor, some authors suggested that MIS 6 glaciation could have played a role in the  
852 final abandonment of Acheulean industries (Moncel et al., 2020; Valensi et al., 2005). It is hard to claim  
853 that specific environmental pressures favoured Levallois technology over bifacial production, as these  
854 lithic technologies seem to have co-existed in Western Europe since MIS 12-11 over several  
855 glacial/interglacial cycles (Baena et al., 2017; Moncel et al., 2020), including extremely cold stages (like  
856 MIS 12 and 10). This “mosaic” pattern for the lower to middle palaeolithic transition, although at least  
857 partly imputable to the large dating uncertainties, points toward more complex processes leading to  
858 the generalization of Middle Palaeolithic industries from MIS 5. Interestingly, the end of the Lower to  
859 Middle Palaeolithic transition is also associated with a shift in the morphology of human remains, from  
860 “Early Neanderthals” (MIS 7-5) to “Classical Neanderthals” (MIS 5-3) (Di Vincenzo and Manzi, 2023).  
861 Sites like La Chaise (Abri Suard), Lazaret and Altamura provide fossil evidence for these “Early  
862 Neanderthals” which share characteristics with earlier Middle Pleistocene populations, and with later  
863 Neanderthals (Buzi et al., 2025; Couture-Veschambre et al., 2021; de Lumley, 2018). Genetic data also  
864 support an important population shift in western Europe sometimes around the transition from MIS 6  
865 to MIS 5 (Peyrègne et al., 2019). Therefore, an important population reorganization seems to have  
866 occurred at the time of the final Acheulean industries, leading to the onset of the so-called “Classical  
867 neanderthal world” in western Eurasia, with generalized Middle Palaeolithic industries and established  
868 Neanderthal morphological features. The role of environmental changes occurring during MIS 6 in this  
869 population reorganization remains poorly understood.

870 Changes in land use and mobility pattern have been evidenced in north-central Iberia, and can  
871 be viewed as adaptations to the severe climatic conditions of MIS 6 evidenced in the ODP 976 sequence  
872 during pollen zone/phase 2-: increasing mobility, more short-term occupations and reliance on more  
873 local resources for subsistence strategies (Diez-Martín, 2010; Diez-Martín et al., 2008; Rios-Garaizar,  
874 2016; Sánchez-Yustos, 2009). According to this view, the emergence of the “classical Neanderthal”  
875 world in Europe after the MIS 6/5 transition corresponds to the initialization of dynamics of repeated  
876 population contraction and expansion in response to the Upper Pleistocene instability (Sánchez-  
877 Yustos, 2009). However,

a mis en forme : Anglais (États-Unis)

a mis en forme : Anglais (États-Unis)

a mis en forme : Anglais (États-Unis)

a mis en forme : Anglais (États-Unis)

Code de champ modifié

Code de champ modifié

878 -identifying cultural phases in the archaeological sequences linked with specific climatic  
879 episodes is generally hindered by the poor resolution of the archaeological record and chronological  
880 data. Among the sites identified in this synthesis, Lazaret and Bolomor caves probably present the  
881 most informative and well-dated sequences with several archaeological layers dated to MIS 6.

a mis en forme : Espace Avant : 0 pt

882 Cueva del Bolomor stands out in the Iberian Peninsula record as it provided an exceptionally  
883 long and continuous record of human presence, and the oldest evidence of fire use in Spain during the  
884 Middle Palaeolithic (Vidal-Matutano et al., 2019). Climate changes during MIS 6 documented in  
885 Bolomor's sediments through multiple proxies are consistent with the different phases identified in  
886 the ODP 976 record, with a more humid and cool phase at the beginning of MIS 6, and the most arid  
887 phase taking place at the middle of Phase III (layers X-VIII) (Arsuaga et al., 2012; Fernández Peris et al.,  
888 2008). The site is described as a climatic refugium where Mediterranean vegetation persisted during  
889 the colder phase of MIS 6 thanks to the coastal reservoir character of the site (Ochando et al., 2019).  
890 No clear change in lithic production has been identified in the MIS 6 layers of Bolomor: according to  
891 Fernández Peris (2008), archaeological layers XII to VII (Phase III, MIS 6) are all dominated by limestone  
892 flakes with few retouches, few recycling, and the presence non-Acheulean macro-lithic elements.  
893 These layers are characterized by expeditive flaking (including Levallois *débitage*) relying on local raw-  
894 material, pointing toward a high degree of mobility and search for immediate effectiveness. It is thus  
895 hard to distinguish different techno-cultural tendencies during this phase. The most visible change in  
896 the archaeological sequence occurs in layer VI (MIS 5) which shows an intensification of lithic  
897 production dominated by flint, the production of more specialized tools including microlithic elements  
898 and associated to more intense and stable occupation in the cave (Fernández Peris et al., 2008).  
899 Therefore, a clear behavioural change in the technological and economical exploitation of raw  
900 materials is identified at the beginning of MIS 5. Faunal remains show a large and constant diversity,  
901 including abundant micro supporting both short-term and long-term not-specialized occupation, with  
902 no clear change in the site's function across the sequence (Blasco et al., 2013).

a mis en forme : Anglais (Royaume-Uni)

a mis en forme : Anglais (Royaume-Uni)

903 Lazaret Cave, in south-eastern France, shows a very distinct scheme: the lower to middle  
904 Palaeolithic transition is well documented in the archaeological sequence (Unit CII and CIII), with the  
905 progressive replacement of large bifacial tools production by more standardized and smaller flakes  
906 (Cauche, 2012). Levallois *débitage* is already present and well-mastered in the lower MIS 6 levels,  
907 although rare, and becomes dominant in the upper levels (early MIS 5). Therefore, a subdivision of unit  
908 CII can be made with a lower interval rich in handaxes, and an upper layer characterized as "final  
909 Acheulean" with rare handaxes and more abundant flakes. Faunal assemblages are very constant  
910 throughout MIS 6, with the large dominance of red deers and rare presence of cold species (*Rangifer*

a mis en forme : Police :Italique

911 tarandus, Coelodonta antiquitatis). Thus, the climatic oscillations of MIS 6 do not seem to have  
912 influenced different hunting strategies or prey selection by human populations at Lazaret Cave, as large  
913 game hunting of red deer prevailed (Valensi et al., 2013).

a mis en forme : Anglais (Royaume-Uni)

914 Therefore, Lazaret and Bolomor caves are examples of different strategies of site exploitation\*  
915 and technological evolution during MIS 6: Lazaret Cave represents a specialized red-deer hunting camp  
916 evidencing a progressive change from Lower to Middle Palaeolithic tools, while Cueva del Bolomor can  
917 be characterized as a short-term camp with more generalized hunting and stable expeditive Middle  
918 Palaeolithic industry. Despite these differences both sites provide evidence for a change in lithic  
919 assemblages occurring at the end of MIS 6/ beginning of MIS 5: the disappearance of handaxes and  
920 generalization of Levallois flakes in Lazaret, and the intensification and standardization of flint flaxes  
921 in Bolomor.

a mis en forme : Espace Avant : 12 pt

922 ~~Changes in land use and mobility pattern have been evidenced in north-central Iberia, and can~~  
923 ~~be viewed as adaptations to the severe climatic conditions of MIS 6: increasing mobility, more short-~~  
924 ~~term occupations and reliance on more local resources for subsistence strategies (Diez Martín, 2010;~~  
925 ~~Diez Martín et al., 2008; Rios Garaizar, 2016; Sánchez Yustos, 2009). According to this view, the~~  
926 ~~emergence of the "classical Neanderthal" world in Europe after the MIS 6/5 transition corresponds to~~  
927 ~~the initialization of dynamics of repeated population contraction and expansion in response to the~~  
928 ~~Upper Pleistocene instability (Sánchez Yustos, 2009).~~

929 ~~Indeed, the~~The fast climate dynamics during Termination II as evidenced in the ODP 976  
930 paleoenvironmental record could have represented a critical period for human population. At the end  
931 of MIS 6, more sites have been identified in the Iberian Peninsula than Southern France, showing the  
932 latter could have represented a climate refugium~~a~~ at the time of maximum glacial expansion, with  
933 more intense human occupation regionally. Many of these late MIS 6 sites present a chronological  
934 boundary at the top of the sequence compatible with the onset of Termination II around 136 ka BP,  
935 and with Heinrich Stadial~~HS~~-11, within the dating uncertainty: Matalascañas, Tarrazona, Los Aljezares,  
936 Bolomor Unit III, Almonda, Pegos do Tejo, Puente Pino, Arlanpe Unit SQ2, Lazaret Unit CII, Payre layer  
937 D, Vauffrey unit IV, and Pech de l'Azé II layer 5-. The extreme character of this event in the South-  
938 Western Mediterranean as expressed in the ODP 976 sequence could have put further environmental  
939 pressure on hominin groups already diminished. A niche modelling approach based on 41 sites of  
940 Western Eurasia since 145 ka BP has shown that the projected potential niche space ~~reconstructed~~  
941 for Neanderthals at the end of MIS 6 (~145ka BP)- ~~was very reduced~~~~is very reduced~~, and concentrated  
942 in Western Europe (Yaworsky et al., 2024). This coincides with the end of pollen zone/phase 2 in the  
943 ODP 976 record, the most cold and arid phase of the penultimate Glacial before HS11. Then, the

944 authors reconstruct a progressive expansion of Neanderthal potential niche space between 145 and  
945 130 ka, compatible with the climatic warming and moistening during pollen zone/phase 3 in the ODP  
946 976 record (Yaworsky et al., 2024). The temporal resolution of the model (1000 years) does not allow  
947 to detect the impact of HS11 on the niche projection, and only a small slowdown and decline of the  
948 projected niche is visible at ~130 ka BP, before the MIS 5e optimum (Yaworsky et al., 2024, Fig. 5). A  
949 regional study focused on North-Western Spain ~~also~~ argued in favour of a demographic vacuum at the  
950 end of MIS 6, compatible with HS11 and leading to a population reorganization implying ~~population~~  
951 ~~retreat-contraction~~ or micro-extinction, before the generalization of Middle Palaeolithic industries ~~and~~  
952 during MIS 5 (Sánchez-Yustos and Díez-Martín, 2015). According to the same authors, following this  
953 crisis, Neanderthal population entered a “reorganisation phase” leading to demographical stability  
954 (Peyrégne et al., 2019) and more technological standardization, visible in the explosion of the number  
955 of sites in Europe in general, especially after the MIS 5e climatic optimum (Bringmans, 2007; Lewis et  
956 al., 2011; Wenzel, 2007).- This statement is supported by niche modelling which shows a peak in  
957 projected potential niche space of Neanderthal during MIS 5e (Yaworsky et al., 2024), and by recent  
958 genetic data which provided evidence for at least two radiation events linked with the environmental  
959 conditions of the last interglacial (Vernot et al., 2021), and Neanderthal population continuity since  
960 ~120 ka BP (Peyrégne et al., 2019). Thus, HS11 did not lead to complete extinction of hominin groups  
961 but might have induced deep demographical and technological reorganization, representing the first  
962 and one of the most intense abrupt changes that Neanderthal population had to face in South-Western  
963 Europe before the Last Glacial largest oscillations (HS4-46). According to this view, the emergence of  
964 the “classical Neanderthal” world in Europe after the MIS 6/5 transition corresponds to the  
965 initialization of dynamics of repeated population contraction and expansion in response to the Upper  
966 Pleistocene instability, especially during MIS 4-2 (Sánchez-Yustos, 2009). In that sense, the subdued  
967 environmental instability during MIS 6 evidenced in the OD-P976 record compared to the last glacial  
968 period (Section 5.5 and Fig. 9) could also have implications for human populations, with less  
969 fragmented (although harsh) habitats and more stable (although reduced) population during MIS 6.  
970 This hypothesis remains however hard to test based on the very different nature and quality of  
971 preservation of the archaeological record during MIS 6 compared to MIS 4-2 (e.g. Charton et al.,  
972 2025),(Peyrégne et al., 2019)(Vernot et al., 2021)~~Thus, HS11 did not lead to complete extinction of~~  
973 ~~hominin groups but might have induced deep demographical and technological reorganization,~~  
974 ~~representing the first and one of the most intense abrupt changes that Neanderthal population had to~~  
975 ~~face in South-Western Europe before the Last Glacial largest oscillations (HS4-6).~~

976

## 6. Conclusion

The ODP 976 record sheds light on the environmental and climate changes during MIS 6 in the SW Mediterranean. The sequence is characterized by the high representation of *Cedrus* and Ericaceae pollen, resulting from the combined influence of African and Atlantic input respectively. ODP 976 position, at the confluence of Mediterranean versus Atlantic, and Eurasian versus African climatic areas, is ideal to decipher the processes behind orbital and sub-orbital climate dynamics during past glaciations. Three main phases have been distinguished during MIS 6 with different trends in vegetation and climate changes. Millennial-scale oscillations are recorded especially during the early part of MIS 6 (~187-166 ka BP) through the rapid increases of temperate and Mediterranean pollen, some of which are ~~consistent similar to with Antarctic and millennial-scale warming D-O-like~~ events identified in the ice-core and marine temperature records, ~~and as well as~~ other palynological sequences in the Mediterranean region. This Early MIS 6 phase is characterized by overall warmer and wetter climate conditions, in agreement with other paleoclimate archives in the Mediterranean showing enhanced moisture availability at the beginning of MIS 6. This phase of enhanced moisture availability was likely connected with enhanced Asian and African monsoon activity and was probably at the origin of the deposition of ~~the an~~ Organic Rich Layer 607 in the Alboran Sea and sapropel S6 in the eastern Mediterranean. The second phase (165-144 ka BP) shows the establishment of full glacial conditions in the Mediterranean, with the maximum spread of steppe and semi-desert vegetation associated to cold and arid climate conditions and limited rapid oscillations. Finally, the final stages of MIS 6 are marked by increased humidity and the development of Ericaceae, with moderate millennial-scale oscillations seen in the vegetation record. Termination II is very particular in the ODP 976 record, with the continuous increase of temperate and Mediterranean vegetation being contemporaneous to a major episode of steppe expansion and aridity increase identified as ~~Heinrich Stadial 11~~ HS11. This event shows a particular three phases or “~~double-UV~~” shape, in agreement with other records, and ~~probably~~ had a major impact on the SW Mediterranean ~~region~~ environments. A comparison with the changes occurring during the last glacial period (MIS ~~42-42~~) inferred from the same core highlighted the limited duration, frequency and intensity of MIS 6 millennial climate events compared ~~to~~ the last Glacial D-O cycles and Heinrich Events (MIS ~~2-44-2~~). These results support a subdued impact of the millennial-scale climate oscillations on the continental vegetation in the Mediterranean region during the Penultimate glaciation compared to the Last Glacial. The only exception is HS11, which stands out by its notable intensity and duration and is of particular interest to understand the mechanisms behind Termination II.

Human populations continuously inhabited the SW Mediterranean territory during MIS 6. While few sites are available and robustly dated to MIS 6 in Italy, Southern France and the Iberian

1011 Peninsula appear to have been intensely populated, supporting their nature of Pleistocene Climate  
1012 refugia. More ecological data from well-dated archaeological sites during MIS 6 would be needed to  
1013 increase the quality of human-environmental dynamics comparison. However, the synthesis drawn in  
1014 the present study highlights the extreme nature of events characterizing Termination II, and  
1015 particularly HS11, which could have represented an important environmental crisis for human  
1016 population at that time, catalysing the end of the Lower to Middle Palaeolithic Transition and the onset  
1017 of the “classical” Neanderthal world through a drastic population ~~contraction~~bottleneck.

## 1018 7. Acknowledgments

1019

1020 We want to thank the three anonymous reviewers and the editor for their very helpful  
1021 comments on this manuscript. We acknowledge the International Ocean Drilling Project and the  
1022 MARUM Bremen Core Repository for making available the ODP 976 samples. The sample processing  
1023 was funded by the CNRS and the MNHN. We thank the European Research Council (ERC) under the  
1024 European Union’s HORIZON1.1 research program (LATEUROPE project, grant agreement ID  
1025 101052653) for funding this publication. L. Charton doctoral contract ~~is~~was funded by the French  
1026 Ministère de l’Enseignement Supérieur et de la Recherche at the doctoral school ED 227 of the  
1027 Muséum National d’Histoire Naturelle, Paris. The international cotutorship with the University of  
1028 Florence is supported by the Ecole Franco-Italienne Vinci grant (project C2-166). We thank Lionel  
1029 Dubost for assistance in laboratory treatment of samples to HF. We are grateful to Francisco Sierro for  
1030 sharing the isotopic data on AICC2012 timescale, to Jon Camuera for the pollen data from Padul and  
1031 to Katherine Roucoux for the pollen data from Ioannina. This is an ISEM contribution.

## 1032 8. Supplements

1033

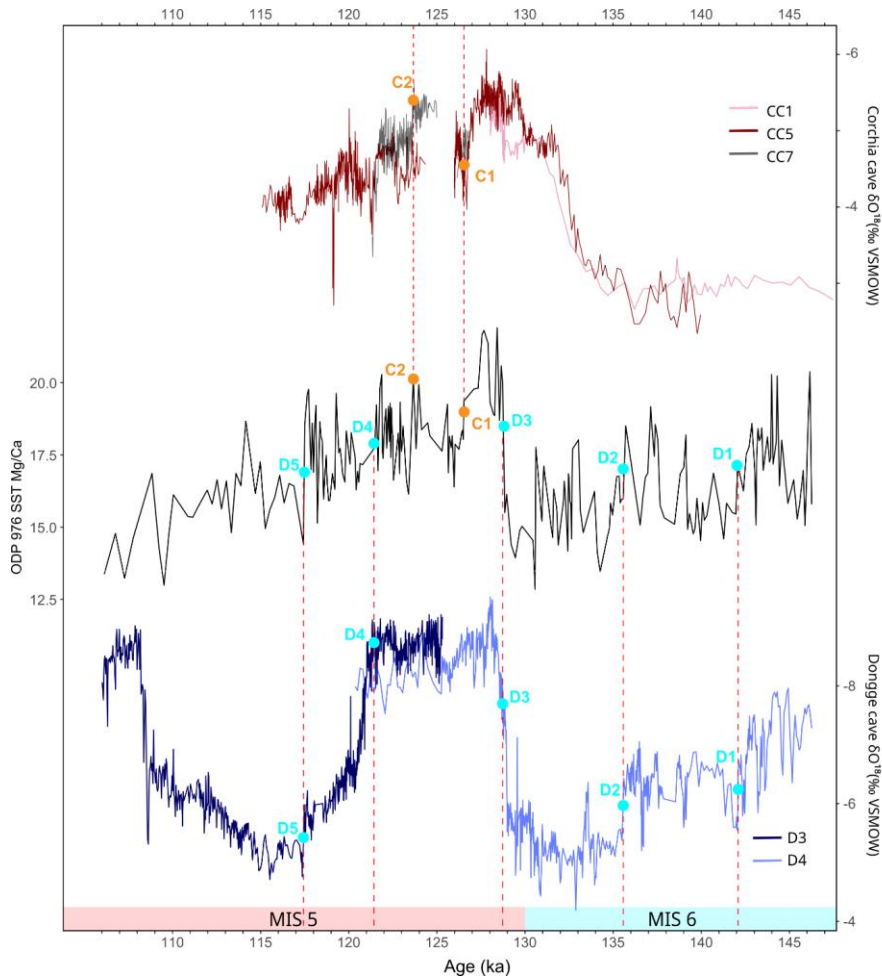


**Fig. S1:** Correlation between the ODP 976 Mg/Ca-based Sea Surface Temperatures (Jiménez-Amat & Zahn, 2015) and the Dongge Cave (Kelly et al., 2006) and Corchia Cave (Drysdale et al., 2009) speleothem oxygen isotope records (adapted from Jiménez-Amat & Zahn, 2015).

a mis en forme : Espace Avant : Automatique, Après : Automatique

a mis en forme le tableau

a mis en forme : Police : (Par défaut) Times New Roman, 12 pt, Français (France)

a mis en forme : Français (France)

a mis en forme : Justifié

a mis en forme : Police : Non Gras, Français (France)

a mis en forme : Français (France)

a mis en forme : Police : Non Gras, Français (France)

a mis en forme : Français (France)

Code de champ modifié

a mis en forme : Français (France)

a mis en forme : Français (France)

a mis en forme : Français (France)

1034

1035

1036

1037

1038

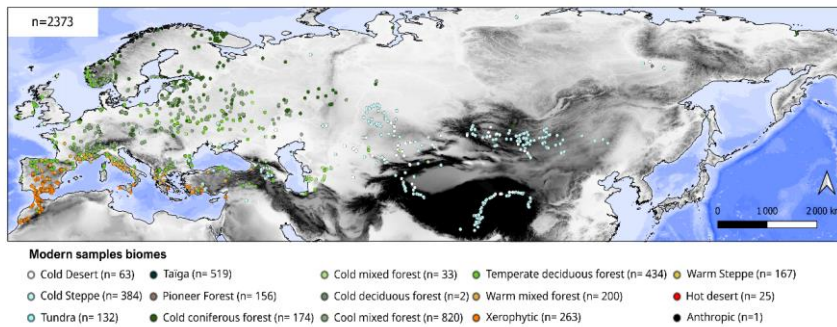
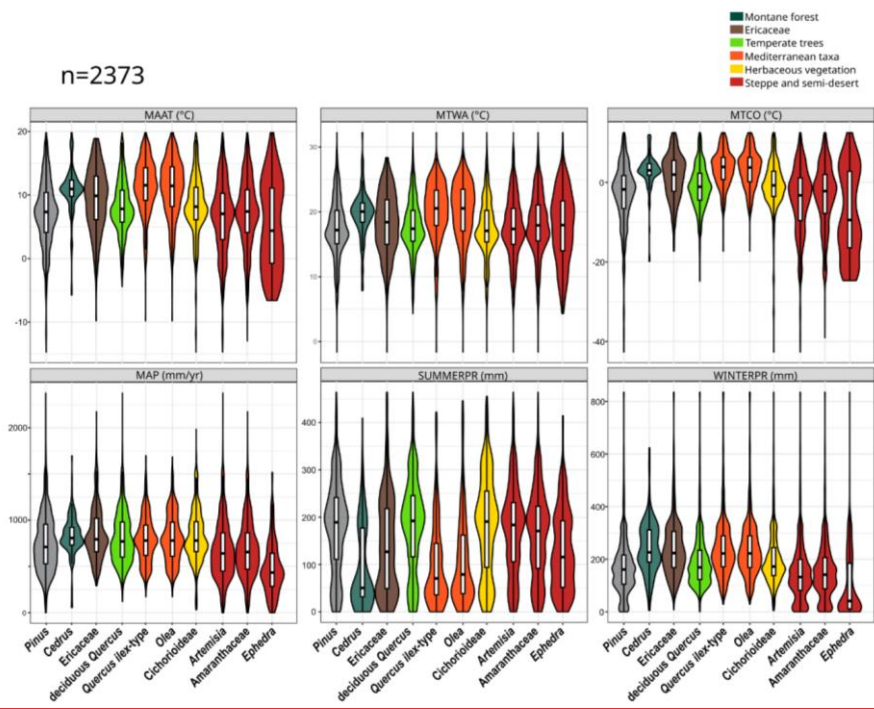


**Fig. S2.** Distribution of modern pollen samples from the Eurasian Pollen Database used for the multimethod pollen-based climatic reconstructions, coloured by biome attribution. The dataset was compiled by Peyron et al. (2013, 2017) and updated by Dugerdil et al. (2021) and Robles et al. (2023).

a mis en forme le tableau

a mis en forme : Police :Gras

a mis en forme : Justifié



a mis en forme le tableau

**Fig. S3.** Tolerance spectra of the ten main pollen taxa identified in the ODP 976 record to the six reconstructed climatic parameters, based on the modern Eurasian pollen database (2373 samples). The violin plots show the taxa abundance depending on the climate parameter values (based on pollen abundance).

1040

1041

1042

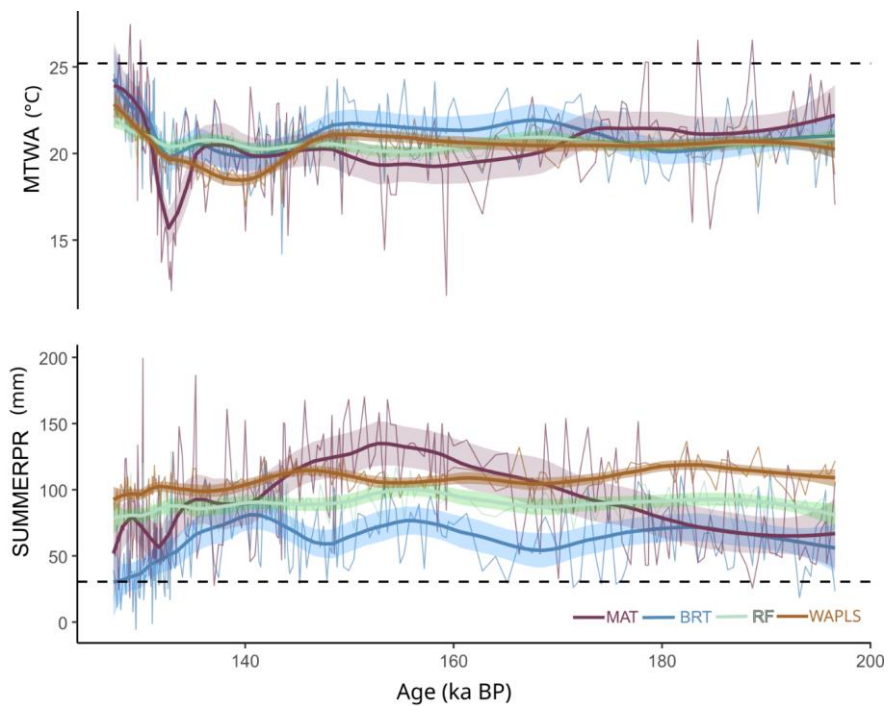


**Fig. S4.** MIS 6 multimethod pollen-based climatic reconstructions of summer precipitation (SUMMERPR) and Mean Temperature of the Warmest Month (MTWA) from the ODP 976 pollen record.

1043

1044



1048 [8.9. References](#)

1049

- 1050 de Abreu, L., Shackleton, N. J., Schönfeld, J., Hall, M., and Chapman, M.: Millennial-scale oceanic  
 1051 climate variability off the Western Iberian margin during the last two glacial periods, *Marine Geology*,  
 1052 196, 1–20, [https://doi.org/10.1016/S0025-3227\(03\)00046-X](https://doi.org/10.1016/S0025-3227(03)00046-X), 2003.
- 1053 Allen, J. R. M. and Huntley, B.: Last Interglacial palaeovegetation, palaeoenvironments and  
 1054 chronology: a new record from Lago Grande di Monticchio, southern Italy, *Quaternary Science  
 1055 Reviews*, 28, 1521–1538, <https://doi.org/10.1016/j.quascirev.2009.02.013>, 2009.
- 1056 Álvarez-Alonso, D.: First Neanderthal settlements in northern Iberia: The Acheulean and the  
 1057 emergence of Mousterian technology in the Cantabrian region, *Quaternary International*, 326–327,  
 1058 288–306, <https://doi.org/10.1016/j.quaint.2012.12.023>, 2014.
- 1059 Aranguren, B., Grimaldi, S., Benvenuti, M., Capalbo, C., Cavanna, F., Cavulli, F., Ciani, F., Comencini,  
 1060 G., Giuliani, C., Grandinetti, G., Mariotti Lippi, M., Masini, F., Mazza, P. P. A., Pallecchi, P., Santaniello,  
 1061 F., Savorelli, A., and Revedin, A.: Poggetti Vecchi (Tuscany, Italy): A late Middle Pleistocene case of  
 1062 human–elephant interaction, *Journal of Human Evolution*, 133, 32–60,  
 1063 <https://doi.org/10.1016/j.jhevol.2019.05.013>, 2019.
- 1064 Arsuaga, J. L., Fernández Peris, J., Gracia-Téllez, A., Quam, R., Carretero, J. M., Barciela González, V.,  
 1065 Blasco, R., Cuartero, F., and Sañudo, P.: Fossil human remains from Bolomor Cave (Valencia, Spain),  
 1066 *Journal of Human Evolution*, 62, 629–639, <https://doi.org/10.1016/j.jhevol.2012.02.002>, 2012.
- 1067 Auffret, G.-A., Pastouret, L., Chamley, H., and Lanoix, F.: Influence of the prevailing current regime on  
 1068 sedimentation in the Alboran Sea, *Deep Sea Research and Oceanographic Abstracts*, 21, 839–849,  
 1069 [https://doi.org/10.1016/0011-7471\(74\)90003-5](https://doi.org/10.1016/0011-7471(74)90003-5), 1974.
- 1070 Aureli, D. and Ronchitelli, A.: The Lower Tyrrhenian Versant: was it a techno-cultural area during the  
 1071 Middle Palaeolithic? Evolution of the lithic industries of the Riparo del Molare sequence in the frame  
 1072 of Neanderthal peopling dynamics in Italy, 59–94, 2018.
- 1073 Ayalon, A., Bar-Matthews, M., and Kaufman, A.: Climatic conditions during marine oxygen isotope  
 1074 stage 6 in the eastern Mediterranean region from the isotopic composition of speleothems of Soreq  
 1075 Cave, Israel, *Geology*, 30, [https://doi.org/10.1130/0091-7613\(2002\)030<0303:CCDMOI>2.0.CO;2](https://doi.org/10.1130/0091-7613(2002)030<0303:CCDMOI>2.0.CO;2),  
 1076 2002a.
- 1077 Ayalon, A., Bar-Matthews, M., and Kaufman, A.: Climatic conditions during marine oxygen isotope  
 1078 stage 6 in the eastern Mediterranean region from the isotopic composition of speleothems of Soreq  
 1079 Cave, Israel, *Geol*, 30, 303, [https://doi.org/10.1130/0091-7613\(2002\)030<0303:CCDMOI>2.0.CO;2](https://doi.org/10.1130/0091-7613(2002)030<0303:CCDMOI>2.0.CO;2),  
 1080 2002b.
- 1081 Baena, J., Moncel, M.-H., Cuartero, F., Chacón Navarro, M. G., and Rubio, D.: Late Middle Pleistocene  
 1082 genesis of Neanderthal technology in Western Europe: The case of Payre site (south-east France),  
 1083 *Quaternary International*, 436, 212–238, <https://doi.org/10.1016/j.quaint.2014.08.031>, 2017.
- 1084 Bailey, G., Carrión, J., Fa, D., Finlayson, C., Finlayson, G., and Vidal, J.: The coastal shelf of the  
 1085 Mediterranean and beyond: Corridor and refugium for human populations in the Pleistocene  
 1086 Introduction, *Quaternary Science Reviews*, 27, 2095–2099,  
 1087 <https://doi.org/10.1016/j.quascirev.2008.08.005>, 2008.

a mis en forme : Gauche, Retrait : Première ligne : 0  
 cm, Interligne : Multiple 1,08 li

1088 Bajo, P., Drysdale, R. N., Woodhead, J. D., Hellstrom, J. C., Hodell, D., Ferretti, P., Voelker, A. H. L.,  
1089 Zanchetta, G., Rodrigues, T., Wolff, E., Tyler, J., Frisia, S., Spötl, C., and Fallick, A. E.: Persistent  
1090 influence of obliquity on ice age terminations since the Middle Pleistocene transition, *Science*, 367,  
1091 1235–1239, <https://doi.org/10.1126/science.aaw1114>, 2020.

1092 Barbante, C., Barnola, J.-M., Becagli, S., Beer, J., Bigler, M., Boutron, C., Blunier, T., Castellano, E.,  
1093 Cattani, O., Chappellaz, J., Dahl-Jensen, D., Debret, M., Delmonte, B., Dick, D., Falourd, S., Faria, S.,  
1094 Federer, U., Fischer, H., Freitag, J., Frenzel, A., Fritzsche, D., Fundel, F., Gabrielli, P., Gaspari, V.,  
1095 Gersonde, R., Graf, W., Grigoriev, D., Hamann, I., Hansson, M., Hoffmann, G., Hutterli, M. A.,  
1096 Huybrechts, P., Isaksson, E., Johnsen, S., Jouzel, J., Kaczmarek, M., Karlin, T., Kaufmann, P., Kipfstuhl,  
1097 S., Kohno, M., Lambert, F., Lambrecht, A., Lambrecht, A., Landais, A., Lawer, G., Leuenberger, M.,  
1098 Littot, G., Loulergue, L., Lüthi, D., Maggi, V., Marino, F., Masson-Delmotte, V., Meyer, H., Miller, H.,  
1099 Mulvaney, R., Narcisi, B., Oerlemans, J., Oerter, H., Parrenin, F., Petit, J.-R., Raisbeck, G., Raynaud, D.,  
1100 Röthlisberger, R., Ruth, U., Rybak, O., Severi, M., Schmitt, J., Schwander, J., Siegenthaler, U., Siggaard-  
1101 Andersen, M.-L., Spahni, R., Steffensen, J. P., Stenni, B., Stocker, T. F., Tison, J.-L., Traversi, R., Udisti,  
1102 R., Valero-Delgado, F., van den Broeke, M. R., van de Wal, R. S. W., Wagenbach, D., Wegner, A.,  
1103 Weiler, K., Wilhelms, F., Winther, J.-G., Wolff, E., and EPICA Community Members: One-to-one  
1104 coupling of glacial climate variability in Greenland and Antarctica, *Nature*, 444, 195–198,  
1105 <https://doi.org/10.1038/nature05301>, 2006.

1106 Bard, E., Delaygue, G., Rostek, F., Antonioli, F., Silenzi, S., and Schrag, D. P.: Hydrological conditions  
1107 over the western Mediterranean basin during the deposition of the cold Sapropel 6 (ca. 175 kyr BP),  
1108 *Earth and Planetary Science Letters*, 202, 481–494, [https://doi.org/10.1016/S0012-821X\(02\)00788-4](https://doi.org/10.1016/S0012-821X(02)00788-4),  
1109 2002a.

1110 Bard, E., Antonioli, F., and Silenzi, S.: Sea-level during the penultimate interglacial period based on a  
1111 submerged stalagmite from Argentarola Cave (Italy), *Earth and Planetary Science Letters*, 196, 135–  
1112 146, [https://doi.org/10.1016/S0012-821X\(01\)00600-8](https://doi.org/10.1016/S0012-821X(01)00600-8), 2002b.

1113 Barker, S. and Knorr, G.: Millennial scale feedbacks determine the shape and rapidity of glacial  
1114 termination, *Nat Commun*, 12, 2273, <https://doi.org/10.1038/s41467-021-22388-6>, 2021.

1115 Barker, S., Knorr, G., Edwards, R. L., Parrenin, F., Putnam, A. E., Skinner, L. C., Wolff, E., and Ziegler,  
1116 M.: 800,000 Years of Abrupt Climate Variability, *Science*, 334, 347–351,  
1117 <https://doi.org/10.1126/science.1203580>, 2011.

1118 Bayr, D., Plaza, M. P., Gilles, S., Kolek, F., Leier-Wirtz, V., Traidl-Hoffmann, C., and Damialis, A.: Pollen  
1119 long-distance transport associated with symptoms in pollen allergics on the German Alps: An old  
1120 story with a new ending?, *Sci Total Environ*, 881, 163310,  
1121 <https://doi.org/10.1016/j.scitotenv.2023.163310>, 2023.

1122 Bazin, L., Landais, A., Lemieux-Dudon, B., Toyé Mahamadou Kele, H., Veres, D., Parrenin, F.,  
1123 Martinerie, P., Ritz, C., Capron, E., Lipenkov, V., Loutre, M.-F., Raynaud, D., Vinther, B., Svensson, A.,  
1124 Rasmussen, S. O., Severi, M., Blunier, T., Leuenberger, M., Fischer, H., Masson-Delmotte, V.,  
1125 Chappellaz, J., and Wolff, E.: An optimized multi-proxy, multi-site Antarctic ice and gas orbital  
1126 chronology (AICC2012): 120–800 ka, *Climate of the Past*, 9, 1715–1731,  
1127 <https://doi.org/10.5194/cp-9-1715-2013>, 2013.

1128 Benvenuti, M., Bahain, J.-J., Capalbo, C., Capretti, C., Ciani, F., D’Amico, C., Esu, D., Giachi, G.,  
1129 Giuliani, C., Gliozzi, E., Lazzeri, S., Macchioni, N., Lippi, M. M., Masini, F., Mazza, P. P. A., Pallecchi, P.,  
1130 Revedin, A., Savorelli, A., Spadi, M., Sozzi, L., Vietti, A., Voltaggio, M., and Aranguren, B.:

- 1131 Paleoenvironmental context of the early Neanderthals of Poggetti Vecchi for the late middle  
1132 Pleistocene of Central Italy, *Quat. res.*, 88, 327–344, <https://doi.org/10.1017/qua.2017.51>, 2017.
- 1133 Bermúdez de Castro, J. M. and Martínón-Torres, M.: A new model for the evolution of the human  
1134 Pleistocene populations of Europe, *Quaternary International*, 295, 102–112,  
1135 <https://doi.org/10.1016/j.quaint.2012.02.036>, 2013.
- 1136 Bicho, N. and Carvalho, M.: Peninsular southern Europe refugia during the Middle Palaeolithic: an  
1137 introduction, *J Quaternary Science*, 37, 133–135, <https://doi.org/10.1002/jqs.3410>, 2022.
- 1138 Bisschop, K., Mortier, F., Etienne, R. S., and Bonte, D.: Transient local adaptation and source–sink  
1139 dynamics in experimental populations experiencing spatially heterogeneous environments,  
1140 *Proceedings of the Royal Society B: Biological Sciences*, 286, 20190738,  
1141 <https://doi.org/10.1098/rspb.2019.0738>, 2019.
- 1142 Blasco, R., Rosell, J., Fernández Peris, J., Arsuaga, J. L., Bermúdez de Castro, J. M., and Carbonell, E.:  
1143 Environmental availability, behavioural diversity and diet: a zooarchaeological approach from the  
1144 TD10-1 sublevel of Gran Dolina (Sierra de Atapuerca, Burgos, Spain) and Bolomor Cave (Valencia,  
1145 Spain), *Quaternary Science Reviews*, 70, 124–144, <https://doi.org/10.1016/j.quascirev.2013.03.008>,  
1146 2013.
- 1147 Bond, G., Heinrich, H., Broecker, W., Labeyrie, L., McManus, J., Andrews, J., Huon, S., Jantschik, R.,  
1148 Clasen, S., Simet, C., Tedesco, K., Klas, M., Bonani, G., and Ivy, S.: Evidence for massive discharges of  
1149 icebergs into the North Atlantic ocean during the last glacial period, *Nature*, 360, 245–249,  
1150 <https://doi.org/10.1038/360245a0>, 1992.
- 1151 Bond, G., Broecker, W., Johnsen, S., McManus, J., Labeyrie, L., Jouzel, J., and Bonani, G.: Correlations  
1152 between climate records from North Atlantic sediments and Greenland ice, *Nature*, 365, 143–147,  
1153 <https://doi.org/10.1038/365143a0>, 1993.
- 1154 Bond, G., Showers, W., Cheseby, M., Lotti, R., Almasi, P., Demenocal, P., Priore, P., Cullen, H., Hajdas,  
1155 I., and Bonani, G.: A pervasive millennial-scale cycle in the North Atlantic Holocene and glacial  
1156 climates, *sci*, 278, 1257, <https://doi.org/10.1126/science.278.5341.1257>, 1997.
- 1157 Bond, G. C., Showers, W., Elliot, M., Evans, M., Lotti, R., Hajdas, I., Bonani, G., and Johnson, S.: The  
1158 North Atlantic's 1-2 kyr climate rhythm: Relation to Heinrich events, Dansgaard/Oeschger cycles and  
1159 the Little Ice Age, *Washington DC American Geophysical Union Geophysical Monograph Series*, 112,  
1160 35–58, <https://doi.org/10.1029/GM112p0035>, 1999.
- 1161 Boswell, S. M., Toucanne, S., Pitel-Roudaut, M., Creyts, T. T., Eynaud, F., and Bayon, G.: Enhanced  
1162 surface melting of the Fennoscandian Ice Sheet during periods of North Atlantic cooling, *Geology*, 47,  
1163 664–668, <https://doi.org/10.1130/G46370.1>, 2019.
- 1164 Bout-Roumazielles, V., Combourieu Nebout, N., Peyron, O., Cortijo, E., Landais, A., and Masson-  
1165 Delmotte, V.: Connection between South Mediterranean climate and North African atmospheric  
1166 circulation during the last 50,000yrBP North Atlantic cold events, *Quaternary Science Reviews*, 26,  
1167 3197–3215, <https://doi.org/10.1016/j.quascirev.2007.07.015>, 2007.
- 1168 ter Braak, C. and Juggins, S.: Weighted Averaging Partial Least Squares Regression (WA-PLS): An  
1169 Improved Method for Reconstructing Environmental Variables from Species Assemblages,  
1170 *Hydrobiologia*, 269–270, 485–502, <https://doi.org/10.1007/BF00028046>, 1993.

a mis en forme : Anglais (États-Unis)

- 1171 Bradtmöller, M., Pastoors, A., Weninger, B., and Weniger, G.-C.: The repeated replacement model –  
1172 Rapid climate change and population dynamics in Late Pleistocene Europe, *Quaternary International*,  
1173 247, 38–49, <https://doi.org/10.1016/j.quaint.2010.10.015>, 2012.
- 1174 Brauer, A., Allen, J. R. M., Mingram, J., Dulski, P., Wulf, S., and Huntley, B.: Evidence for last  
1175 interglacial chronology and environmental change from Southern Europe, *Proceedings of the*  
1176 *National Academy of Sciences*, 104, 450–455, <https://doi.org/10.1073/pnas.0603321104>, 2007.
- 1177 Bringmans, P.: First Evidence of Neanderthal Presence in Northwest Europe during the Late Saalian  
1178 “Zeifen Interstadial” (MIS 6.01) found at the VLL and VLB Sites at Veldwezelt-Hezerwater, Belgium,  
1179 *Journal of Archaeology of Northwest Europe*, 1, 2007.
- 1180 Broecker, W. S. and Henderson, G. M.: The sequence of events surrounding Termination II and their  
1181 implications for the cause of glacial-interglacial CO<sub>2</sub> changes, *Paleoceanography*, 13, 352–364, 1998.
- 1182 Burns, S. J., Welsh, L. K., Scroxton, N., Cheng, H., and Edwards, R. L.: Millennial and orbital scale  
1183 variability of the South American Monsoon during the penultimate glacial period, *Sci Rep*, 9, 1234,  
1184 <https://doi.org/10.1038/s41598-018-37854-3>, 2019.
- 1185 Buzi, C., Profico, A., Lorenzo, C., and Manzi, G.: The first preserved nasal cavity in the human fossil  
1186 record: The Neanderthal from Altamura, *Proceedings of the National Academy of Sciences*, 122,  
1187 e2426309122, <https://doi.org/10.1073/pnas.2426309122>, 2025.
- 1188 Cacho, I., Grimalt, J. O., Pelejero, C., Canals, M., Sierro, F. J., Flores, J. A., and Shackleton, N.:  
1189 Dansgaard-Oeschger and Heinrich event imprints in Alboran Sea paleotemperatures,  
1190 *Paleoceanography*, 14, 698–705, <https://doi.org/10.1029/1999PA900044>, 1999.
- 1191 Cacho, I., Shackleton, N., Elderfield, H., Sierro, F. J., and Grimalt, J. O.: Glacial rapid variability in deep-  
1192 water temperature and  $\delta^{18}O$  from the Western Mediterranean Sea, *Quaternary Science Reviews*, 25,  
1193 3294–3311, <https://doi.org/10.1016/j.quascirev.2006.10.004>, 2006.
- 1194 Camuera, J., Jiménez-Moreno, G., Ramos-Román, M. J., García-Alix, A., Toney, J. L., Anderson, R. S.,  
1195 Jiménez-Espejo, F., Bright, J., Webster, C., Yanes, Y., and Carrión, J. S.: Vegetation and climate  
1196 changes during the last two glacial-interglacial cycles in the western Mediterranean: A new long  
1197 pollen record from Padul (southern Iberian Peninsula), *Quaternary Science Reviews*, 205, 86–105,  
1198 <https://doi.org/10.1016/j.quascirev.2018.12.013>, 2019.
- 1199 Camuera, J., Ramos-Román, M. J., Jiménez-Moreno, G., García-Alix, A., Ilvonen, L., Ruha, L., Gil-  
1200 Romera, G., González-Sampériz, P., and Seppä, H.: Past 200 kyr hydroclimate variability in the  
1201 western Mediterranean and its connection to the African Humid Periods, *Sci Rep*, 12, 9050,  
1202 <https://doi.org/10.1038/s41598-022-12047-1>, 2022.
- 1203 Caro Gómez, J. A., Díaz Del Olmo, F., Artigas, R. C., Recio Espejo, J. M., and Barrera, C. B.:  
1204 Geoarchaeological alluvial terrace system in Tarazona: Chronostratigraphical transition of Mode 2 to  
1205 Mode 3 during the middle-upper pleistocene in the Guadalquivir River valley (Seville, Spain),  
1206 *Quaternary International*, 243, 143–160, <https://doi.org/10.1016/j.quaint.2011.04.022>, 2011.
- 1207 Chapman, M. R. and Shackleton, N. J.: Global ice-volume fluctuations, North Atlantic ice-rafting  
1208 events, and deep-ocean circulation changes between 130 and 70 ka, *Geology*, 27, 795,  
1209 [https://doi.org/10.1130/0091-7613\(1999\)027<0795:GIVFNA>2.3.CO;2](https://doi.org/10.1130/0091-7613(1999)027<0795:GIVFNA>2.3.CO;2), 1999.
- 1210 Chappellaz, J., Brook, E., Blunier, T., and Malaizé, B.: CH<sub>4</sub> and  $\delta^{18}O$  of O<sub>2</sub> records from Antarctic and  
1211 Greenland ice: A clue for stratigraphic disturbance in the bottom part of the Greenland Ice Core

a mis en forme : Anglais (États-Unis)

a mis en forme : Anglais (États-Unis)

1212 Project and the Greenland Ice Sheet Project 2 ice cores, *J. Geophys. Res.*, 102, 26547–26557,  
1213 <https://doi.org/10.1029/97JC00164>, 1997.

1214 Charton, L.: Vegetation and climate changes during the Middle to Upper Palaeolithic transition in the  
1215 southwestern Mediterranean: What happened to the last Neanderthals during Heinrich stadial 4?,  
1216 *Quaternary Science Reviews*, 2025.

1217 Charton, L., Combourieu-Nebout, N., Bertini, A., Lebreton, V., Peyron, O., Robles, M., Sassoone, D.,  
1218 and Moncel, M.-H.: Vegetation and climate changes during the Middle to Upper Palaeolithic  
1219 transition in the southwestern Mediterranean: What happened to the last Neanderthals during  
1220 Heinrich stadial 4?, 2025.

1221 Cheddadi, R. and Rossignol-Strick, M.: Eastern Mediterranean Quaternary paleoclimates from pollen  
1222 and isotope records of marine cores in the Nile Cone Area, *Paleoceanography*, 10, 291–300,  
1223 <https://doi.org/10.1029/94PA02672>, 1995.

1224 Cheng, H., Edwards, R. L., Wang, Y., Kong, X., Ming, Y., Kelly, M. J., Wang, X., Gallup, C. D., and Liu, W.:  
1225 A penultimate glacial monsoon record from Hulu Cave and two-phase glacial terminations, *Geology*,  
1226 34, 217–220, <https://doi.org/10.1130/G22289.1>, 2006.

1227 Chevalier, M., Davis, B. A. S., Heiri, O., Seppä, H., Chase, B. M., Gajewski, K., Lacourse, T., Telford, R.  
1228 J., Finsinger, W., Guiot, J., Köhler, N., Maezumi, S. Y., Tipton, J. R., Carter, V. A., Brussel, T., Phelps, L. N.,  
1229 Dawson, A., Zanon, M., Vallé, F., Nolan, C., Mauri, A., de Vernal, A., Izumi, K., Holmström, L.,  
1230 Marsicek, J., Goring, S., Sommer, P. S., Chaput, M., and Kupriyanov, D.: Pollen-based climate  
1231 reconstruction techniques for late Quaternary studies, *Earth-Science Reviews*, 210,  
1232 <https://doi.org/10.1016/j.earscirev.2020.103384>, 2020.

1233 Colleoni, F., Wekerle, C., Näslund, J.-O., Brandefelt, J., and Masina, S.: Constraint on the penultimate  
1234 glacial maximum Northern Hemisphere ice topography ( $\approx 140$  kyrs BP), *Quaternary Science Reviews*,  
1235 137, 97–112, <https://doi.org/10.1016/j.quascirev.2016.01.024>, 2016.

1236 Combourieu-Nebout, N., Turon, J. L., Zahn, R., Capotondi, L., Londeix, L., and Pahnke, K.: Enhanced  
1237 aridity and atmospheric high-pressure stability over the western Mediterranean during the North  
1238 Atlantic cold events of the past 50 k.y., *Geol*, 30, 863, [https://doi.org/10.1130/0091-7613\(2002\)030<0863:EAAAHP>2.0.CO;2](https://doi.org/10.1130/0091-7613(2002)030<0863:EAAAHP>2.0.CO;2), 2002.

1240 Combourieu-Nebout, N., Peyron, O., Dormoy, I., Desprat, S., Célia, B., Kotthoff, U., and Marret, F.:  
1241 Rapid climatic variability in the west Mediterranean during the last 25 000 years from high resolution  
1242 pollen data, *Climate of the Past*, 5, <https://doi.org/10.5194/cpd-5-671-2009>, 2009.

1243 Cortina, A., Sierro, F. J., Flores, J. A., Martrat, B., and Grimalt, J. O.: The response of SST to insolation  
1244 and ice sheet variability from MIS 3 to MIS 11 in the northwestern Mediterranean Sea (Gulf of Lions),  
1245 *Geophysical Research Letters*, 42, 10,366-10,374, <https://doi.org/10.1002/2015GL065539>, 2015.

1246 Couture-Veschambre, C., López-Onaindia, D., Sala, N., Arlegi, M., Balzeau, A., Crevecoeur, I.,  
1247 Maureille, B., Tournepiche, J.-F., and Gómez-Olivencia, A.: Reassessment of the Neandertal fossil  
1248 collection from Abri Suard (La Chaise de Vouthon, Charente, France), *Bulletins et mémoires de la*  
1249 *Société d'Anthropologie de Paris. BMSAP*, 33, <https://doi.org/10.4000/bmsap.6982>, 2021.

1250 Cueto, S., Preysler, J., Pérez-González, A., Torres, C., Pérez, I., and Miguel, J.: Acheulian flint quarries  
1251 in the Madrid Tertiary basin, central Iberian Peninsula: First data obtained from geoarchaeological  
1252 studies, *Quaternary International*, 411, <https://doi.org/10.1016/j.quaint.2016.01.041>, 2016.

1253 Cunha, P. P., Almeida, N. A. C., Aubry, T., Martins, A. A., Murray, A. S., Buylaert, J.-P., Sohbati, R.,  
1254 Raposo, L., and Rocha, L.: Records of human occupation from Pleistocene river terrace and aeolian  
1255 sediments in the Arneiro depression (Lower Tejo River, central eastern Portugal), *Geomorphology*,  
1256 165–166, 78–90, <https://doi.org/10.1016/j.geomorph.2012.02.017>, 2012.

1257 Cunha, P. P., Martins, A. A., Buylaert, J.-P., Murray, A. S., Raposo, L., Mozzi, P., and Stokes, M.: New  
1258 data on the chronology of the Vale do Forno sedimentary sequence (Lower Tejo River terrace  
1259 staircase) and its relevance as a fluvial archive of the Middle Pleistocene in western Iberia,  
1260 *Quaternary Science Reviews*, 166, 204–226, <https://doi.org/10.1016/j.quascirev.2016.11.001>, 2017.

1261 Damialis, A., Kaimakamis, E., Konoglou, M., Akritidis, I., Traidl-Hoffmann, C., and Gioulekas, D.:  
1262 Estimating the abundance of airborne pollen and fungal spores at variable elevations using an  
1263 aircraft: how high can they fly?, *Sci Rep*, 7, 44535, <https://doi.org/10.1038/srep44535>, 2017.

1264 Dansgaard, W., Johnsen, S. J., Clausen, H. B., Dahl-Jensen, D., Gundestrup, N. S., Hammer, C. U.,  
1265 Hvidberg, C. S., Steffensen, J. P., Sveinbjörnsdóttir, A. E., and Jouzel, J.: Evidence for general  
1266 instability of past climate from a 250-kyr ice-core record, *Nature*, 364, 218–220, 1993.

1267 Davtian, N. and Bard, E.: A new view on abrupt climate changes and the bipolar seesaw based on  
1268 paleotemperatures from Iberian Margin sediments, *Proceedings of the National Academy of  
1269 Sciences*, 120, e2209558120, <https://doi.org/10.1073/pnas.2209558120>, 2023.

1270 Dennell, R. W., Martínón-Torres, M., and Bermúdez de Castro, J. M.: Hominin variability, climatic  
1271 instability and population demography in Middle Pleistocene Europe, *Quaternary Science Reviews*,  
1272 30, 1511–1524, <https://doi.org/10.1016/j.quascirev.2009.11.027>, 2011.

1273 D’Errico, F. and Sánchez Goñi, M. F. S.: Neandertal extinction and the millennial scale climatic  
1274 variability of OIS 3, *Quaternary Science Reviews*, 22, 769–788, [https://doi.org/10.1016/S0277-3791\(03\)00009-X](https://doi.org/10.1016/S0277-3791(03)00009-X), 2003.

1276 Di Vincenzo, F. and Manzi, G.: Homo heidelbergensis as the Middle Pleistocene common ancestor of  
1277 Denisovans, Neanderthals and modern humans, *Journal of Mediterranean Earth Sciences*, Vol. 15  
1278 (2023): In progress, <https://doi.org/10.13133/2280-6148/18074>, 2023.

1279 Díez-Martín, F.: Evaluating the effect of plowing on the archaeological record: The early middle  
1280 palaeolithic in the river Duero basin plateaus (north-central Spain), *Quaternary International*, 214,  
1281 30–43, <https://doi.org/10.1016/j.quaint.2009.10.024>, 2010.

1282 Díez-Martín, F., Sánchez-Yustos, P., Gómez-González, J. Á., and Gómez De La Rúa, D.: Earlier  
1283 Palaeolithic Settlement Patterns: Landscape Archaeology on the River Duero Basin Plateaus (Castilla y  
1284 León, Spain), *J World Prehist*, 21, 103–137, <https://doi.org/10.1007/s10963-008-9012-0>, 2008.

1285 D’Oliveira, L., Dugerdil, L., Ménot, G., Evin, A., Muller, S., Ansanay-Alex, S., Azuara, J., Bonnet, C.,  
1286 Bremond, L., Shah, M., and Peyron, O.: Reconstructing 15 000 years of southern France temperatures  
1287 from coupled pollen and molecular (branched glycerol dialkyl glycerol tetraether) markers (Canroute,  
1288 Massif Central), *Climate of the Past*, 19, 2127–2156, <https://doi.org/10.5194/cp-19-2127-2023>, 2023.

1289 Drysdale, R. N., Zanchetta, G., Hellstrom, J. C., Fallick, A. E., and Zhao, J.: Stalagmite evidence for the  
1290 onset of the Last Interglacial in southern Europe at  $129 \pm 1$  ka, *Geophysical Research Letters*, 32,  
1291 <https://doi.org/10.1029/2005GL024658>, 2005.

1292 Ehlers, J. and Gibbard, P. L.: The extent and chronology of Cenozoic Global Glaciation, *Quaternary  
1293 International*, 164–165, 6–20, <https://doi.org/10.1016/j.quaint.2006.10.008>, 2007a.

- 1294 Ehlers, J. and Gibbard, P. L.: The extent and chronology of Cenozoic Global Glaciation, *Quaternary*  
1295 *International*, 164–165, 6–20, <https://doi.org/10.1016/j.quaint.2006.10.008>, 2007b.
- 1296 Ehlers, J., Grube, A., Stephan, H.-J., and Wansa, S.: Pleistocene Glaciations of North Germany—New  
1297 Results, in: *Developments in Quaternary Sciences*, vol. 15, Elsevier, 149–162,  
1298 <https://doi.org/10.1016/B978-0-444-53447-7.00013-1>, 2011.
- 1299 Ehlers, J., Gibbard, P. L., and Hughes, P. D.: Chapter 4 - Quaternary Glaciations and Chronology, in:  
1300 *Past Glacial Environments (Second Edition)*, edited by: Menzies, J. and van der Meer, J. J. M., Elsevier,  
1301 77–101, <https://doi.org/10.1016/B978-0-08-100524-8.00003-8>, 2018.
- 1302 Emeis, K., Schulz, H., Struck, U., Rossignol-Strick, M., Erlenkeuser, H., Howell, M., Kroon, D.,  
1303 Mackensen, A., Ishizuka, S., Oba, T., Sakamoto, T., and Koizumi, I.: Eastern Mediterranean surface  
1304 water temperatures and  $\delta^{18}\text{O}$  composition during deposition of sapropels in the late Quaternary,  
1305 *Paleoceanography*, 18, 1005, <https://doi.org/10.1029/2000PA000617>, 2003a.
- 1306 Emeis, K.-C., Schulz, H., Struck, U., Rossignol-Strick, M., Erlenkeuser, H., Howell, M. W., Kroon, D.,  
1307 Mackensen, A., Ishizuka, S., Oba, T., Sakamoto, T., and Koizumi, I.: Eastern Mediterranean surface  
1308 water temperatures and  $\delta^{18}\text{O}$  composition during deposition of sapropels in the late Quaternary,  
1309 *Paleoceanography*, 18, <https://doi.org/10.1029/2000PA000617>, 2003b.
- 1310 Eynaud, F., Zaragosi, S., Scourse, J. D., Mojtahid, M., Bourillet, J. F., Hall, I. R., Penaud, A., Locascio,  
1311 M., and Reijonen, A.: Deglacial laminated facies on the NW European continental margin: The  
1312 hydrographic significance of British-Irish Ice Sheet deglaciation and Fleuve Manche paleoriver  
1313 discharges, *Geochemistry, Geophysics, Geosystems*, 8, <https://doi.org/10.1029/2006GC001496>,  
1314 2007.
- 1315 Faegri, K. and Iversen, J.: *Textbook of Pollen Analysis*, 4th Edition., John Wiley and Sons, Chichester,  
1316 UK, 338 pp., 1964.
- 1317 Fernández Peris, J., Barciela, V., Blasco, R., Cuartero, F., and Sañudo, P.: El Paleolítico Medio en el  
1318 territorio valenciano y la variabilidad tecno-económica de la Cova del Bolomor, *Treballs*  
1319 *d'Arqueologia*, 141–169, 2008.
- 1320 Fernández-Rodríguez, S., Skjøth, C. A., Tormo-Molina, R., Brandao, R., Caeiro, E., Silva-Palacios, I.,  
1321 Gonzalo-Garijo, A., and Smith, M.: Identification of potential sources of airborne *Olea* pollen in the  
1322 Southwest Iberian Peninsula, *Int J Biometeorol*, 58, 337–348, <https://doi.org/10.1007/s00484-012-0629-4>, 2014.
- 1324 Finlayson, C. and Carrión, J. S.: Rapid ecological turnover and its impact on Neanderthal and other  
1325 human populations, *Trends in Ecology & Evolution*, 22, 213–222,  
1326 <https://doi.org/10.1016/j.tree.2007.02.001>, 2007.
- 1327 Fletcher, W. J. and Sánchez Goñi, M. F.: Orbital- and sub-orbital-scale climate impacts on vegetation  
1328 of the western Mediterranean basin over the last 48,000 yr, *Quaternary Research*, 70, 451–464,  
1329 <https://doi.org/10.1016/j.yqres.2008.07.002>, 2008.
- 1330 Fletcher, W. J., Sánchez Goñi, M. F., Allen, J. R. M., Cheddadi, R., Combourieu-Nebout, N., Huntley, B.,  
1331 Lawson, I., Londeix, L., Magri, D., Margari, V., Müller, U. C., Naughton, F., Novenko, E., Roucoux, K.,  
1332 and Tzedakis, P. C.: Millennial-scale variability during the last glacial in vegetation records from  
1333 Europe, *Quaternary Science Reviews*, 29, 2839–2864,  
1334 <https://doi.org/10.1016/j.quascirev.2009.11.015>, 2010.

a mis en forme : Anglais (États-Unis)

a mis en forme : Espagnol (Espagne)

a mis en forme : Anglais (États-Unis)

1335 Foerster, V., Asrat, A., Bronk Ramsey, C., Brown, E. T., Chapot, M. S., Deino, A., Duesing, W., Grove,  
1336 M., Hahn, A., Junginger, A., Kaboth-Bahr, S., Lane, C. S., Opitz, S., Noren, A., Roberts, H. M.,  
1337 Stockhecke, M., Tiedemann, R., Vidal, C. M., Vogelsang, R., Cohen, A. S., Lamb, H. F., Schaebitz, F.,  
1338 and Trauth, M. H.: Pleistocene climate variability in eastern Africa influenced hominin evolution, *Nat*  
1339 *Geosci*, 15, 805–811, <https://doi.org/10.1038/s41561-022-01032-y>, 2022.

1340 Follieri, M., Magri, D., and Sadori, L.: A 250 000-years pollen record from Valle di Castiglione (Roma),  
1341 *Pollen et Spores*, 30, 329–356, 1988.

1342 Fontana, F., Nenzioni, G., and Peretto, C.: The southern Po plain area (Italy) in the mid-late  
1343 Pleistocene: Human occupation and technical behaviours, *Quaternary International*, 223, 465–471,  
1344 <https://doi.org/10.1016/j.quaint.2010.02.013>, 2010.

1345 Gouzy, A., Malaizé, B., Pujol, C., and Charlier, K.: Climatic “pause” during Termination II identified in  
1346 shallow and intermediate waters off the Iberian margin, *Quaternary Science Reviews*, 23, 1523–1528,  
1347 <https://doi.org/10.1016/j.quascirev.2004.03.002>, 2004.

1348 von Grafenstein, R., Zahn, R., and Tiedemann, R.: Planktonic  $\delta^{18}O$  records at Sites 976 and 977,  
1349 Alboran Sea: stratigraphy, forcing, and paleoceanographic implications. In Curry, W.B., Shackleton,  
1350 N.J., and Richter, C., *Proceedings Ocean Drilling Program Scientific Results*, 154, 299–318, 1999.

1351 Guiot, J.: Methodology of the last climatic cycle reconstruction in France from pollen data,  
1352 *Palaeogeography, Palaeoclimatology, Palaeoecology*, 80, 49–69, [https://doi.org/10.1016/0031-](https://doi.org/10.1016/0031-0182(90)90033-4)  
1353 [0182\(90\)90033-4](https://doi.org/10.1016/0031-0182(90)90033-4), 1990.

1354 Guiot, J., Pons, A., De Beaulieu, J. L., and Reille, M.: A 140,000-year continental climate  
1355 reconstruction from two European pollen records, *Nature*, 338, 309–313,  
1356 <https://doi.org/10.1038/338309a0>, 1989.

1357 Guiot, J., De Beaulieu, J. L., Cheddadi, R., David, F., Poncelet, P., and Reille, M.: The climate in Western  
1358 Europe during the last Glacial/Interglacial cycle derived from pollen and insect remains,  
1359 *Palaeogeography, Palaeoclimatology, Palaeoecology*, 103, 73–93, [https://doi.org/10.1016/0031-](https://doi.org/10.1016/0031-0182(93)90053-L)  
1360 [0182\(93\)90053-L](https://doi.org/10.1016/0031-0182(93)90053-L), 1993.

1361 Heinrich, H.: Origin and Consequences of Cyclic Ice Rafting in the Northeast Atlantic Ocean During the  
1362 Past 130,000 Years, *Quaternary Research*, 29, 142–152, [https://doi.org/10.1016/0033-](https://doi.org/10.1016/0033-5894(88)90057-9)  
1363 [5894\(88\)90057-9](https://doi.org/10.1016/0033-5894(88)90057-9), 1988.

1364 Held, F., Cheng, H., Edwards, R. L., Tüysüz, O., Koç, K., and Fleitmann, D.: Dansgaard-Oeschger cycles  
1365 of the penultimate and last glacial period recorded in stalagmites from Türkiye, *Nat Commun*, 15,  
1366 1183, <https://doi.org/10.1038/s41467-024-45507-5>, 2024.

1367 Hemming, S. R.: Heinrich events: Massive late Pleistocene detritus layers of the North Atlantic and  
1368 their global climate imprint, *Reviews of Geophysics*, 42, <https://doi.org/10.1029/2003RG000128>,  
1369 2004.

1370 Hérisson, D., Brenet, M., Cliquet, D., Moncel, M.-H., Richter, J., Scott, B., Van Baelen, A., Di Modica,  
1371 K., Loecker, D., Ashton, N., Bourguignon, L., Delagnes, A., Faivre, J.-P., Folgado-Lopez, M., Locht, J.-L.,  
1372 Pope, M., Raynal, J.-P., Roebroeks, W., Santagata, C., and Peer, P.: The emergence of the Middle  
1373 Palaeolithic in north-western Europe and its southern fringes, *Quaternary International*, 411,  
1374 <https://doi.org/10.1016/j.quaint.2016.02.049>, 2016.

1375 Hersbach, H., Bell, B., Berrisford, P., Hirahara, S., Horányi, A., Muñoz-Sabater, J., Nicolas, J., Peubey,  
1376 C., Radu, R., Schepers, D., Simmons, A., Soci, C., Abdalla, S., Abellan, X., Balsamo, G., Bechtold, P.,  
1377 Biavati, G., Bidlot, J., Bonavita, M., De Chiara, G., Dahlgren, P., Dee, D., Diamantakis, M., Dragani, R.,  
1378 Flemming, J., Forbes, R., Fuentes, M., Geer, A., Haimberger, L., Healy, S., Hogan, R. J., Hólm, E.,  
1379 Janisková, M., Keeley, S., Laloyaux, P., Lopez, P., Lupu, C., Radnoti, G., de Rosnay, P., Rozum, I.,  
1380 Vamborg, F., Villaume, S., and Thépaut, J.-N.: The ERA5 global reanalysis, *Quarterly Journal of the*  
1381 *Royal Meteorological Society*, 146, 1999–2049, <https://doi.org/10.1002/qj.3803>, 2020.

1382 Hodell, D. A., Channell, J. E. T., Curtis, J. H., Romero, O. E., and Röhl, U.: Onset of “Hudson Strait”  
1383 Heinrich events in the eastern North Atlantic at the end of the middle Pleistocene transition (~640  
1384 ka)?, *Paleoceanography*, 23, 2008PA001591, <https://doi.org/10.1029/2008PA001591>, 2008.

1385 Hodell, D. A., Crowhurst, S. J., Lourens, L., Margari, V., Nicolson, J., Rolfe, J. E., Skinner, L. C., Thomas,  
1386 N. C., Tzedakis, P. C., Mlenek-Vautravets, M. J., and Wolff, E. W.: A 1.5-million-year record of orbital  
1387 and millennial climate variability in the North Atlantic, *Clim. Past*, 19, 607–636,  
1388 <https://doi.org/10.5194/cp-19-607-2023>, 2023.

1389 Hodge, E., Richards, D., Smart, P., Andreo, B., Hoffmann, D., Matthey, D., and González-Ramón, A.:  
1390 Effective precipitation in southern Spain (~ 266 to 46 ka) based on a speleothem stable carbon  
1391 isotope record, *Quaternary Research*, 69, 447–457, <https://doi.org/10.1016/j.yqres.2008.02.013>,  
1392 2008.

1393 Hublin, J. J.: The origin of Neandertals, *Proceedings of the National Academy of Sciences*, 106,  
1394 16022–16027, <https://doi.org/10.1073/pnas.0904119106>, 2009.

1395 Jiménez-Amat, P. and Zahn, R.: Offset timing of climate oscillations during the last two glacial-  
1396 interglacial transitions connected with large-scale freshwater perturbation, *Paleoceanography*, 30,  
1397 768–788, <https://doi.org/10.1002/2014PA002710>, 2015.

1398 Jiménez-Moreno, G., Anderson, R. S., Ramos-Román, M. J., Camuera, J., Mesa-Fernández, J. M.,  
1399 García-Alix, A., Jiménez-Espejo, F. J., Carrión, J. S., and López-Avilés, A.: The Holocene Cedrus pollen  
1400 record from Sierra Nevada (S Spain), a proxy for climate change in N Africa, *Quaternary Science*  
1401 *Reviews*, 242, 106468, <https://doi.org/10.1016/j.quascirev.2020.106468>, 2020.

1402 Johnsen, S. J., Clausen, H. B., Dansgaard, W., Fuhrer, K., Gundestrup, N., Hammer, C. U., Iversen, P.,  
1403 Jouzel, J., Stauffer, B., and Steffensen, J. P.: Irregular glacial interstadials recorded in a new Greenland  
1404 record, *Nature*, 359, 311–313, 1992.

1405 Jouzel, J., Masson-Delmotte, V., Cattani, O., Dreyfus, G., Falourd, S., Hoffmann, G., Minster, B.,  
1406 Nouet, J., Barnola, J. M., Chappellaz, J., Fischer, H., Gallet, J. C., Johnsen, S., Leuenberger, M.,  
1407 Loulergue, L., Luethi, D., Oerter, H., Parrenin, F., Raisbeck, G., Raynaud, D., Schilt, A., Schwander, J.,  
1408 Selmo, E., Souchez, R., Spahni, R., Stauffer, B., Steffensen, J. P., Stenni, B., Stocker, T. F., Tison, J. L.,  
1409 Werner, M., and Wolff, E. W.: Orbital and millennial Antarctic climate variability over the past  
1410 800,000 years, *Science*, 317, 793–796, <https://doi.org/10.1126/science.1141038>, 2007.

1411 Kallel, N., Duplessy, J.-C., Labeyrie, L., Fontugne, M., Paterne, M., and Montacer, M.: Mediterranean  
1412 pluvial periods and sapropel formation over the last 200 000 years, *Palaeogeography*,  
1413 *Palaeoclimatology, Palaeoecology*, 157, 45–58, [https://doi.org/10.1016/S0031-0182\(99\)00149-2](https://doi.org/10.1016/S0031-0182(99)00149-2),  
1414 2000.

1415 Kelly, M., Edwards, R., Cheng, H., Yuan, D., Cai, Y., Zhang, M., Lin, Y., and An, Z.: High resolution  
1416 characterization of the Asian Monsoon between 146,000 and 99,000 years B.P. from Dongge Cave,

1417 China and global correlation of events surrounding Termination II, *Palaeogeography,*  
1418 *Palaeoclimatology, Palaeoecology*, 236, 20–38, <https://doi.org/10.1016/j.palaeo.2005.11.042>, 2006.

1419 Key, A. J. M., Jarić, I., and Roberts, D. L.: Modelling the end of the Acheulean at global and continental  
1420 levels suggests widespread persistence into the Middle Palaeolithic, *Humanit Soc Sci Commun*, 8, 55,  
1421 <https://doi.org/10.1057/s41599-021-00735-8>, 2021.

1422 Koltai, G., Spötl, C., Shen, C.-C., Wu, C.-C., Rao, Z., Palcsu, L., Kele, S., Surányi, G., and Bárányi-Kevei, I.:  
1423 A penultimate glacial climate record from southern Hungary, *Journal of Quaternary Science*, 32, 946–  
1424 956, <https://doi.org/10.1002/jqs.2968>, 2017.

1425 Koutsodendris, A., Dakos, V., Fletcher, W. J., Knipping, M., Kotthoff, U., Milner, A. M., Müller, U. C.,  
1426 Kaboth-Bahr, S., Kern, O. A., Kolb, L., Vakhrameeva, P., Wulf, S., Christanis, K., Schmiedl, G., and  
1427 Pross, J.: Atmospheric CO<sub>2</sub> forcing on Mediterranean biomes during the past 500 kyrs, *Nat Commun*,  
1428 14, 1664, <https://doi.org/10.1038/s41467-023-37388-x>, 2023.

1429 Laskar, J., Robutel, P., Joutel, F., Gastineau, M., Correia, A. C. M., and Levrard, B.: A long-term  
1430 numerical solution for the insolation quantities of the Earth, *A&A*, 428, 261–285,  
1431 <https://doi.org/10.1051/0004-6361:20041335>, 2004.

1432 Lewis, S., Ashton, N., and Jacobi, R.: 9 - Testing Human Presence During the Last Interglacial (MIS 5e):  
1433 A Review of the British Evidence, in: *Developments in Quaternary Sciences*, vol. 14, edited by:  
1434 Ashton, N., Lewis, S. G., and Stringer, C., Elsevier, 125–164, <https://doi.org/10.1016/B978-0-444-53597-9.00009-1>, 2011.

1436 Li, T.-Y., Shen, C.-C., Huang, L.-J., Jiang, X.-Y., Yang, X.-L., Mii, H.-S., Lee, S.-Y., and Lo, L.: Stalagmite-  
1437 inferred variability of the Asian summer monsoon during the penultimate glacial–interglacial period,  
1438 *Climate of the Past*, 10, 1211–1219, <https://doi.org/10.5194/cp-10-1211-2014>, 2014.

1439 Lionello, P., Malanotte-Rizzoli, P., Boscolo, R., Alpert, P., Artale, V., Li, L., Luterbacher, J., May, W.,  
1440 Trigo, R., Tsimplis, M., Ulbrich, U., and Xoplaki, E.: The Mediterranean climate: An overview of the  
1441 main characteristics and issues, in: *Developments in Earth and Environmental Sciences*, vol. 4, edited  
1442 by: Lionello, P., Malanotte-Rizzoli, P., and Boscolo, R., Elsevier, 1–26, [https://doi.org/10.1016/S1571-9197\(06\)80003-0](https://doi.org/10.1016/S1571-9197(06)80003-0), 2006.

1444 Lisiecki, L. and Raymo, M.: Pliocene-Pleistocene stack of 57 globally distributed benthic 18O records.,  
1445 *Paleoceanography*, 20, <https://doi.org/10.1029/2004PA001071>, 2005.

1446 Lisiecki, L. E. and Stern, J. V.: Regional and global benthic  $\delta^{18}\text{O}$  stacks for the last glacial cycle,  
1447 *Paleoceanography*, 31, 1368–1394, <https://doi.org/10.1002/2016PA003002>, 2016.

1448 Liu, J., Fang, N., Wang, F., Yang, F., and Ding, X.: Features of ice-rafted debris (IRD) at IODP site U1312  
1449 and their palaeoenvironmental implications during the last 2.6 Myr, *Palaeogeography,*  
1450 *Palaeoclimatology, Palaeoecology*, 511, 364–378, <https://doi.org/10.1016/j.palaeo.2018.09.002>,  
1451 2018.

1452 de Lumley, M. A.: Les restes humains fossiles de la grotte du Lazaret. Généralités, approche  
1453 démographique., in: *Les restes humains fossiles de la grotte du Lazaret, Nice, Alpes-Maritimes. Des*  
1454 *Homo erectus européens évolués en voie de néandertalisation*, CNRS Editions, 217–220, 2018.

1455 Macklin, M. G., Fuller, I. C., Lewin, J., Maas, G. S., Passmore, D. G., Rose, J., Woodward, J. C., Black, S.,  
1456 Hamlin, R. H. B., and Rowan, J. S.: Correlation of fluvial sequences in the Mediterranean basin over

a mis en forme : Anglais (États-Unis)

a mis en forme : Anglais (États-Unis)

1457 the last 200 ka and their relationship to climate change, *Quaternary Science Reviews*, 21, 1633–  
1458 1641, [https://doi.org/10.1016/S0277-3791\(01\)00147-0](https://doi.org/10.1016/S0277-3791(01)00147-0), 2002.

1459 Magri, D. and Parra, I.: Late Quaternary western Mediterranean pollen records and African winds,  
1460 *Earth and Planetary Science Letters*, 200, 401–408, [https://doi.org/10.1016/S0012-821X\(02\)00619-2](https://doi.org/10.1016/S0012-821X(02)00619-2),  
1461 2002.

1462 Margari, V., Skinner, L. C., Tzedakis, P. C., Ganopolski, A., Vautravers, M., and Shackleton, N. J.: The  
1463 nature of millennial-scale climate variability during the past two glacial periods, *Nature Geosci*, 3,  
1464 127–131, <https://doi.org/10.1038/ngeo740>, 2010.

1465 Margari, V., Skinner, L., Hodell, D., Martrat, B., Toucanne, S., Gibbard, P., Lunkka, J., and Tzedakis, C.:  
1466 Land-ocean changes on orbital and millennial time scales and the penultimate glaciation, *Geology*,  
1467 <https://doi.org/10.1130/G35070.1>, 2014.

1468 Martrat, B., Grimalt, J. O., Lopez-Martinez, C., Cacho, I., Sierro, F. J., Flores, J. A., Zahn, R., Canals, M.,  
1469 Curtis, J. H., and Hodell, D. A.: Abrupt Temperature Changes in the Western Mediterranean over the  
1470 Past 250,000 Years, *Science*, 306, 1762–1765, <https://doi.org/10.1126/science.1101706>, 2004.

1471 Martrat, B., Grimalt, J. O., Shackleton, N. J., de Abreu, L., Hutterli, M. A., and Stocker, T. F.: Four  
1472 Climate Cycles of Recurring Deep and Surface Water Destabilizations on the Iberian Margin, *Science*,  
1473 317, 502–507, <https://doi.org/10.1126/science.1139994>, 2007.

1474 Martrat, B., Jimenez-Amat, P., Zahn, R., and Grimalt, J. O.: Similarities and dissimilarities between the  
1475 last two deglaciations and interglaciations in the North Atlantic region, *Quaternary Science Reviews*,  
1476 99, 122–134, <https://doi.org/10.1016/j.quascirev.2014.06.016>, 2014.

1477 Masson-Delmotte, V., Stenni, B., Pol, K., Braconnot, P., Cattani, O., Falourd, S., Kageyama, M., Jouzel,  
1478 J., Landais, A., Minster, B., Barnola, J. M., Chappellaz, J., Krinner, G., Johnsen, S., Röthlisberger, R.,  
1479 Hansen, J., Mikolajewicz, U., and Otto-Bliesner, B.: EPICA Dome C record of glacial and interglacial  
1480 intensities, *Quaternary Science Reviews*, 29, 113–128,  
1481 <https://doi.org/10.1016/j.quascirev.2009.09.030>, 2010.

1482 Mathias, C., Bourguignon, L., Brenet, M., Grégoire, S., and Moncel, M.-H.: Between new and  
1483 inherited technical behaviours: a case study from the Early Middle Palaeolithic of Southern France,  
1484 *Archaeol Anthropol Sci*, 12, 146, <https://doi.org/10.1007/s12520-020-01114-1>, 2020.

1485 Matthews, A., Affek, H. P., Ayalon, A., Vonhof, H. B., and Bar-Matthews, M.: Eastern Mediterranean  
1486 climate change deduced from the Soreq Cave fluid inclusion stable isotopes and carbonate clumped  
1487 isotopes record of the last 160 ka, *Quaternary Science Reviews*, 272, 107223,  
1488 <https://doi.org/10.1016/j.quascirev.2021.107223>, 2021.

1489 McCarron, A. P., Bigg, G. R., Brooks, H., Leng, M. J., Marshall, J. D., Ponomareva, V., Portnyagin, M.,  
1490 Reimer, P. J., and Rogerson, M.: Northwest Pacific ice-rafted debris at 38°N reveals episodic ice-sheet  
1491 change in late Quaternary Northeast Siberia, *Earth and Planetary Science Letters*, 553, 116650,  
1492 <https://doi.org/10.1016/j.epsl.2020.116650>, 2021.

1493 McManus, J. F., Oppo, D. W., and Cullen, J. L.: A 0.5-Million-Year Record of Millennial-Scale Climate  
1494 Variability in the North Atlantic, *Science*, 283, 971–975,  
1495 <https://doi.org/10.1126/science.283.5404.971>, 1999.

1496 Melchionna, M., Di Febbraro, M., Carotenuto, F., Rook, L., Mondanaro, A., Castiglione, S., Serio, C.,  
1497 Vero, V. A., Tesone, G., Piccolo, M., Diniz-Filho, J. A. F., and Raia, P.: Fragmentation of Neanderthals'

1498 pre-extinction distribution by climate change, *Palaeogeography, Palaeoclimatology, Palaeoecology*,  
1499 496, 146–154, <https://doi.org/10.1016/j.palaeo.2018.01.031>, 2018.

1500 Menviel, L., Capron, E., Govin, A., Dutton, A., Tarasov, L., Abe-Ouchi, A., Drysdale, R. N., Gibbard, P.  
1501 L., Gregoire, L., He, F., Ivanovic, R. F., Kageyama, M., Kawamura, K., Landais, A., Otto-Bliesner, B. L.,  
1502 Oyabu, I., Tzedakis, P. C., Wolff, E., and Zhang, X.: The penultimate deglaciation: protocol for  
1503 Paleoclimate Modelling Intercomparison Project (PMIP) phase 4 transient numerical simulations  
1504 between 140 and 127 ka, version 1.0, *Geoscientific Model Development*, 12, 3649–3685,  
1505 <https://doi.org/10.5194/gmd-12-3649-2019>, 2019.

1506 Michel, V., Shen, G., Shen, C.-C., Duval, M., Woodhead, J., Chou, Y.-M., Hu, H.-M., Wu, C.-C., Kan, Y.-  
1507 C., Yang, H., Yu, T.-L., Gallet, S., and Valensi, P.: Datations radioisotopiques (U-Th, U-Pb) et  
1508 paléodosimétriques (ESR) des plus anciens sites préhistoriques des Alpes-Maritimes: la grotte du  
1509 Vallonnet, le site de plein air de Terra Amata et la grotte du Lazaret, in: *Bulletin du Musée*  
1510 *d'Anthropologie préhistorique de Monaco*, vol. 61, 65–80, 2022.

1511 Moncel, M., Vaissié, E., Marin, J., Fernandes, P., Abrunhosa, A., Hardy, B., Richard, M., Torres, C., and  
1512 Baena, J.: Early Middle Palaeolithic Occupations Dated to MIS 7 at the Abri du Maras (Ardèche,  
1513 Southeast France), *Journal of Paleolithic Archaeology*, 2025.

1514 Moncel, M.-H., Ashton, N., Arzarello, M., Fontana, F., Lamotte, A., Scott, B., Muttillio, B., Berruti, G.,  
1515 Nenzioni, G., Tuffreau, A., and Peretto, C.: Early Levallois core technology between Marine Isotope  
1516 Stage 12 and 9 in Western Europe, *Journal of Human Evolution*, 139, 102735,  
1517 <https://doi.org/10.1016/j.jhevol.2019.102735>, 2020.

1518 Moseley, G. E., Spötl, C., Cheng, H., Boch, R., Min, A., and Edwards, R. L.: Termination-II  
1519 interstadial/stadial climate change recorded in two stalagmites from the north European Alps,  
1520 *Quaternary Science Reviews*, 127, 229–239, <https://doi.org/10.1016/j.quascirev.2015.07.012>, 2015.

1521 Mudie, P.: Pollen distribution in recent marine sediments, eastern Canada, *Canadian Journal of Earth*  
1522 *Sciences*, 19, 729–747, <https://doi.org/10.1139/e82-062>, 2011.

1523 Murat, A. (Ed.): Chapitre 41 : Pliocene–pleistocene occurrence of sapropels in the western  
1524 mediterranean sea and their relation to eastern mediterranean sapropels, in: *Proceedings of the*  
1525 *Ocean Drilling Program, 161 Scientific Results*, vol. 161, Ocean Drilling Program,  
1526 <https://doi.org/10.2973/odp.proc.sr.161.1999>, 1999.

1527 Nehme, C., Verheyden, S., Breitenbach, S. F. M., Gillikin, D. P., Verheyden, A., Cheng, H., Edwards, R.  
1528 L., Hellstrom, J., Noble, S. R., Farrant, A. R., Sahy, D., Goovaerts, T., Salem, G., and Claeys, P.: Climate  
1529 dynamics during the penultimate glacial period recorded in a speleothem from Kanaan Cave,  
1530 Lebanon (central Levant), *Quaternary Research*, 90, 10–25, <https://doi.org/10.1017/qua.2018.18>,  
1531 2018.

1532 Nehme, C., Kluge, T., Verheyden, S., Nader, F., Charalambidou, I., Weissbach, T., Gucel, S., Cheng, H.,  
1533 Edwards, R. L., Satterfield, L., Eiche, E., and Claeys, P.: Speleothem record from Pentadactylos cave  
1534 (Cyprus): new insights into climatic variations during MIS 6 and MIS 5 in the Eastern Mediterranean,  
1535 *Quaternary Science Reviews*, 250, 106663, <https://doi.org/10.1016/j.quascirev.2020.106663>, 2020.

1536 Obrochta, S. P., Crowley, T. J., Channell, J. E. T., Hodell, D. A., Baker, P. A., Seki, A., and Yokoyama, Y.:  
1537 Climate variability and ice-sheet dynamics during the last three glaciations, *Earth and Planetary*  
1538 *Science Letters*, 406, 198–212, <https://doi.org/10.1016/j.epsl.2014.09.004>, 2014.

a mis en forme : Anglais (États-Unis)

- 1539 Ochando, J., Carrión, J. S., Blasco, R., Fernández, S., Amorós, G., Munuera, M., Sañudo, P., and  
1540 Fernández Peris, J.: Silvicolous Neanderthals in the far West: the mid-Pleistocene palaeoecological  
1541 sequence of Bolomor Cave (Valencia, Spain), *Quaternary Science Reviews*, 217, 247–267,  
1542 <https://doi.org/10.1016/j.quascirev.2019.03.015>, 2019.
- 1543 Okuda, M., Yasuda, Y., and Setoguchi, T.: Middle to Late Pleistocene vegetation history and climatic  
1544 changes at Lake Kopais, Southeast Greece, *Boreas*, 30, 73–82, <https://doi.org/10.1111/j.1502-3885.2001.tb00990.x>, 2001.
- 1546 Oppo, D. W., Keigwin, L. D., McManus, J. F., and Cullen, J. L.: Persistent suborbital climate variability  
1547 in marine isotope stage 5 and termination II, *Paleoceanography*, 16, 280–292,  
1548 <https://doi.org/10.1029/2000PA000527>, 2001.
- 1549 Oppo, D. W., McManus, J. F., and Cullen, J. L.: Evolution and demise of the Last Interglacial warmth in  
1550 the subpolar North Atlantic, *Quaternary Science Reviews*, 25, 3268–3277,  
1551 <https://doi.org/10.1016/j.quascirev.2006.07.006>, 2006.
- 1552 Ovsepyan, E. A. and Murdmaa, I. O.: Response of the bering sea to Heinrich Event 11, *Lithol Miner  
1553 Resour*, 52, 442–446, <https://doi.org/10.1134/S0024490217060062>, 2017.
- 1554 Panera, J., Torres, T., Pérez-González, A., Ortiz, J. E., Rubio-Jara, S., and Val, D. U. del: Geocronología  
1555 de la Terraza Compleja de Arganda en el valle del río Jarama (Madrid, España), *Estudios Geológicos*,  
1556 67, 495–504, <https://doi.org/10.3989/egeol.40550.204>, 2011.
- 1557 Panera, J., Rubio-Jara, S., Yravedra, J., Blain, H.-A., Sesé, C., and Pérez-González, A.: Manzanares  
1558 Valley (Madrid, Spain): A good country for Proboscideans and Neanderthals, *Quaternary  
1559 International*, 326–327, 329–343, <https://doi.org/10.1016/j.quaint.2013.09.009>, 2014.
- 1560 Penaud, A., Eynaud, F., Turon, J. L., Zaragosi, S., Malaizé, B., Toucanne, S., and Bourillet, J. F.: What  
1561 forced the collapse of European ice sheets during the last two glacial periods (150 ka B.P. and  
1562 18 ka cal B.P.)? Palynological evidence, *Palaeogeography, Palaeoclimatology, Palaeoecology*, 281,  
1563 66–78, <https://doi.org/10.1016/j.palaeo.2009.07.012>, 2009.
- 1564 Penaud, A., Eynaud, F., Voelker, A. H. L., and Turon, J.-L.: Palaeohydrological changes over the last 50  
1565 ky in the central Gulf of Cadiz: complex forcing mechanisms mixing multi-scale processes,  
1566 *Biogeosciences*, 13, 5357–5377, <https://doi.org/10.5194/bg-13-5357-2016>, 2016.
- 1567 Pereira, T., Cunha, P. P., Martins, A. A., Nora, D., Paixão, E., Figueiredo, O., Raposo, L., Henriques, F.,  
1568 Caninas, J., Moura, D., and Bridgland, D. R.: Geoarchaeology of the Cobrinhos site (Vila Velha de  
1569 Ródão, Portugal) - a record of the earliest Mousterian in western Iberia, *Journal of Archaeological  
1570 Science: Reports*, 24, 640–654, <https://doi.org/10.1016/j.jasrep.2018.11.026>, 2019.
- 1571 Pérez-Asensio, J. N., Frigola, J., Pena, L. D., Sierro, F. J., Reguera, M. I., Rodríguez-Tovar, F. J., Dorador,  
1572 J., Asioli, A., Kuhlmann, J., Huhn, K., and Cacho, I.: Changes in western Mediterranean thermohaline  
1573 circulation in association with a deglacial Organic Rich Layer formation in the Alboran Sea,  
1574 *Quaternary Science Reviews*, 228, 106075, <https://doi.org/10.1016/j.quascirev.2019.106075>, 2020.
- 1575 Peyrégne, S., Slon, V., Mafessoni, F., de Filippo, C., Hajdinjak, M., Nagel, S., Nickel, B., Essel, E., Le  
1576 Cabec, A., Wehrberger, K., Conard, N. J., Kind, C. J., Posth, C., Krause, J., Abrams, G., Bonjean, D., Di  
1577 Modica, K., Toussaint, M., Kelso, J., Meyer, M., Pääbo, S., and Prüfer, K.: Nuclear DNA from two early  
1578 Neandertals reveals 80,000 years of genetic continuity in Europe, *Science Advances*, 5, eaaw5873,  
1579 <https://doi.org/10.1126/sciadv.aaw5873>, 2019.

a mis en forme : Espagnol (Espagne)

a mis en forme : Anglais (États-Unis)

1580 Pini, R., Ravazzi, C., and Donegana, M.: Pollen stratigraphy, vegetation and climate history of the last  
1581 215 ka in the Azzano Decimo core (plain of Friuli, north-eastern Italy), *Quaternary Science Reviews*,  
1582 28, 1268–1290, <https://doi.org/10.1016/j.quascirev.2008.12.017>, 2009.

1583 Prasad, A. M., Iverson, L. R., and Liaw, A.: Newer Classification and Regression Tree Techniques:  
1584 Bagging and Random Forests for Ecological Prediction, *Ecosystems*, 9, 181–199,  
1585 <https://doi.org/10.1007/s10021-005-0054-1>, 2006.

1586 Quézel, P.: *Réflexions sur l'évolution de la flore et de la végétation au Maghreb Méditerranéen*, Ibis  
1587 Press., Paris, 117 pp., 2000.

1588 Raia, P., Mondanaro, A., Melchionna, M., Di Febbraro, M., Diniz-Filho, J. A., Rangel, T., Holden, P.,  
1589 Carotenuto, F., Edwards, N., Lima-Ribeiro, M., Profico, A., Maiorano, L., Castiglione, S., Serio, C., and  
1590 Rook, L.: Past Extinctions of Homo Species Coincided with Increased Vulnerability to Climatic Change,  
1591 *One Earth*, 3, 480–490, <https://doi.org/10.1016/j.oneear.2020.09.007>, 2020.

1592 Railsback, L. B., Gibbard, P. L., Head, M. J., Voarintsoa, N. R. G., and Toucanne, S.: An optimized  
1593 scheme of lettered marine isotope substages for the last 1.0 million years, and the  
1594 climatostratigraphic nature of isotope stages and substages, *Quaternary Science Reviews*, 111, 94–  
1595 106, <https://doi.org/10.1016/j.quascirev.2015.01.012>, 2015.

1596 Rasmussen, S. O., Bigler, M., Blockley, S. P., Blunier, T., Buchardt, S. L., Clausen, H. B., Cvijanovic, I.,  
1597 Dahl-Jensen, D., Johnsen, S. J., Fischer, H., Gkinis, V., Guillevic, M., Hoek, W. Z., Lowe, J. J., Pedro, J.  
1598 B., Popp, T., Seierstad, I. K., Steffensen, J. P., Svensson, A. M., Vallelonga, P., Vinther, B. M., Walker,  
1599 M. J. C., Wheatley, J. J., and Winstrup, M.: A stratigraphic framework for abrupt climatic changes  
1600 during the Last Glacial period based on three synchronized Greenland ice-core records: refining and  
1601 extending the INTIMATE event stratigraphy, *Quaternary Science Reviews*, 106, 14–28,  
1602 <https://doi.org/10.1016/j.quascirev.2014.09.007>, 2014.

1603 Rasmussen, T. L., Oppo, D. W., Thomsen, E., and Lehman, S. J.: Deep sea records from the southeast  
1604 Labrador Sea: Ocean circulation changes and ice-rafting events during the last 160,000 years,  
1605 *Paleoceanography*, 18, <https://doi.org/10.1029/2001PA000736>, 2003.

1606 Regattieri, E., Zanchetta, G., Drysdale, R. N., Isola, I., Hellstrom, J. C., and Roncioni, A.: A continuous  
1607 stable isotope record from the penultimate glacial maximum to the Last Interglacial (159–121 ka)  
1608 from Tana Che Urla Cave (Apuan Alps, central Italy), *Quaternary Research*, 82, 450, 2014.

1609 Renault, L., Oguz, T., Pascual, A., Vizoso, G., and Tintore, J.: Surface circulation in the Alborán Sea  
1610 (western Mediterranean) inferred from remotely sensed data, *J. Geophys. Res.*, 117, 2011JC007659,  
1611 <https://doi.org/10.1029/2011JC007659>, 2012.

1612 Rios-Garaizar, J.: Early Middle Palaeolithic occupations at Ventalaperra cave (Cantabrian Region,  
1613 Northern Iberian Peninsula), *Journal of Lithic Studies*, 3, <https://doi.org/10.2218/jls.v3i1.1287>, 2016.

1614 Robles, M., Peyron, O., Ménot, G., Brugiapaglia, E., Wulf, S., Appelt, O., Blache, M., Vannièrè, B.,  
1615 Dugerdil, L., Paura, B., Ansanay-Alex, S., Cromartie, A., Charlet, L., Guédron, S., De Beaulieu, J.-L., and  
1616 Joannin, S.: Climate changes during the Lateglacial in South Europe: new insights based on pollen and  
1617 brGDGTs of Lake Matese in Italy, <https://doi.org/10.5194/cp-2022-54>, 2022.

1618 Robles, M., Peyron, O., Ménot, G., Elisabetta, B., Wulf, S., Appelt, O., Blache, M., Vannièrè, B.,  
1619 Dugerdil, L., Paura, B., Ansanay-Alex, S., Cromartie, A., Charlet, L., Guedron, S., de Beaulieu, Jacques-  
1620 L., and Joannin, S.: Climate changes during the Late Glacial in southern Europe: new insights based on

a mis en forme : Anglais (États-Unis)

1621 pollen and brGDGTs of Lake Matese in Italy, 19, 493–515, <https://doi.org/10.5194/cp-19-493-2023>,  
1622 2023.

1623 Rogerson, M., Cacho, I., Jimenez-Espejo, F., Reguera, M. I., Sierro, F. J., Martinez-Ruiz, F., Frigola, J.,  
1624 and Canals, M.: A dynamic explanation for the origin of the western Mediterranean organic-rich  
1625 layers, *Geochemistry, Geophysics, Geosystems*, 9, <https://doi.org/10.1029/2007GC001936>, 2008.

1626 Rohling, E. J., Marino, G., and Grant, K. M.: Mediterranean climate and oceanography, and the  
1627 periodic development of anoxic events (sapropels), *Earth-Science Reviews*, 143, 62–97,  
1628 <https://doi.org/10.1016/j.earscirev.2015.01.008>, 2015.

1629 Rohling, E. J., Hibbert, F. D., Williams, F. H., Grant, K. M., Marino, G., Foster, G. L., Hennekam, R., de  
1630 Lange, G. J., Roberts, A. P., Yu, J., Webster, J. M., and Yokoyama, Y.: Differences between the last two  
1631 glacial maxima and implications for ice-sheet,  $\delta^{18}\text{O}$ , and sea-level reconstructions, *Quaternary  
1632 Science Reviews*, 176, 1–28, <https://doi.org/10.1016/j.quascirev.2017.09.009>, 2017.

1633 Rojo, J., Orlandi, F., Pérez-Badia, R., Aguilera, F., Ben Dhiab, A., Bouziane, H., Díaz de la Guardia, C.,  
1634 Galán, C., Gutiérrez-Bustillo, A. M., Moreno-Grau, S., Msallem, M., Trigo, M. M., and Fornaciari, M.:  
1635 Modeling olive pollen intensity in the Mediterranean region through analysis of emission sources,  
1636 *Science of The Total Environment*, 551–552, 73–82, <https://doi.org/10.1016/j.scitotenv.2016.01.193>,  
1637 2016.

1638 Roucoux, K. H., de Abreu, L., Shackleton, N. J., and Tzedakis, P. C.: The response of NW Iberian  
1639 vegetation to North Atlantic climate oscillations during the last 65kyr, *Quaternary Science Reviews*,  
1640 24, 1637–1653, <https://doi.org/10.1016/j.quascirev.2004.08.022>, 2005.

1641 Roucoux, K. H., Tzedakis, P. C., Lawson, I. T., and Margari, V.: Vegetation history of the penultimate  
1642 glacial period (Marine isotope stage 6) at Ioannina, north-west Greece, *Journal of Quaternary  
1643 Science*, 26, 616–626, <https://doi.org/10.1002/jqs.1483>, 2011.

1644 Rousseau, D.-D., Antoine, P., Boers, N., Lagroix, F., Ghil, M., Lomax, J., Fuchs, M., Debret, M.,  
1645 Christine, H., Moine, O., Gauthier, C., Jordanova, D., and Jordanova, N.: Dansgaard-Oeschger-like  
1646 events of the penultimate climate cycle: the loess point of view, *Climate of the Past*, 16, 713–727,  
1647 <https://doi.org/10.5194/cp-16-713-2020>, 2020.

1648 Rubio-Jara, S. and Panera, J.: Unravelling an essential archive for the European Pleistocene. The  
1649 human occupation in the Manzanares valley (Madrid, Spain) throughout nearly 800,000 years,  
1650 *Quaternary International*, 520, 5–22, <https://doi.org/10.1016/j.quaint.2018.08.007>, 2019.

1651 Rubio-Jara, S., Panera, J., Rodríguez-de-Tembleque, J., Santonja, M., and Pérez-González, A.: Large  
1652 flake Acheulean in the middle of Tagus basin (Spain): Middle stretch of the river Tagus valley and  
1653 lower stretches of the rivers Jarama and Manzanares valleys, *Quaternary International*, 411, 349–  
1654 366, <https://doi.org/10.1016/j.quaint.2015.12.023>, 2016.

1655 Ruddiman, W. F.: Late Quaternary deposition of ice-rafted sand in the subpolar North Atlantic (lat 40°  
1656 to 65°N), *Geol Soc America Bull*, 88, 1813, [https://doi.org/10.1130/0016-  
1657 7606\(1977\)88<1813:LQDOIS>2.0.CO;2](https://doi.org/10.1130/0016-7606(1977)88<1813:LQDOIS>2.0.CO;2), 1977.

1658 Sadori, L., Koutsodendris, A., Panagiotopoulos, K., Masi, A., Bertini, A., Combourieu-Nebout, N.,  
1659 Francke, A., Kouli, K., Joannin, S., Mercuri, A. M., Peyron, O., Torri, P., Wagner, B., Zanchetta, G.,  
1660 Sinopoli, G., and Donders, T. H.: Pollen-based paleoenvironmental and paleoclimatic change at Lake  
1661 Ohrid (south-eastern Europe) during the past 500 ka, *Biogeosciences*, 13, 1423–1437,  
1662 <https://doi.org/10.5194/bg-13-1423-2016>, 2016.

a mis en forme : Anglais (États-Unis)

- 1663 Salonen, J. S., Korpela, M., Williams, J. W., and Luoto, M.: Machine-learning based reconstructions of  
1664 primary and secondary climate variables from North American and European fossil pollen data, *Sci*  
1665 *Rep*, 9, 15805, <https://doi.org/10.1038/s41598-019-52293-4>, 2019.
- 1666 Sánchez Goñi, M.: The climatic and environmental context of the Late Pleistocene, in: *Updating*  
1667 *Neanderthals. Understanding Behavioural Complexity in the Late Middle Palaeolithic.*,  
1668 Elsevier/Academic Press, London, 165–169, <https://doi.org/10.1016/B978-0-12-823498-3.00012-1>,  
1669 2022.
- 1670 Sánchez Goñi, M. F.: Millennial-scale variability during the last glacial in vegetation records from  
1671 Europe, *Quaternary Science Reviews*, 2010.
- 1672 Sánchez Goñi, M. S., I, C., J, T., J, G., F, S., J, P., J, G., and N, S.: Synchronicity between marine and  
1673 terrestrial responses to millennial scale climatic variability during the last glacial period in the  
1674 Mediterranean region, *Climate Dynamics*, 19, 95, 2002.
- 1675 Sánchez-Laulhé, J. M., Jansa, A., and Jiménez, C.: Alboran Sea Area Climate and Weather, in: *Alboran*  
1676 *Sea - Ecosystems and Marine Resources*, edited by: Báez, J. C., Vázquez, J.-T., Camiñas, J. A., and  
1677 Malouli Idrissi, M., Springer International Publishing, Cham, 31–83, [https://doi.org/10.1007/978-3-](https://doi.org/10.1007/978-3-030-65516-7_3)  
1678 [030-65516-7\\_3](https://doi.org/10.1007/978-3-030-65516-7_3), 2021.
- 1679 Sánchez-Yustos, P.: El paleolítico antiguo en la cuenca del Duero. Instrumentos teóricos para la  
1680 construcción de un modelo interpretativo de arqueología económica, 2009.
- 1681 Sánchez-Yustos, P. and Diez-Martín, F.: Dancing to the rhythms of the Pleistocene? Early Middle  
1682 Paleolithic population dynamics in NW Iberia (Duero Basin and Cantabrian Region), *Quaternary*  
1683 *Science Reviews*, 121, <https://doi.org/10.1016/j.quascirev.2015.05.005>, 2015.
- 1684 Santonja, M., Pérez-González, A., Panera, J., Rubio-Jara, S., and Méndez-Quintas, E.: The coexistence  
1685 of Acheulean and Ancient Middle Palaeolithic techno-complexes in the Middle Pleistocene of the  
1686 Iberian Peninsula, *Quaternary International*, 411, 367–377,  
1687 <https://doi.org/10.1016/j.quaint.2015.04.056>, 2016.
- 1688 Santonja, M., Pérez-González, A., Baena, J., Panera, J., Méndez-Quintas, E., Uribebarrea, D., Demuro,  
1689 M., Arnold, L., Abrunhosa, A., and Rubio-Jara, S.: The Acheulean of the Upper Guadiana River Basin  
1690 (Central Spain). Morphostratigraphic Context and Chronology, *Front. Earth Sci.*, 10,  
1691 <https://doi.org/10.3389/feart.2022.912007>, 2022.
- 1692 Sasso, D., Lebreton, V., Combouieu-Nebout, N., Peyron, O., and Moncel, M.-H.:  
1693 Palaeoenvironmental changes in the southwestern Mediterranean (ODP site 976, Alboran sea) during  
1694 the MIS 12/11 transition and the MIS 11 interglacial and implications for hominin populations,  
1695 *Quaternary Science Reviews*, 304, 108010, <https://doi.org/10.1016/j.quascirev.2023.108010>, 2023.
- 1696 Sasso, D., Combouieu-Nebout, N., Peyron, O., Bertini, A., Toti, F., Lebreton, V., and Moncel, M.-H.:  
1697 Pollen-based climatic reconstructions for the interglacial analogues of MIS 1 (MIS 19, 11, and 5) in  
1698 the southwestern Mediterranean: insights from ODP Site 976, *Clim. Past*, 21, 489–515,  
1699 <https://doi.org/10.5194/cp-21-489-2025>, 2025.
- 1700 Savannah, M., Eelco, R., Timme, D., Katharine, G., Jörg, K., Gianluca, M., Francesca, S., Francesca, C.,  
1701 Caterina, M., Anna, S., and Alessandra, N.: The “glacial” sapropel S6 (172 ka; MIS 6): A multiproxy  
1702 approach to solve a Mediterranean “cold case,” *Palaeogeography, Palaeoclimatology, Palaeoecology*,  
1703 650, 112384, <https://doi.org/10.1016/j.palaeo.2024.112384>, 2024.

a mis en forme : Espagnol (Espagne)

a mis en forme : Anglais (États-Unis)

1704 Scott, B.: *Becoming Neanderthals: the earlier British middle palaeolithic*, Oxbow books, Oxford, 2011.

1705 Shackleton, N. J.: Oxygen isotopes, ice volume and sea level, *Quaternary Science Reviews*, 6, 183–  
1706 190, [https://doi.org/10.1016/0277-3791\(87\)90003-5](https://doi.org/10.1016/0277-3791(87)90003-5), 1987.

1707 Shackleton, N. J., Hall, M. A., and Vincent, E.: Phase relationships between millennial-scale events  
1708 64,000–24,000 years ago, *Paleoceanography*, 15, 565–569, <https://doi.org/10.1029/2000PA000513>,  
1709 2000.

1710 Shackleton, N. J., Sánchez-Goñi, M. F., Pailler, D., and Lancelot, Y.: Marine Isotope Substage 5e and  
1711 the Eemian Interglacial, *Global and Planetary Change*, 36, 151–155, [https://doi.org/10.1016/S0921-8181\(02\)00181-9](https://doi.org/10.1016/S0921-8181(02)00181-9), 2003.

1713 Shackleton, N. J., Fairbanks, R. G., Chiu, T., and Parrenin, F.: Absolute calibration of the Greenland  
1714 time scale: implications for Antarctic time scales and for  $\Delta^{14}C$ , *Quaternary Science Reviews*, 23,  
1715 1513–1522, <https://doi.org/10.1016/j.quascirev.2004.03.006>, 2004.

1716 Shaw, A., Bates, M., Conneller, C., Gamble, C., Julien, M.-A., McNabb, J., Pope, M., and Scott, B.: The  
1717 archaeology of persistent places: the Palaeolithic case of La Cotte de St Brelade, Jersey, *Antiquity*, 90,  
1718 1437–1453, <https://doi.org/10.15184/aqy.2016.212>, 2016.

1719 Shin, J., Nehrbass-Ahles, C., Grilli, R., Chowdhry Beeman, J., Parrenin, F., Teste, G., Landais, A.,  
1720 Schmidely, L., Silva, L., Schmitt, J., Bereiter, B., Stocker, T. F., Fischer, H., and Chappellaz, J.:  
1721 Millennial-scale atmospheric CO<sub>2</sub> variations during the Marine Isotope Stage 6 period (190–  
1722 135&thinsp;ka), *Climate of the Past*, 16, 2203–2219, <https://doi.org/10.5194/cp-16-2203-2020>, 2020.

1723 Sierro, F. J. and Andersen, N.: An exceptional record of millennial-scale climate variability in the  
1724 southern Iberian Margin during MIS 6: Impact on the formation of sapropel S6, *Quaternary Science  
1725 Reviews*, 286, 107527, <https://doi.org/10.1016/j.quascirev.2022.107527>, 2022.

1726 Sierro, F. J., Hodell, D. A., Andersen, N., Azibeiro, L. A., Jimenez-Espejo, F. J., Bahr, A., Flores, J. A.,  
1727 Ausin, B., Rogerson, M., Lozano-Luz, R., Lebreiro, S. M., and Hernandez-Molina, F. J.: Mediterranean  
1728 Overflow Over the Last 250 kyr: Freshwater Forcing From the Tropics to the Ice Sheets,  
1729 *Paleoceanography and Paleoclimatology*, 35, e2020PA003931,  
1730 <https://doi.org/10.1029/2020PA003931>, 2020.

1731 Silva, P. G., López-Recio, M., Tapias, F., Roquero, E., Morín, J., Rus, I., Carrasco-García, P., Giner-  
1732 Robles, J. L., Rodríguez-Pascua, M. A., and Pérez-López, R.: Stratigraphy of the Arriaga Palaeolithic  
1733 sites. Implications for the geomorphological evolution recorded by thickened fluvial sequences within  
1734 the Manzanares River valley (Madrid Neogene Basin, Central Spain), *Geomorphology*, 196, 138–161,  
1735 <https://doi.org/10.1016/j.geomorph.2012.10.019>, 2013.

1736 Sinopoli, G., Peyron, O., Masi, A., Holtvoeth, J., Francke, A., Wagner, B., and Sadori, L.: Pollen-based  
1737 temperature and precipitation changes in the Ohrid Basin (western Balkans) between 160 and 70 ka,  
1738 *Climate of the Past*, 15, 53–71, <https://doi.org/10.5194/cp-15-53-2019>, 2019.

1739 Skinner, L. C. and Shackleton, N. J.: Deconstructing Terminations I and II: revisiting the glacioeustatic  
1740 paradigm based on deep-water temperature estimates, *Quaternary Science Reviews*, 25, 3312–3321,  
1741 <https://doi.org/10.1016/j.quascirev.2006.07.005>, 2006a.

1742 Skinner, L. C. and Shackleton, N. J.: Deconstructing Terminations I and II: revisiting the glacioeustatic  
1743 paradigm based on deep-water temperature estimates, *Quaternary Science Reviews*, 25, 3312–3321,  
1744 <https://doi.org/10.1016/j.quascirev.2006.07.005>, 2006b.

a mis en forme : Anglais (États-Unis)

- 1745 Stocker, T. F.: The Seesaw Effect, *Science*, 282, 61–62, <https://doi.org/10.1126/science.282.5386.61>,  
1746 1998.
- 1747 Sumner, G., Homar, V., and Ramis, C.: Precipitation seasonality in eastern and southern coastal Spain,  
1748 *Intl Journal of Climatology*, 21, 219–247, <https://doi.org/10.1002/joc.600>, 2001.
- 1749 Svendsen, J. I., Alexanderson, H., Astakhov, V. I., Demidov, I., Dowdeswell, J. A., Funder, S., Gataullin,  
1750 V., Henriksen, M., Hjort, C., Houmark-Nielsen, M., Hubberten, H. W., Ingólfsson, Ó., Jakobsson, M.,  
1751 Kjær, K. H., Larsen, E., Lokrantz, H., Lunkka, J. P., Lyså, A., Mangerud, J., Matiouchkov, A., Murray, A.,  
1752 Möller, P., Niessen, F., Nikolskaya, O., Polyak, L., Saarnisto, M., Siegert, C., Siegert, M. J., Spielhagen,  
1753 R. F., and Stein, R.: Late Quaternary ice sheet history of northern Eurasia, *Quaternary Science*  
1754 *Reviews*, 23, 1229–1271, <https://doi.org/10.1016/j.quascirev.2003.12.008>, 2004.
- 1755 Terradillos-Bernal, M., Demuro, M., Arnold, L. J., Jordá-Pardo, J. F., Clemente-Conte, I., Benito-Calvo,  
1756 A., and Díez Fernández-Lomana, J. C.: San Quirce (Palencia, Spain): new chronologies for the Lower to  
1757 Middle Palaeolithic transition of south-west Europe, *Journal of Quaternary Science*, 38, 21–37,  
1758 <https://doi.org/10.1002/jqs.3460>, 2023.
- 1759 Thabet, A. A., Maas, A. E., Lawson, G. L., and Tarrant, A. M.: Life cycle and early development of the  
1760 thecosomatous pteropod *Limacina retroversa* in the Gulf of Maine, including the effect of elevated  
1761 CO<sub>2</sub> levels, *Mar Biol*, 162, 2235–2249, <https://doi.org/10.1007/s00227-015-2754-1>, 2015.
- 1762 Torres, C., Tapias, F., Demuro, M., Arnold, L., Arriolabengoa, M., Pérez, S., and Preysler, J.: The  
1763 Acheulian site of Cantera Vieja (Madrid, Spain) and the Lower to Middle Palaeolithic transition in  
1764 central Spain, <https://doi.org/10.21203/rs.3.rs-4195503/v1>, 2024.
- 1765 Toucanne, S., Zaragosi, S., Bourillet, J. F., Cremer, M., Eynaud, F., Van Vliet-Lanoë, B., Penaud, A.,  
1766 Fontanier, C., Turon, J. L., Cortijo, E., and Gibbard, P. L.: Timing of massive ‘Fleuve Manche’  
1767 discharges over the last 350 kyr: insights into the European ice-sheet oscillations and the European  
1768 drainage network from MIS 10 to 2, *Quaternary Science Reviews*, 28, 1238–1256,  
1769 <https://doi.org/10.1016/j.quascirev.2009.01.006>, 2009.
- 1770 Tzedakis, P. C.: Long-term tree populations in northwest Greece through multiple Quaternary  
1771 climatic cycles, *Nature*, 364, 437–440, <https://doi.org/10.1038/364437a0>, 1993.
- 1772 Tzedakis, P. C.: Towards an understanding of the response of southern European vegetation to  
1773 orbital and suborbital climate variability, *Quaternary Science Reviews*, 24, 1585–1599,  
1774 <https://doi.org/10.1016/j.quascirev.2004.11.012>, 2005.
- 1775 Tzedakis, P. C., Frogley, M. R., Lawson, I. T., Preece, R. C., Cacho, I., and de Abreu, L.: Ecological  
1776 thresholds and patterns of millennial-scale climate variability: The response of vegetation in Greece  
1777 during the last glacial period, *Geology*, 32, 109, <https://doi.org/10.1130/G20118.1>, 2004.
- 1778 Tzedakis, P. C., Hooghiemstra, H., and Pälike, H.: The last 1.35 million years at Tenaghi Philippon:  
1779 revised chronostratigraphy and long-term vegetation trends, *Quaternary Science Reviews*, 25, 3416–  
1780 3430, <https://doi.org/10.1016/j.quascirev.2006.09.002>, 2006.
- 1781 Tzedakis, P. C., Drysdale, R. N., Margari, V., Skinner, L. C., Menviel, L., Rhodes, R. H., Taschetto, A. S.,  
1782 Hodell, D. A., Crowhurst, S. J., Hellstrom, J. C., Fallick, A. E., Grimalt, J. O., McManus, J. F., Martrat, B.,  
1783 Mokeddem, Z., Parrenin, F., Regattieri, E., Roe, K., and Zanchetta, G.: Enhanced climate instability in  
1784 the North Atlantic and southern Europe during the Last Interglacial, *Nat Commun*, 9, 4235,  
1785 <https://doi.org/10.1038/s41467-018-06683-3>, 2018.

1786 Valensi, P., Aouraghe, H., Bailon, S., Cauche, D., Combier, J., Desclaux, E., Gagnepain, J., Gaillard, C.,  
1787 Khatib, S., Lumley, H., Moigne, A.-M., Moncel, M.-H., and Notter, O.: Les peuplements préhistoriques  
1788 dans le sud-est de la France à la fin du Pléistocène moyen : 400 - 120 000 ans. Terra Amata, Orgnac 3,  
1789 Baume Bonne, Lazaret. Cadre géochronologique et biostratigraphique, paléoenvironnements et  
1790 évolution culturelle des derniers anténéandertaliens., 2005.

1791 Valensi, P., Michel, V., El Guennouni, K., and Liouville, M.: New data on human behavior from a  
1792 160,000 year old Acheulean occupation level at Lazaret cave, south-east France: An  
1793 archaeozoological approach, *Quaternary International*, 316,  
1794 <https://doi.org/10.1016/j.quaint.2013.10.034>, 2013.

1795 Vernot, B., Zavala, E., Gómez-Olivencia, A., Jacobs, Z., Slon, V., Mafessoni, F., Romagné, F., Pearson,  
1796 A., Petr, M., Sala, N., Pablos, A., Aranburu, A., Bermúdez de Castro, J.-M., Carbonell, E., Li, B.,  
1797 Krajcarz, M., Krivoschapkin, A., Kolobova, K., Kozlikin, M., and Meyer, M.: Unearthing Neanderthal  
1798 population history using nuclear and mitochondrial DNA from cave sediments, *Science*, 372,  
1799 eabf1667, <https://doi.org/10.1126/science.abf1667>, 2021.

1800 Vidal-Matutano, P., Blasco, R., Sañudo, P., and Fernández Peris, J.: The Anthropogenic Use of  
1801 Firewood During the European Middle Pleistocene: Charcoal Evidence from Levels XIII and XI of  
1802 Bolomor Cave, Eastern Iberia (230–160 ka), *Environmental Archaeology*, 24, 269–284,  
1803 <https://doi.org/10.1080/14614103.2017.1406026>, 2019.

1804 Voelker, A. H. L. and de Abreu, L.: A Review of Abrupt Climate Change Events in the Northeastern  
1805 Atlantic Ocean (Iberian Margin): Latitudinal, Longitudinal, and Vertical Gradients, in: *Abrupt Climate*  
1806 *Change: Mechanisms, Patterns, and Impacts*, American Geophysical Union (AGU), 15–37,  
1807 <https://doi.org/10.1029/2010GM001021>, 2011.

1808 Wagner, B., Vogel, H., Francke, A., Friedrich, T., Donders, T., Lacey, J. H., Leng, M. J., Regattieri, E.,  
1809 Sadori, L., Wilke, T., Zanchetta, G., Albrecht, C., Bertini, A., Combourieu-Nebout, N., Cvetkoska, A.,  
1810 Giaccio, B., Grazhdani, A., Hauffe, T., Holtvoeth, J., Joannin, S., Jovanovska, E., Just, J., Kouli, K.,  
1811 Kousis, I., Koutsodendris, A., Krastel, S., Lagos, M., Leicher, N., Levkov, Z., Lindhorst, K., Masi, A.,  
1812 Melles, M., Mercuri, A. M., Nomade, S., Nowaczyk, N., Panagiotopoulos, K., Peyron, O., Reed, J. M.,  
1813 Sagnotti, L., Sinopoli, G., Stelbrink, B., Sulpizio, R., Timmermann, A., Tofilovska, S., Torri, P., Wagner-  
1814 Cremer, F., Wonik, T., and Zhang, X.: Mediterranean winter rainfall in phase with African monsoons  
1815 during the past 1.36 million years, *Nature*, 573, 256–260, [https://doi.org/10.1038/s41586-019-1529-](https://doi.org/10.1038/s41586-019-1529-0)  
1816 0, 2019.

1817 Wainer, K., Genty, D., Blamart, D., Daëron, M., Bar-Matthews, M., Vonhof, H., Dublyansky, Y., Pons-  
1818 Branchu, E., Thomas, L., Calsteren, P., Quinif, Y., and Caillon, N.: Speleothem record of the last 180 ka  
1819 in Villars cave (SW France): Investigation of a large  $\delta^{18}\text{O}$  shift between MIS6 and MIS5, *Quaternary*  
1820 *Science Reviews - QUATERNARY SCI REV*, 30, 130–146,  
1821 <https://doi.org/10.1016/j.quascirev.2010.07.004>, 2011.

1822 Wainer, K., Genty, D., Blamart, D., Bar-Matthews, M., Quinif, Y., and Plagnes, V.: Millennial climatic  
1823 instability during penultimate glacial period recorded in a south-western France speleothem,  
1824 *Palaeogeography, Palaeoclimatology, Palaeoecology*, 376, 122–131,  
1825 <https://doi.org/10.1016/j.palaeo.2013.02.026>, 2013.

1826 Wang, Q., Wang, Y., Shao, Q., Liang, Y., Zhang, Z., and Kong, X.: Millennial-scale Asian monsoon  
1827 variability during the late Marine Isotope Stage 6 from Hulu Cave, China, *Quat. res.*, 90, 394–405,  
1828 <https://doi.org/10.1017/qua.2018.75>, 2018.

a mis en forme : Anglais (États-Unis)

a mis en forme : Anglais (États-Unis)

1829 Wang, Y. J., Cheng, H., Edwards, R. L., An, Z. S., Wu, J. Y., Shen, C. C., and Dorale, J. A.: A high-  
1830 resolution absolute-dated late Pleistocene Monsoon record from Hulu Cave, China, *Science*, 294,  
1831 2345–2348, <https://doi.org/10.1126/science.1064618>, 2001.

1832 Wenzel, S.: Neanderthal presence and behaviour in central and Northwestern Europe during MIS 5e,  
1833 in: *Developments in Quaternary Sciences*, 173–193, <https://doi.org/10.13140/2.1.2747.7442>, 2007.

1834 White, M. J. and Pettitt, P. B.: The British Late Middle Palaeolithic: An Interpretative Synthesis of  
1835 Neanderthal Occupation at the Northwestern Edge of the Pleistocene World, *Journal of World*  
1836 *Prehistory*, 24, <https://doi.org/10.1007/s10963-011-9043-9>, 2011.

1837 Willis, K. J., Bennett, K. D., Walker, D., Gamble, C., Davies, W., Pettitt, P., and Richards, M.: Climate  
1838 change and evolving human diversity in Europe during the last glacial, *Philosophical Transactions of*  
1839 *the Royal Society of London. Series B: Biological Sciences*, 359, 243–254,  
1840 <https://doi.org/10.1098/rstb.2003.1396>, 2004.

1841 Wilson, G. P., Frogley, M. R., Hughes, P. D., Roucoux, K. H., Margari, V., Jones, T. D., Leng, M. J., and  
1842 Tzedakis, P. C.: Persistent millennial-scale climate variability in Southern Europe during Marine  
1843 Isotope Stage 6, *Quaternary Science Advances*, 3, 100016,  
1844 <https://doi.org/10.1016/j.qsa.2020.100016>, 2021.

1845 Xue, G., Cai, Y., Ma, L., Cheng, X., Cheng, H., Edwards, R. L., Li, D., and Tan, L.: A new speleothem  
1846 record of the penultimate deglacial: Insights into spatial variability and centennial-scale instabilities  
1847 of East Asian monsoon, *Quaternary Science Reviews*, 210, 113–124,  
1848 <https://doi.org/10.1016/j.quascirev.2019.02.023>, 2019.

1849 Yaworsky, P. M., Nielsen, E. S., and Nielsen, T. K.: The Neanderthal niche space of Western Eurasia  
1850 145 ka to 30 ka ago, *Sci Rep*, 14, 7788, <https://doi.org/10.1038/s41598-024-57490-4>, 2024.

1851 Yravedra, J., Rubio-Jara, S., Panera, J., Made, J. van der, and Pérez-González, A.: Neanderthal diet in  
1852 fluvial environments at the end of the Middle Pleistocene/early Late Pleistocene of PRERESA site in  
1853 the Manzanares Valley (Madrid, Spain), *Quaternary International*, 520, 72–83,  
1854 <https://doi.org/10.1016/j.quaint.2018.01.030>, 2019.

1855 Zahn, R., Comas, M. C., and Klaus, A. (Eds.): *Proceedings of the Ocean Drilling Program*, 161 Scientific  
1856 *Results*, Ocean Drilling Program, <https://doi.org/10.2973/odp.proc.sr.161.1999>, 1999.

1857 Zhang, J., Zolitschka, B., Högrefe, I., Tsukamoto, S., Binot, F., and Frechen, M.: High-resolution  
1858 luminescence-dated sediment record for the last two glacial-interglacial cycles from Rodderberg,  
1859 Germany, *Quaternary Geochronology*, 82, 101535, <https://doi.org/10.1016/j.quageo.2024.101535>,  
1860 2024.

1861 Ziegler, M., Tuenter, E., and Lourens, L.: The precession phase of the boreal summer monsoon as  
1862 viewed from the eastern Mediterranean (ODP Site 968), *Quaternary Science Reviews*, 29,  
1863 <https://doi.org/10.1016/j.quascirev.2010.03.011>, 2010.

1864